University of Strathclyde

Strathclyde Institute of Pharmacy and

Biomedical Sciences

Improved routes to bioprocessing of biopharmaceuticals by a marine fungus

Tantima Kumlung

A thesis presented in fulfilment of the requirements for the degree of Doctor of Philosophy

June 2012

This thesis is the result of the author's original research. It has been composed by the author and has not been previously submitted for examination which has led to the award of a degree.

Signed:

Date:

Acknowledgement

First and foremost, I would like to express my sincere gratitude to my supervisors, Prof. Brian McNeil, Dr. Linda Harvey, and Dr. RuAngelie Edrada-Ebel for their support, encouragement and guidance throughout my studies. Also sincere thanks to Dr. RuAngelie Edrada-Ebel for her assistance with NMR experimentation and NMR interpretation.

I am grateful for marine microorganisms which were kindly supplied by Aquapharm Biodiscovery Ltd., and I would also like to express my sincere appreciation to Dr Andrew Mearns Spragg for his guidance and valuable discussion.

I am also thankful to my wonderful colleagues and friends in the Strathclyde Fermentation Centre, Dr. Mariana Fazenda, Dr. Payal Roy Choudhury, Dr. Manal Eshelli, Dr. Ioannis Voulgaris, Dr. Ebtihaj Jambi (my best friend, and winner forever), Ivo Kretzers, Melissa Black and the craziest chemist Peter Gardner. I wish to thank the lab technician, Walter McEwan, for his magic hands and excellent technical support; and Dr Zhang Tong for helping with LC-MS. I want to give thanks to my friends, who supported me with warmth and friendship during my study in Glasgow, Dr. Juyen Fu, Dr. Hibah Aldawsari and her kids, Christina Victoria Viegelmann. Also my sincere thanks to my beloved friend, Dr. Utsana Puapermpoonsiri who always encouraged and given moral support when I was down.

I would like to thank the Thai Government for funding my study.

Last but not least many thanks to my grandma who passed away two years ago, my parents and family for their continuous love and support.

Table of Contents

LIST OF FIGURES

LIST OF TABLES

LIST OF ABBREVIATIONS

acetyl-CoA	acetyl coenzyme A
ACP	acyl carrier protein
Acs	acetyl CoA synthetase
Adh	alcohol dehydrogenase
Ald	aldehyde dehydrogenase
APCI	atmospheric pressure chemical ionisation
AT	acyltransferase
CI	chemical ionisation
COSY	correlation spectroscopy
DESI	desorption electrospray ionisation
DI	desorption ionisation
DMPP	dimethylallyl pyrophosphate
DOT	dissolved oxygen tension
EI	electron impact
ESI	electrospray ionisation
EPS	exopolysaccharides
Fbp1	fructose-1,6-bisphosphatase 1
FPP	farnesyl pyrophosphate

Gal	galactokinase
Glk	glucokinase
GPP	geranyl pyrophosphate
h	Planck's constant
HMBC	heteronuclear multiple bond correlation
HMG-CoA	hydroxymethylglutaryl coenzyme A
HPLC	high-performance liquid chromatography
HRFTMS	high-resolution Fourier transform mass spectrometry
HSQC	heteronuclear single quantum coherence
Hxk	hexokinase
IEX	ion-exchange
IO	Instant Ocean
IPP	isopentenyl pyrophosphate
J	the coupling constant
β-KS	beta-ketoacyl synthase
LC-MS	liquid chromatography–mass spectrometry
MALDI	matrix-assisted laser desorption/ionisation
MS	mass spectrometry
MS/MS	tandem mass spectrometry

MYGP	Malt yeast glucose peptone media
NMR	Nuclear Magnetic Resonance
NP	normal-phase
PDA	Potato dextrose agar
PDB	Potato dextrose broth
Pdc	pyruvate-decarboxylase
Pdh	pyruvate dehydrogenase
Pfk	phosphofructokinase
Pgl	6-phosphogluconolactonase
PKSs	polyketides synthase pathway
ppm	parts per million
Pyk	pyruvate kinase isoenzymes
RP	reversed-phase
SEC	size-exclusion chromatography
STR	stirred tank
β_o	the strength of the external magnetic field
γ	the strength of the nuclear magnet
ΔE	the energy
ν_o	the Larmor frequency
φ	water potential

φg	gravimetric potential
φm	matric potential
φp	turgor potential
$\varphi \pi$	osmotic potential

ABSTRACT

The marine-derived fungus, *Trichoderma pseudokonningii* was isolated from seawater at Oban, Scotland and provided by Aquapharm Biodiscovery Ltd. The aim of this project was to investigate a microorganism that can produce bioactive secondary metabolites as well as to develop efficient cultivation and production processes on a small scale which could be finally scaled up to a fermenter system. Current findings show that salinity has a very clear influence upon growth and sporulation of this fungus. A dereplication study of its secondary metabolites was carried out using - LTQ-Orbitrap-HRFTMS and high resolution NMR. With the aid of an automated label-free differential expression software, SIEVE v.1.2 and MZmine v.2.2, the presence of four bioactive compounds were identified including virescenoside B, gemfibrozil, γ-linolenic acid, and a lovastatin derivative. Scale-up of the production of the probably new lovastatin congener was chosen because of the high market value of lovastatin in the world. From LC-MS quantification results, PDA without the Instant Ocean (IO) gave the maximum yield of the lovastatin congener (6.13 μg/plate). NMR analysis also confirmed the presence of a structure related to lovastatin produced in cultures of AQP 4097 which has a difference in chemical shifts of the olefinic protons. Moreover, increasing the initial glucose concentration and dissolved oxygen tension in the medium promoted the growth of this strain; however, the higher agitation speed was associated with adverse affects both on mycelial morphology and production of the lovastatin derivative by AQP 4097. Slowly utilized carbon sources, such as glycerol, promoted the production of the lovastatin derivative, and also affected culture morphology of AQP 4097 which was transformed from loose fluffy aggregates into denser larger pellets within 72 hours after inoculation. Conclusively, a lovastatin

derivative was successfully produced from the marine-derived fungus (*Trichoderma pseudokonningii*) by shake flask and fermentation vessel process. In the scale up of the production of the described lovastatin congener the appropriate conditions that include glucose consumption, dissolved oxygen, carbon source, and agitation speed have to be carefully considered in order to obtain the highest yield as well as to maintain the mycelial morphology.

Chapter 1 Introduction

1. Introduction

1.1. Overview of natural products

The word nature originated from the Latin word, *natura*, and natural is an adjective referring to something that is present in or produced by nature and not artificial or man-made (Spainhour, 2005). Thus, a natural product is defined as any chemical compound derived from plants, microorganisms, invertebrates and vertebrates (Bhat *et al.*, 2005). Natural products derived from microorganisms can be divided into two groups depending on their function; primary and secondary metabolites. Compounds which occur in all cells and play a crucial role in metabolism and reproduction of those cells, are known as primary metabolites, and included in this group are nucleic acids, common amino acids and sugars. Secondary metabolites are compounds that are not involved in the normal growth, development, or reproduction of an organism, and may often play an important role in interspecies defences. These properties of secondary metabolites make them attractive for scientists to study.

The first historical indication that humans relied on a natural product to take care of their health was the discovery of the remnants of medicinal herbs in Neanderthal remains (Holt and Chandra, 2002). Hippocrates, considered the Father of Medicine, wrote a treatise known as *Corpus Hippocraticum*, which covered the usage of mainly plant-based mixtures in Greece and the Roman Empire. A philosopher and natural scientist, Theophrastus, in approximately 300 BC, wrote a History of Plants in which he addressed the medicinal qualities of herbs and the ability to cultivate them. The Greek botanist, Pedanious Dioscorides, in approximately AD 100, produced a work entitled

De Materia Medica, which is still a very well-known European document on the use of herbs in medicine.

In addition to Europe, in the Middle East, the first records on the use of natural products in medicine were written in cuneiform in Mesopotamia on clay tablets and date to approximately 2600 BC (Nakanishi, 1999). There is also documented use of various herbs in Egypt in 1500 B.C. The best known of these documents is the Ebers Papyrus, which reported nearly 1000 different substances and formulations, most of which are plant-based medicines including opium, cannabis, linseed, aloe and garlic. Another well-known book, The Canon of Medicine is an encyclopaedia of Greek and Roman medicine compiled by Ibn Sīnā, a Persian philosopher and physician; originally written in Arabic, the book was later translated into a number of other languages, including Latin, Chinese, Hebrew, German, French, and English (Nakanishi, 1999). Buss and Butler (2010) described some records of the use of natural products, approximately 1000 plant derived-medicines, including oils of *Cedrus* species (cedar) and *Cupressus sempervirens* (cypress), *Glycyrrhiza glabra* (liquorice), *Commiphora* species (myrrh) and *Papaver somniferum* (poppy juice) for treatment of various ailments.

Asia is another part of the world that has a long history of using natural medicines to cure or prevent diseases. Holt and Chandra (2002) noted that Chinese herbal guides were used as far back as 2000 BC. The Nei Ching is one of the earliest health science anthologies ever produced, and dates back to 3000 BC (Nakanishi, 1999). The drug encyclopaedia during the Ming Dynasty entitled Pen-ts'as kang mu was written by Li Shih-Chen in AD 1596 and comprised of 1898 herbal drugs and 8160 prescriptions. In India around 1000 BC, a collection of Ayurvedic hymns described the use of over 1000

different herbs. This work served as the basis for Tibetan Medicine translated from Sanskrit during the eighth century (Bhat, *et al.* 2005).

Newman *et al.* (2000) reported that the first commercial pure natural product introduced for therapeutic use is generally considered to be the narcotic morphine, marketed by Merck in 1826 and the first semi-synthetic pure drug based on a natural product, aspirin, was introduced by Bayer in 1899.

Natural products can be classified into 2 major groups based on their habitat, terrestrial and marine habitats. The first group, natural products from terrestrial habitats are divided into two subgroups including terrestrial plants, and terrestrial microorganisms. Natural products from marine habitats are also divided into 2 subgroups including marine organisms, and marine microorganisms.

Natural products from terrestrial plants, were first recorded on clay tablets from Mesopotamia around 2600 BC which identified poppy capsule latex (*Papaver somniferum)* as one of the substances in Babylonian prescriptions, and showed that human beings have known how to use plant substances as drugs for a long time; even nowadays drugs-derived from plants such as cocaine, codeine, digitoxin, and quinine, in addition to morphine are still in use (Newman *et al*., 2000; Butler, 2004). At the beginning, these medicines-derived from plants were used as a crude product, for example, tinctures, teas, poultices, powders and other herbal formulations (Balick and Cox, 1997). More recently, compound isolation, characterisation and elucidation techniques have improved. However, compound developments from plant-derived products still face a challenge; the major problem is the natural product can be isolated in small quantities which are not enough to optimise and develop their use in a clinical trials. In addition, bioactive compound

production relies on environmental factors such as climate, season, and herbivore pressure (Balunas and Kinghorn, 2005). Sometimes unpredictable quantities of product are due to the plant not being the real source of the compound, such as toxol which is produced from an endophytic fungus associated with Pacific yew (Stierle *et al*., 1993). Five important drugs derived from plants that have been approved for use include Apomorphine hydrochloride, Arteether, Galantamine hydrobromide, Nitisinone, and Tiotropium bromide (Young-Won, 2006).

In the early 20th century, the Golden Age of antibiotics, natural products from terrestrial microorganisms, were developed after Sir Alexander Fleming discovered the first antibiotic, penicillin, from the fungus *Penicillium notatum* in 1928 for which he was awarded the Nobel Prize. Fleming was followed by Selman Waksman, who received the Nobel Prize in Physiology or Medicine in 1952, after discovering the first antibiotic remedy for tuberculosis, streptomycin, from the soil-actinobacterium *Streptomyces griseus*. Waksman's discovery lead to the later discovery of several antibiotics, including actinomycin, clavacin, streptothricin, streptomycin, grisein, neomycin, fradicin, candicidin, and candidin (Buss and Butler, 2010).

Microbes are an alternative source of bioactive compounds to traditional medicinal sources such as those extracted from plants, which have a limitation because they depend on seasonal changes or are protected under the convention on biological diversity, which limits substantial recollection (Buss and Butler, 2010). The advantages of using microbes for searching for new bioactive compounds is that they are renewable resources, i.e. they can be cultured in the laboratory and on a large scale necessary for manufacture. Moreover, they can be found everywhere on Earth; they can live in the air, on

land, and in fresh or salt water environments; even in extreme environments (high and low temperatures, high pressure, acidity/alkalinity).

McWilliams (2011) stated that the total global market for microbes and microbial products was worth more than $144 billion in 2010. The 2011 market was projected to exceed $156 billion, and up to $259 billion by 2016, reflecting a 10.7% projected compound annual growth rate (CAGR) between 2011 and 2016. Only the cost of market for microbes, which can be identified as biofertilizers, biopesticides, and probiotics, totalled nearly $4.5 billion in 2010. The market for microbes was projected to approach $4.9 billion in 2011 and $6.8 billion by 2016, a CAGR of 6.9% over the forecast period. The Healthcare sector costs more than 60% of the total market for microbes and microbial products. This sector was valued at $90.5 billion in 2010, increasing to $100.4 billion in 2011 and $169 billion by 2016, a CAGR of 11% over the forecast period.

The generic names of forty-nine natural products obtained from terrestrial microorganisms that have been commercialised in the global market (including the source and application of product) are listed in Appendix I. Most of them are produced by yeast. In addition to these products another twenty-four substances are undergoing clinical trial. (Young-Won, *et al.* 2006).

Natural products from marine habitats: marine organisms and marine microorganisms have attracted biologists and chemists around the world for the last five decades due to their considerable biodiversity that has been found in the oceans that cover over 70% of the world. Bhakuni and Rawat (2005) stated that approximately 16,000 marine natural products have been isolated from marine organisms and reported in approximately 6,800

publications. In addition to these publications there are approximately another 9,000 publications that cover syntheses, reviews, biological activity and ecological studies. In 1974, two marine-derived natural products (cytarabine, Ara-C and vidarabine, Ara-A) were approved by the Food and Drug Administration (FDA) to be part of the pharmacopeia used to treat human diseases and thirty years later, another, Ziconotide (Prialt®) for the treatment of moderate to severe pain in 2004. Trabectedin (ET-743) from Yondelis® company followed received European approval in 2007 for the treatment of soft tissue sarcoma, and in 2009 for ovarian carcinoma (Mayer *et al*., 2010). Biosynthesis studies of marine metabolites face a problem due to the slow synthesis rate of metabolites in marine organisms, particularly if the organism is slow growing. Another problem is that understanding of the metabolic processes in the marine environment is still very limited. Marine organisms are different from other living organism because they commonly live in symbiotic associations; for example, the association between sponges and microalgae or bacteria (or both) and that between coral (or dinoflagellates) and gorgonians is well known. The pathway for the transfer of nutrients, which is the main key to understanding the metabolic production between symbiotic partners, is also still to be identified.

Normally in the terrestrial environment, bacteria and fungi are prime producers of antagonistic substances; in the ocean these organisms are expected to perform a similar role. There are some lead products from marine microorganisms that are in Phase III clinical trials for the treatment of cancer such as Soblidotin (TZT 1027), isolated from marine cyanobacteria (Young-Won, *et al.* 2006). Three other compounds Plinabulin (NPI-2358), Tasidotin, and Synthadotin (ILX-651), isolated from marine fungi and marine bacteria respectively are in phase II Clinical trials. In addition, Marizomib

(Salinosporamide A; NPI-0052), isolated from marine bacteria are in Phase I Clinical trials (Young-Won, *et al.* 2006). Besides these compounds, there are one hundred and six lead compounds isolated from marine fungi and eighty four lead compounds isolated from marine bacteria which have bioactive properties. These are summarised in Appendix II. One key player in the marine natural products field, in Scotland is a company called Aquapharm Biodiscovery Ltd. based in Oban that develops next generation pharmaceuticals and novel, naturally derived functional food and personal care ingredients and products from marine organisms. One of their strategies is to collaborate with researchers to research and commercialise their pharmaceutical candidates. Therefore, they are interested in searching and elucidating the structure of marine-derived compounds, optimising compound production by their organisms, investigating scale-up of growth of the organism, and production of particular commercially relevant compounds. One compound that is attractive to Aquapharm® Biodiscovery Limited for future development is lovastatin.

1.2 Lovastatin

1.2.1 History

Lovastatin is a drug which can be classified as a statin, or called a HMG-CoA reductase inhibitor, used for lowering cholesterol levels by inhibiting the enzyme HMG-CoA reductase, which plays an important role in the production of cholesterol in the liver. There are around 10 commercialised statin drugs on the world market. In 2009, the market intelligence group IMS National Sales Perspectives TM (Top 15 U.S Pharmaceutical Products by Sales, 2009) reported that Lipitor® (atorvastatin) from Pfizer was in first place on the Top 15 U.S. Prescription Products list, while in 2011 Lipid

Regulators were in third place on the Top Therapeutic Classes list by Spending (Top Therapeutic Classes by Spending, 2011), which cost 20.1 billion US$.

Cholesterol is a crucial biological molecule, which plays an important role in membrane structure as well as being a precursor for the synthesis of steroid hormones and bile acids in the human body. Cholesterol biosynthesis occurs in the cytoplasm and microsomes (Endoplasmic reticulum), produced by the mevalonate pathway as shown in Figure 1.1 At the first step, acetyl-CoA which is derived from an oxidation reaction (e.g., fatty acids or pyruvate) in the mitochondria, and can also be derived from cytoplasmic oxidation of ethanol by acetyl-CoA synthetase, converted to mevalonate by a series of reactions that begins with the formation of HMG-CoA. After that, mevalonate is activated by phosphorylation activity to 5-pyrophosphomevalonate and coverted to isopentenyl pyrophosphate (IPP) an activated isoprenoid molecule via ATP-dependent decarboxylation. Afterwards, isopentenyl pyrophosphate is in equilibrium with its isomer, dimethylallyl pyrophosphate (DMPP). One molecule of IPP condenses with one molecule of DMPP to generate geranyl pyrophosphate (GPP). This further condenses with another IPP molecule to yield farnesyl pyrophosphate (FPP). The NADPH-requiring enzyme, squalene synthase catalyses the head-to-tail condensation of two molecules of FPP, yielding squalene. Squalene undergoes a two-step cyclisation to yield lanosterol. The first reaction is catalysed by squalene monooxygenase, which enzyme uses NADPH as a cofactor to introduce molecular oxygen as an epoxide at the 2, 3 position of squalene. Through a series of 19 additional reactions, lanosterol is converted to cholesterol.

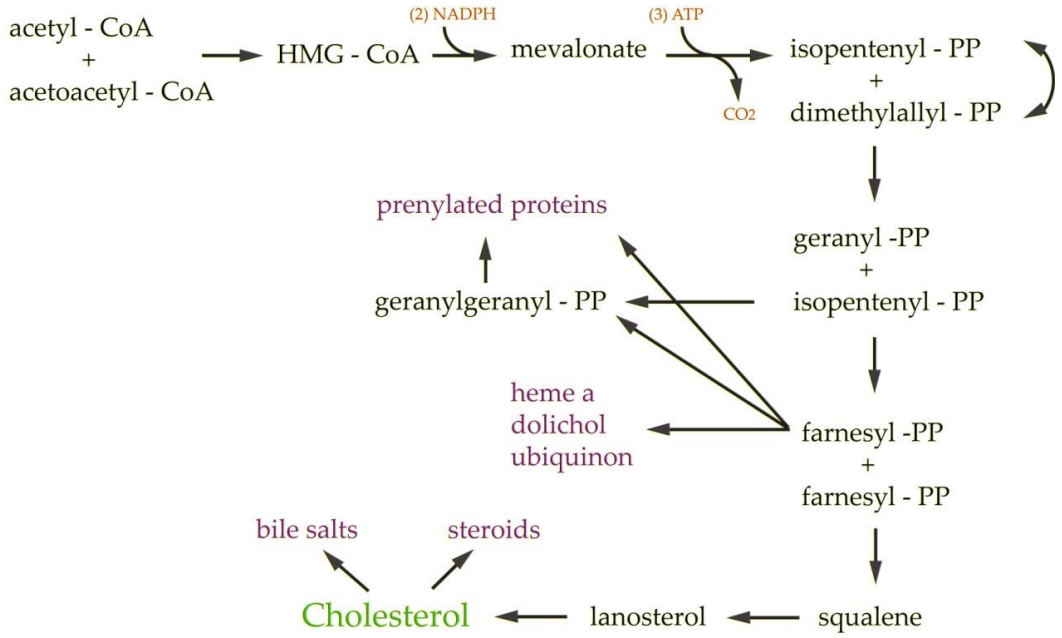

Figure 1.1 Biosynthesis of cholesterol via the mevalonate pathway. Adapted from King (2012)

HMG-CoA reductase inhibitor inhibits the enzyme hydroxymethylglutaryl coenzyme A (HMG-CoA) reductase (that catalyzes the reduction of HMG-CoA to mevalonate during the cholesterol pathway). Albert, *et al.* (1980) stated that the mechanism of enzyme inhibition was based on competitive binding between the HMG-CoA reductase and ß-hydroxyacid form of the statin. This statin has a higher affinity for the receptor than HMG-CoA reductase, so binds in preference preventing the enzyme producing mevalonate and therefore formation of cholesterol.

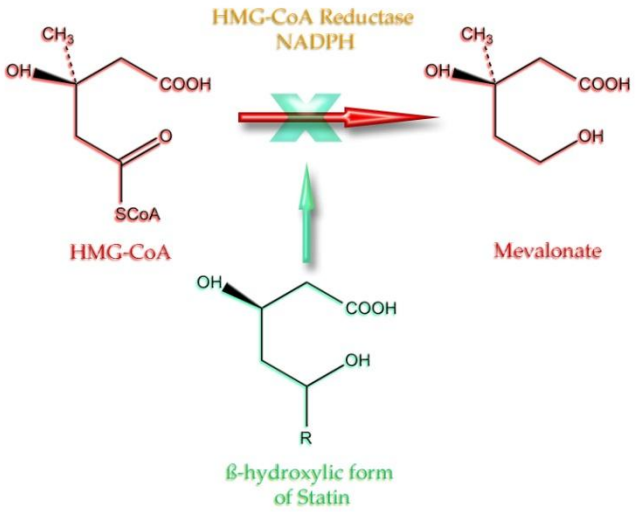

Figure 1.2 The inhibition mechanism of statin to HMG-CoA reductase. Adapted from Endo (2010)

Statin is composed of two important structures, a hexahydro-naphthalene system and a ß-hydroxylactone; their differences are due to side chains (R_1) and methyl groups (R_2) around the ring as shown in Figure 1.3. Natural statins such as lovastatin (or mevinolin, monacolin K, and Mevacor, Merck) contain a methylbutyric side chain (R_1) and a 6-α methyl group (R_2), which is lacking in mevastatin (or compactin, ML-236B, and CS-500). While Pravastatin (or eptastatin and Pravachol, Bristol-Myers Squibb/Sankyo), which has the same C6-hydroxy analogue as mevastatin, has the β-hydroxylactone in the 6-hydroxy sodium salt form instead of methyl groups. In addition, Simvastatin (or Synvinolin and Zocor, Merck) contains an additional methyl group at the C2 position of the side chain.

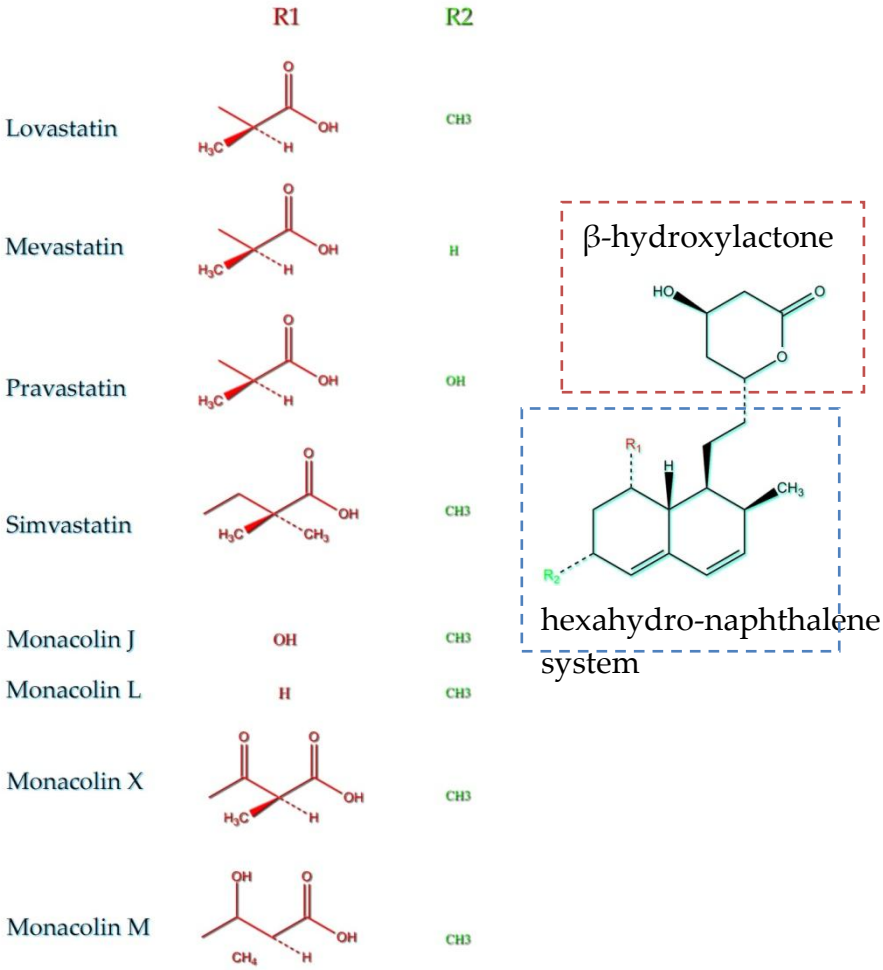

Figure 1.3 Comparison of the differences between the structures of the two side chains (R_1 and R_2) of natural compounds in the statin group. Adapted from Manzoni and Rollini (2002)

The structure of the C8 side chain of lovastatin- or mevastatin-related metabolites such as monacolins X and M have a slightly different composition, and monacolins J and L lack the lovastatin methylbutyric side chain. In monacolin J a hydroxyl group is present at the C8 position, while it is substituted by a hydrogen in monacolin L and dihydromonacolin L (Figure 1.3) (Endo *et al.* 1985; Juzlová *et al.* 1996; Kimura *et al.* 1990; Komagata *et al.* 1989).

As illustrated in Figure 1.4, the structures of the synthetic statins atorvastatin (Lipitor, Parke-Davis), fluvastatin (Lescol, Novartis), and cerivastatin (Baycol and Lipobay, Bayer) are dissimilar from the natural statins. Only the HMG CoA-like structure, which are in hydroxyl acid form, responsible for HMG-CoA reductase inhibition, is similar in both natural and synthetic statins.

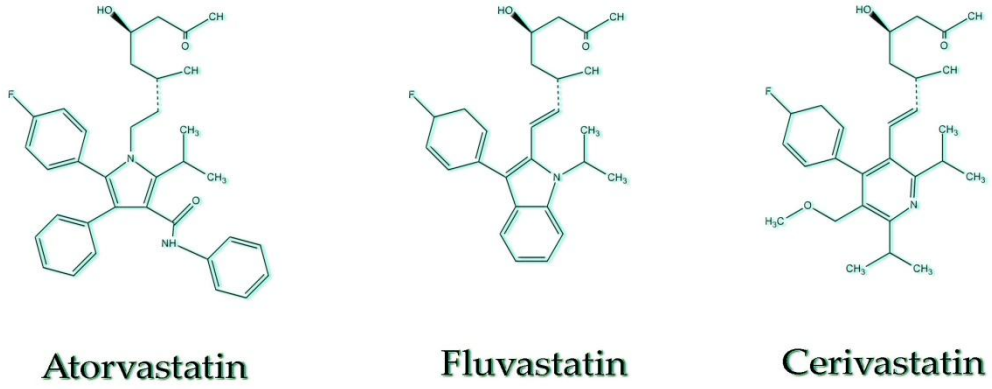

Figure 1.4 Structure of synthetic commercial statins. Adapted from Manzoni and Rollini (2002)

The discovery of the first statin was based on the study of Endo in 1976 who received the Lasker-DeBaker Award for Clinical Medical Research. He screened 6000 fungal extracts for inhibitors of cholesterol biosynthesis in rat and he found two inhibitory compounds (ML-236A and B), which are derived from *P. citrinum* isolated from infected Japanese orange. Lovastatin from Merck was the first HMG-CoA inhibitors to get a permit from the US Food and Drug Administration (FDA) to be tested in clinical trials in 1987 (Brown and Goldstein, 2004). Nowadays commercially natural lovastatin is produced by a variety of filamentous fungi including *Penicillium* species, *Monascus ruber* and *Aspergillus terreus* as a secondary metabolite. Most commercial production is based on *A. terreus* batch fermentation and most of

the literature is focuses on this species (Seenivasan *et al.*, 2008). In 2010, Jaivel isolated and screened lovastatin producing microorganisms from soil and other sources, and found ten fungal cultures which produce lovastatin. Based on the quantification of lovastatin production, *A. terreus* strains JPM1, JPM2, JPM3 and MTCC479 have recorded maximum lovastatin yields, but JPM3 has reported the highest yield of lovastatin followed by JPM1, MTCC479 and JPM2.

1.2.2 Biosynthesis pathway of Lovastatin

Lovastatin is a secondary metabolite which is classified as a polyketides, and is always produced by fungi via the Polyketides synthase pathway. Polyketide synthases, also known as PKSs, are a family of enzymes or enzyme complexes which are divided into three groups including: Type I PKSs which are large, highly modular proteins, Type II PKSs which are aggregates of monofunctional proteins, and Type III PKSs which do not use in full acyl carrier protein (ACP) domains.

Fungal PKS systems fall into the first group, iterative type I PKSs as shown in Figure 1.5. Generally, type I PKSs are multifunctional enzymes organized into modules, each of which harbours a set of distinct domains responsible for the catalysis of one cycle of polyketide chain elongation. Prototypically, a type I PKS elongation module contains minimally three domains—an acyltransferase (AT), ACP and a beta-ketoacyl synthase (KS)—that select, activate, and catalyze a decarboxylative Claisen condensation between the extender unit and the growing polyketide chain, generating a β-KS-ACP intermediate. Optional domains are found between the AT and ACP domains, which carry out the variable set of reductive modifications of the b-keto group before the ensuing cycle of chain extension (Shen, 2003; Staunton

and Weissman, 2001). The pathway of lovastatin synthesis starting from acetyl-CoA and malonyl-CoA can be used by PKSs to assemble the carbon chain with C-methylation, and relatively few of the oxygen functions are retained in the final product. A Diels–Alder reaction accounts for formation of the decalin system at the hexaketide intermediate stage. Unusually, though the PKS carries an enoyl reductase (ER) domain, this function is not activated unless an accessory protein LovC is also present. The product of lovastatin nonaketide synthase is the lactone dihydromonacolin L. Monocolin J is then produced by a synthetic pathway of post-PKS modifications detailed in Figure 1.5. The ester side-chain is produced by a non-iterative type I PKS, lovastatin diketide synthase, which also carries a C-methyltransferase domain. It carries no thioesterase (TE) domain, and the fatty acyl chain appears to be delivered directly from the PKS protein in conjunction with the esterifying enzyme to obtain the final product; lovastatin.

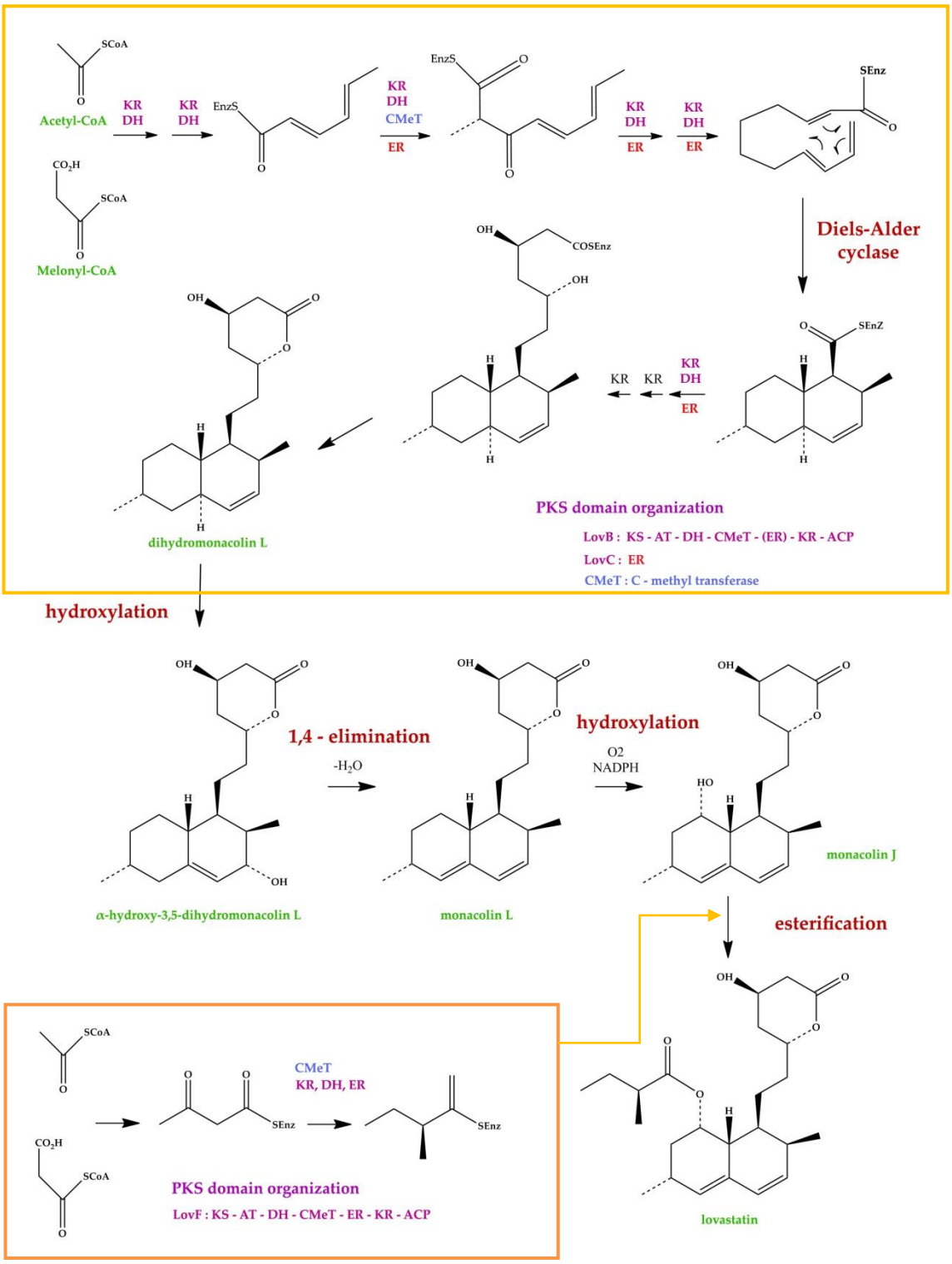

Figure 1.5 Lovastatin biosynthesis pathways. Adapted from Kennedy et al. (1999).

1.3 Analytical methods for extraction and identification of natural product

The extraction of natural products normally depends on the nature of the source material, the target compounds, and the level of required purity (Saker, 2005). If the source of the material is a plant, immediate extract or storage in a freezer to prevent any changes in the profile of metabolites is recommended (Schliemann *et al*., 2001). Whereas if the sources are microbes; clarified the extracted part, microbial cells or liquid medium, should do prior to extraction (Saker, 2005). Hydrophobicity or hydrophilicity properties of the target compounds are also depends on the choice of the solvents. The method to indicate the polarity of the extract as well as the target compounds present in the extract can be determined by drying and redissolving in various solvents covering a range of polarities such as water, methanol, acetonitrile, ethyacetate, chloroform, petroleum ether, hexane (Seidel, 2005). High purity is required should structure elucidation experiments need to be done for further study.

For this project, liquid–liquid extractions following the Bligh and Dyer method (Bligh and Dyer, 1959) or Ebada method (Ebada, 2008) were used.

Two analytical techniques, LC-MS and NMR, were also used extensively.

Liquid chromatography–mass spectrometry (LC-MS, or alternatively HPLC-MS) is an analytical chemistry technique that combines the physical separation capabilities of liquid chromatography (or HPLC) with the mass analysis capabilities of mass spectrometry. LC-MS is a powerful technique, which has very high sensitivity and selectivity.

Chromatographic separations are based on forced transport of the liquid (mobile phase) carrying the analyte mixture through a porous media and the differences in the interactions of the analytes with the surface of this porous media results in different migration times for a mixture of components. High surface area of the interface between mobile and stationary phases is essential for space discrimination of different components in the mixture (Robinson *et al.*, 2005).

Liquid chromatography can be further classified according to the type of interactions of the analyte with the stationary phase surface and according to the relative polarity of the stationary and mobile phases. There are classified into 4 types including, normal-phase (NP), reverse-phase (RP), ion-exchange (IEX) and size-exclusion chromatography (SEC) (Robinson *et al.*, 2005).

For normal-phase HPLC (NP-HPLC), which is the first type of column available for HPLC using polar stationary phases and non-polar mobile phases, analyte molecules compete with the mobile-phase molecules for the adsorption sites on the surface of the stationary phase. The separation depends on the interaction of polar functional groups of the analyte molecule with polar groups on the surface of the packing. Analytes elute from the column starting with the least polar compound followed by other compounds in order of their increasing polarity. Packing materials for stationary phase commonly use porous oxides such as silica (SiO_2) or alumina (Al_2O_3). Mobile phases in normal-phase HPLC are based on nonpolar solvents (for instance hexane and heptane) with the small addition of a polar modifier (for instance, methanol, ethanol, isopropanol, ethyl acetate or chloroform). The mobile phase is generally a binary mixture of

water and a miscible polar organic solvent like methanol, acetonitrile or tetrahydrofuran.

Reverse-phase HPLC (RP-HPLC) acts opposite to normal-phase HPLC; the polarities of mobile and stationary phases are reversed. The surface of the stationary phase in RP-HPLC is hydrophobic and the mobile phase is polar, where mainly water-based solutions are employed. The advantages of RP-HPLC are the ability to discriminate very closely related compounds and the ease of variation of retention and selectivity due to the dispersive forces employed in this separation mode being the weakest intermolecular forces (hydrophobic or van der Waals interactions). This makes the overall background interaction energy in the chromatographic system very low compared to other separation techniques. This low background energy allows for distinguishing very small differences in molecular interactions of closely related analytes. The packing materials used in RP-HPLC are chemically modified porous silica binding with various sizes of the modifier, specific surface area of the adsorbent, and the bonding density. The first of the bonded-phase columns, the octyldecyl–or C18–silica column, has octyldecyl side chains linked to the silica support by Si–O–Si links. These reverse-phase columns with bonded organic phases can be run in less expensive aqueous solvents that are easier to dispose of and less hazardous to use. Another common type of bonded-phase column is the octyl–silica column which has C8 side chains attached to silica through Si–O–Si linkages. The shorter chains allow nonpolar components of the mobile phase to approach closer to the polar support, and they are not as tightly held as they are on a C18–silica column. It takes less nonpolar solvent in the mobile phase to elute nonpolar components off the column in the same time. The mobile phases normally used are water, acetronitrile, methanol, acetone, ethanol,

tetrahydrofuran, and ethylene glycol. DMSO has been used for minor selectivity adjustment; due to high backpressure limitations and/or high background UV absorbance (Robinson *et al.*, 2005).

Another type of liquid chromatography is IEX. The separation of analytes is based on the different affinities of the analyte ions for the oppositely charged ionic centers in the resin or adsorbed counterions in the hydrophobic stationary phase. Analyte retention and selectivity in IEX are strongly dependent on the pH and ionic strength of the mobile phase based on the exclusion of the molecules from the porous space of packing material due to steric hindrance. The hydrodynamic radius of the analyte molecule is the main factor determining its retention. The higher the molecular weight of the molecule, the greater its hydrodynamic radius, which results in faster elution. At the same time, if an analyte molecule interacts (undesired) with the stationary phase, this increase the retention of larger molecules, may confound separation of molecules based solely on their hydrodynamic radius (Robinson *et al.*, 2005).

Mass spectrometry (MS) is a powerful and effective analytical technique in drug discovery and development. This technique is usually used to measure the mass-to-charge ratio of charged particles, determine the elemental composition of a sample or molecule, and elucidate the chemical structures of molecules, such as peptides and other chemical compounds. The MS principle consists of four steps: (1) introduction of the sample; (2) ionisation of the sample molecule to convert the neutral molecules to ions in the gas phase (ionisation method); (3) sorting of the resulting gas-phase ions by mass-to-charge ratios (mass analyser); and (4) detection of the separated ions.

The ideal characteristic of the ion source is providing high ionisation efficiency and a high stability of ions for subsequent mass analysis by mass analyzers. It is advantageous to measure the quantity of a compound using an MS instrument together with chromatographic separation techniques, especially HPLC. There are many ionisation methods that have been invented such as electron impact (EI), chemical ionisation (CI), desorption ionisation (DI), matrix-assisted laser desorption/ionisation (MALDI), desorption electrospray ionisation (DESI), electrospray ionisation (ESI), and atmospheric pressure chemical ionisation (APCI). Kazakevich (2007) summarized the advantages characteristic of each ion source as shown in Table 1.1.

Table 1.1 Comparison of the advantages and disadvantages of different ionisation methods. Adapted from (Robinson *et al.*, 2005).

Ionisation Methods	Ionisation Agents	Strengths	Limitations
EI	Electrons (70eV)	Extensive fragmentation, reproducible spectra, searchable large reference compound EI libraries	Limited to volatile/nonpolar molecules
CI	Gaseous ions	Abundant molecular ions with controllable fragmentation	Limited to nonpolar and moderately polar molecules, limited fragmentation
APCI	Corona discharge/ gaseous ions	Operative at atmospheric pressure, easy interface to HPLC, abundant molecular ions	Limited to low to moderately polar molecules
DI	Energetic particles (atoms, ions), photons	Abundant molecular ions from high mass compounds	Difficult to interface to HPLC
ESI	Electrical/thermal/ pneumatic energy	Operative at atmospheric pressure, easy interface to HPLC, multiple-charged ions for large biomolecules	Poor results for nonpolar molecules, limited fragmentation

Improvements in databases have also reduced the time for dereplication. For example, AntiMarin and MarinLit have the option using a variety of parameters including functional groups to search a compound represented in the sample. Since heteronuclear single quantum coherence (HSQC) and heteronuclear multiple bond correlation (HMBC) data can be acquired rapidly in NMR, many functional groups can be easily identified and used as parameters in database searches and can greatly enhances

dereplication. Although still in its infancy, the ability to create searchable tandem mass spectrometry (MS/MS) fragment libraries provides the first potential avenue for automated dereplication, accurate MS/MS data can help find a unique elemental composition m/z 52–54 of the parent ion. The unique elemental composition can be assigned to small fragments. Use of MS/MS for metabolite identification and structural characterisation can help with the otherwise time-consuming task of data interpretation (Robinson *et al.*, 2005).

One of the most important features in ESI is the formation of multiple charged ions for proteins/peptides In addition; the detection of multiple charged ions provides precise measurements of molecular weights of proteins/peptides via the deconvolution method. A mass accuracy of better than 0.01% can be achieved for proteins with masses up to 100kDa. Another important characteristic of ESI is the softness of the ionisation. It is a very mild process that generates mainly molecular ions with little fragmentation. For small molecules, the singly charged molecular ions usually dominate the mass spectrum. The third characteristic of ESI is the simplicity of the source design and its operation at atmospheric pressure, allowing ESI to be readily coupled to HPLC. It is important to note that a low flow rate (~200μL/min) of the sample solution is required in order to maintain a stable spray in ESI. Thus, flow splitters are often utilized in ESI-LC/MS applications. This does not reduce the concentration sensitivity of ESI since ESI responses are directly related to the concentration of the analyte entering the ion source. However, the mass sensitivity can be substantially increased with a lower flow rate if the same concentration sensitivity is maintained. This has led to the wide use of nano-spray (~nL/min) LC/MS for analysis of proteins and peptides, achieving femtomolar sensitivity.

1.5.2 NMR

NMR is a spectroscopic technique that relies on the magnetic properties of the atomic nucleus. When placed in a strong magnetic field, certain nuclei resonate at a characteristic frequency in the radio frequency range of the electromagnetic spectrum. The variation of resonant frequency will give information to predict the molecular structure in which the atom resides (Neil, 2007).

The first application of proton NMR for metabolism studies occurred in early 1977. Brown *et al.* (1997) studied a suspension of red blood cells using proton NMR and found the signals of lactate, pyruvate, alanine and creatine compounds. Nowadays, NMR is used in various studies in physics, chemistry and biology, to determine the structure and function of macromolecules, study metabolism, and to obtain in vivo images of anatomical structures and functional (physiological) states (Lindon *et al*., 2007).

The NMR theory

Five atoms that have the most important role in NMR experiments are ^{1}H, ^{13}C, ^{31}P, ^{15}N and ^{19}F. ^{1}H has a high sensitivity and vast occurrence in organic compounds, while ^{13}C is found to be a key component of all organic compounds despite occurring at a low abundance (1.1%) when compared to the major isotope of carbon ^{12}C, which has a spin of 0 and therefore is NMR inactive. ^{13}C and ^{31}P often occurs in organic compounds and has moderate relative sensitivity. In addition, ^{15}N is a major component of important biomolecules such as proteins and DNA of organisms and microorganisms. Lastly, ^{19}F has a high relative sensitivity.

Neil (2007) stated that many atoms, including all atoms that have been mentioned before behave as if the positively charged nucleus was spinning on an axis; creating a tiny magnetic field. When placed in a strong external magnetic field, the magnetic nucleus tries to align with it like a compass needle in the earth's magnetic field. As the nucleus is spinning and has angular momentum, the torque exerted by the external field results in a circular motion called precession, similar to a spinning top in the earth's gravitational field.

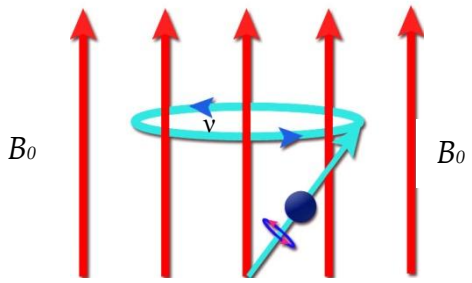

Figure 1.6 Spinning characteristic of an atom in a magnetic field. Adapted from Neil (2007).

The rate of this precession is proportional to the external magnetic field strength and to the strength of the nuclear magnet shown as the equation:

$$\nu_0 = \gamma B_0 / 2\pi$$

where ν_0 is the precession rate (the "Larmor frequency") in Hertz,

γ is the strength of the nuclear magnet (the "magnetogyric ratio")

B_0 is the strength of the external magnetic field.

When an atom is placed in a magnetic field, there are two quantum states, which are called "spin ½". As shown in Figure 1.8, an atom has the spin axis pointing "up" or "down". In the absence of an external magnetic field, these two states have the same energy and are in thermal equilibrium. Exactly one half of a large population of nuclei will be in the "up" state and the other half will be in the "down" state. In a magnetic field, however, the "up" state, which is aligned with the magnetic field, is lower in energy than the "down" state, which is opposed to the magnetic field. As this is a quantum phenomenon, there are no possible states in between. This energy separation or "gap" between the two quantum states is proportional to the strength of the external magnetic field, and increases as the field strength is increased. In a large population of nuclei in thermal equilibrium, slightly more than half will reside in the "up" (lower energy) state and slightly less than half will reside in the "down" (higher energy) state. As in all forms of spectroscopy, it is possible for a nucleus in the lower energy state to absorb a photon of electromagnetic energy and be promoted to the higher energy state (Neil, 2007).

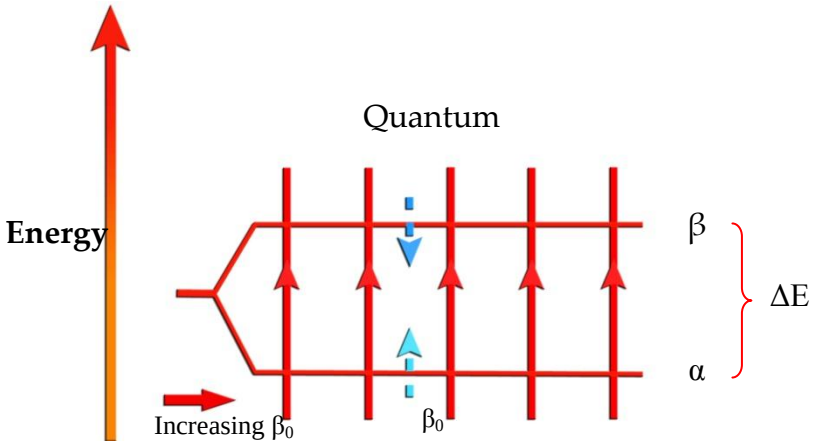

Figure 1.7 A change of quantum state of an atom placed in a magnetic field. Adapted from Neil (2007)

The energy of the photon must exactly match the energy "gap" (ΔE) between the two states, and this energy corresponds to a specific frequency of electromagnetic radiation according to the equation:

$$\Delta E = h\nu_0 = h\gamma B_0/2\pi$$

where h is Planck's constant. The resonant frequency, νo, is in the radio frequency range, identical to the precession frequency (the Larmor frequency).

The other characteristic of the atom which varies slightly depending on the position of that atom within a molecule (the "chemical environment") also provides detailed information about the structure of molecules called ' the chemical shift' measured in parts per million (ppm). It occurs because the bonding electrons create their own small magnetic field that modifies the external magnetic field in the vicinity of the nucleus. Different atoms within a molecule can be identified by their chemical shift, based on molecular symmetry and the predictable effects of nearby electronegative atoms and unsaturated groups as shown in a Figures 1.8 and 1.9.

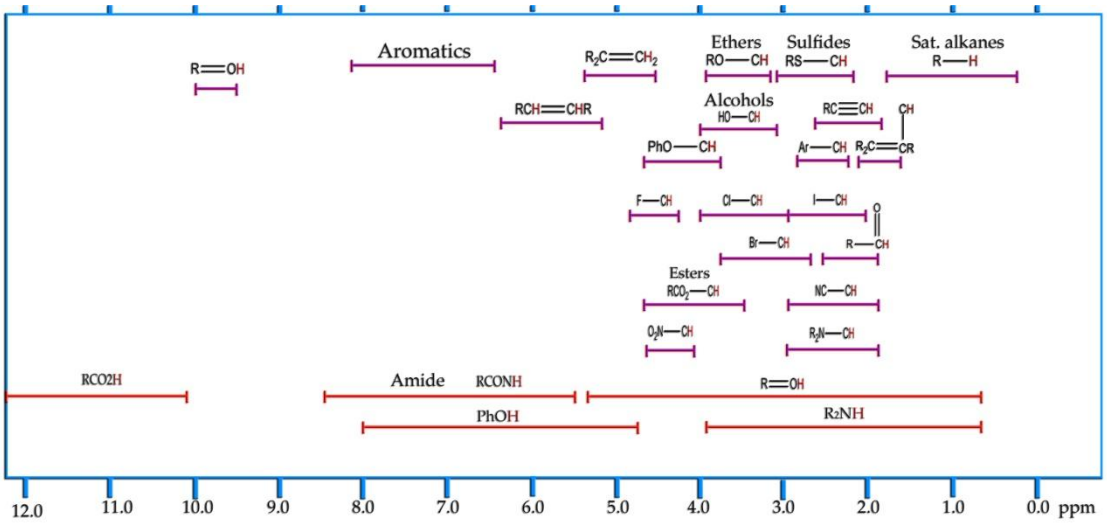

Figure 1.8 Proton chemical shift ranges. Adapted from Organic chemistry Michigan State University website. (http://www.cem.msu.edu/~reusch/OrgPage/nmr.htm). For samples in $CDCl_3$ solution, the δ scale is relative to TMS at δ = 0.

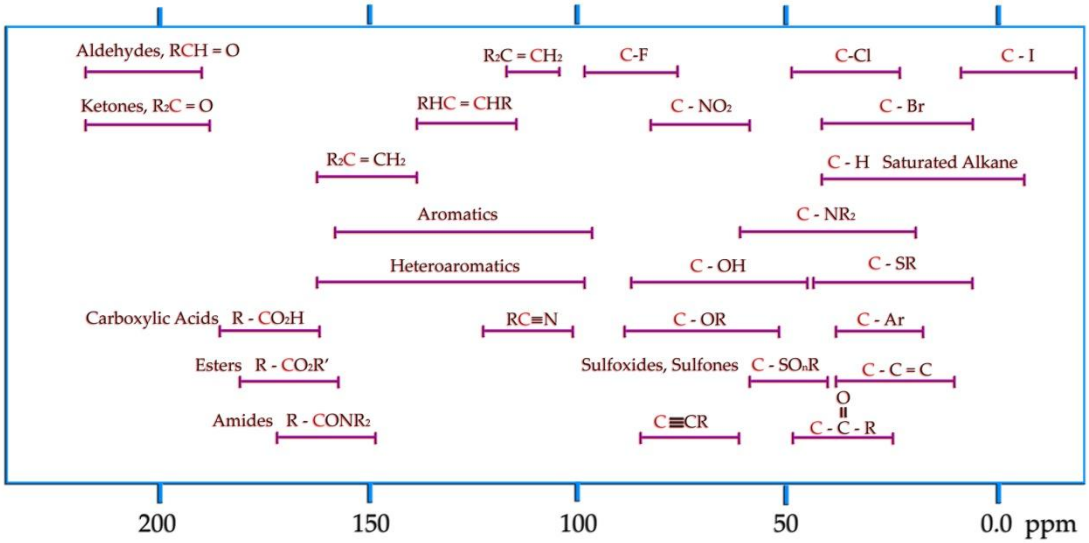

Figure 1.9 ^{13}C chemical shift ranges. Adapted from Organic chemistry Michigan State University website (http://www.cem.msu.edu/~reusch/OrgPage/nmr.htm). For samples in $CDCl_3$ solution, the δ scale is relative to TMS at δ = 0.

The other phenomenon called 'spin–spin splitting' also characterises the structure of a molecule. Consider two protons ($_1H_aC–C_1H_b$) with different chemical shifts on two adjacent carbon atoms in an organic molecule. The magnetic nucleus of H_b can be either aligned with ("up") or against ("down") the magnetic field of the spectrometer as shown in Figure 1.10. From the point of view of H_a, the H_b nucleus magnetic field perturbs the external magnetic field, adding a slight amount to it or subtracting a slight amount from it, depending on the orientation of the H_b nucleus ("up" or "down"). Since roughly 50% of the H_b nuclei are in the "up" state and roughly 50% are in the "down" state, the H_a resonance is "split" by H_b into a pair of resonance peaks of equal intensity (a "doublet") with a separation of J Hz, where J is called the coupling constant measured in Hertz. The relationship is mutual so that H_b experiences the same splitting effect (separation of J Hz) from H_a. This effect is transmitted through bonds and operates only when the two nuclei are very close (three bonds or less) in the bonding network (Neil, 2007).

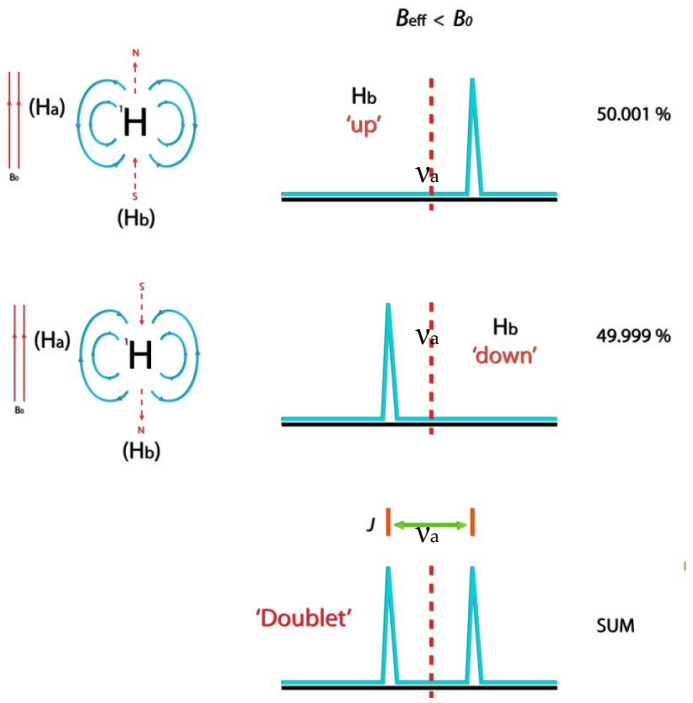

Figure 1.10 A diagram of a 'spin–spin splitting' phenomenon of atom. Adapted from Neil (2007)

If there are larger numbers of neighbouring spins leading to the general case of n neighbouring spins, which split the H_a resonance peak into $n+1$ peaks with an intensity ratio determined by *Pascal's triangle* as show in Figure 1.11.

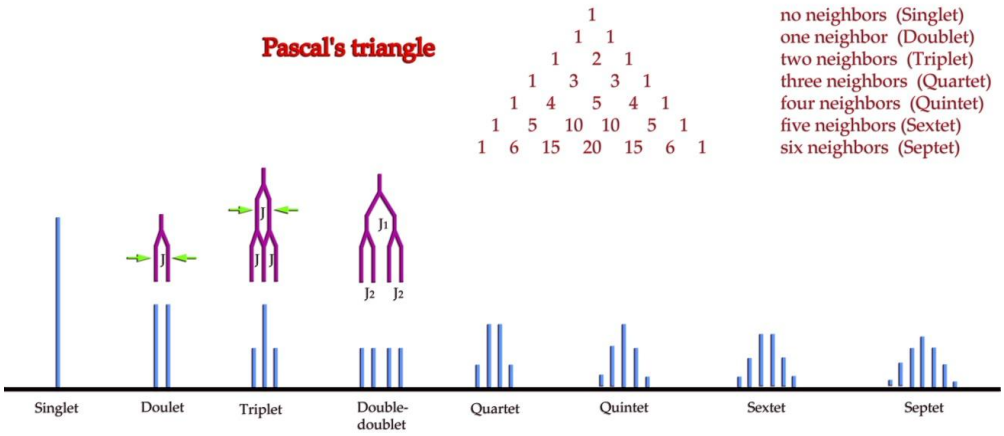

Figure 1.11 A characteristic of a peak of an atom determined following Pascal's triangle rule. Adapted from Neil (2007)

1.4 Scale-up strategies for Bioreactors

Scale-up of a fermentation process from small to large scale usually involves a series of steps and is associated with a great deal of empiricism. It is critically important to develop a protocol for scale-up which maintains the productivity of the desired compound during this process. In general, scale-up in fermentation systems is based on four empirical criteria, such as constant power input per unit volume, constant mixing time, a constant mass transfer coefficient, and constant impeller tip velocity. Burke (2008) critically compared the advantages and disadvantages of each as shown in Table 1.2. Constant impeller tip velocity method is a widely used criterion for scale-up of filamentous microorganisms and the focus here is to seek to achieve a constant shear in the fermenters as the process is scaled up. In filamentous fermentation broths, shear is increased by changing agitator geometry, the inclusion of baffles and by increasing agitation speed (Burke, 2008).

Table 1.2 Scale-up strategies for fermentation process.

Scale-up method	Primary Reference	Engineering correlation	Benefits	Disadvantages
Constant power consumption/	Cooper *et al.*(1944)	Constant K_La directly proportional to gassed power consumption/unit volume	Relatively straightforward correlation, easy to scale factor.	Shear increases with scale increase.
Constant mixing time	Norwood and Metzner (1960)	$N_2 = N_1(D_2/D_1)^{1/4}$ Where N = impeller tip speed D = impeller diameter	Time required for a liquid droplet to be completely and uniformly dispersed in the bulk fluid in an agitated vessel, constant across scales; the mixing should be at the molecular level. Particularly useful for low shear systems with rapid reaction kinetics, often where microbial growth is of secondary importance.	If this scale up method is used, power consumption/unit volume will increase significantly with scale. It is therefore not advisable to use this route unless necessary for mixing-specific issues.
Constant volumetric transfer coefficient	Aiba *et al.* (1973)	Constant K_La used for bubble aeration, i.e. non mechanically agitated systems	Can be useful for nonstandard agitation systems e.g. draught tube or bubble columns. Once optimal aeration efficiency has been demonstrated at small scale, conditions are then found by experiment on the large scale to support the same aeration efficiency. Equations are complex, involving estimations of bubble diameter.	Need a method for monitoring K_La; sulfite oxidation, gassing out or exhaust gas oxygen balance are typical. Difficult with live fermentations.
Constant impeller tip speed	Steel and Maxon (1962)	$N_2 = N_1(V_1/V_2)^{1/3}$ Where N = impeller tip speed D = impeller diameter V = liquid volume	As the maximum shear experienced by the medium is at the tip, then it has been found advantageous for organisms susceptible to shear or mechanical damage, e.g. protozoa or shear-responsive filamentous organisms.	Power consumption/unit volume will decrease.

Adapted from Burke (2008)

1.5 Aims

Trichoderma pseudokoningii, AQP 4097 is a newly isolated fungus, which has not been studied previously. It was kindly supplied by Aquapharm Biodiscovery Ltd (Oban, UK). The isolate was isolated from sea water and maintained on PDA plus Instant Ocean (IO, synthetic sea salt (a detail of IO components are listed in Appendix III)) 33 g/L. In terms of its appearance on such media, the mycelium, initially cream-coloured, gradually turned to greenish, and yellowish colour on sporulation (Figure 1.12).

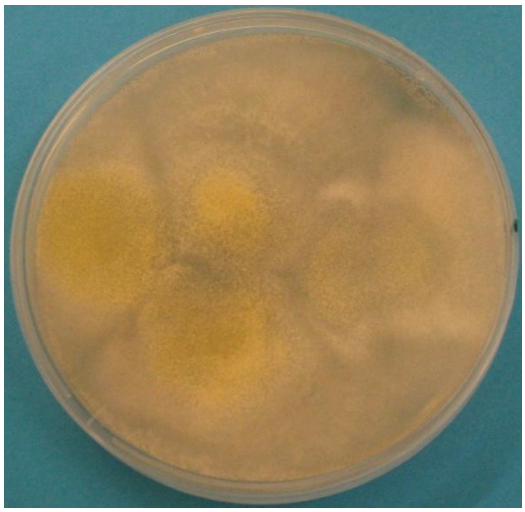

Figure 1.12 Colonies of *Trichoderma pseudokoningii* isolate AQP 4097 cultured on PDA plus 33 g/L IO.

According to Aquapharm Biodiscovery Ltd. their interest arose because of their capability of producing two unsaturated fatty acids; oleic acid (47.69%, w/v) and gamma-linolenic acid (2.76%, w/v). Therefore the objective of this project was to investigate environmental factors affecting growth and production of elucidated bio-actives from this fungus on a lab scale, followed by establishing optimum cultivation and production processes of the

bioproducts in small scale bioreactors (1-2 litres working volume), and finally to examine transfer of production to larger scale fermenter systems (14L or greater volume).

Chapter 2 Materials and Methods

2. Material and Methods

2.1 Microorganisms

Marine microorganism, fungus strain AQP 4097, was isolated from seawater and provided by Aquapharm® Biodiscovery Limited, Oban, UK. This strain is routinely grown on PDA (Oxoid, Basingstoke, UK) prepared with 33 g/L IO (Aquarium Systems, Cedex, France).

2.1.1 Strain preservation

Microorganisms were preserved by two different methods; freezing at -80 degrees Celsius and lyophilisation (Nakasone *et al*., 2004).

Freezing at -80 degrees Celsius, was carried out by culturing the fungus on PDA plus IO for 7 days. The spores were washed with sterile water, and then 500 µl of spore suspension was transferred to a cryotube containing 500 µl of sterile 30% (v/v) glycerol in water. The suspension was mixed well and kept in a CryoBox at – 80 degrees Celsius.

Lyophilisation was performed similarly by culturing the fungus on PDA plus IO for 7 days. After that the spores were washed with 1.5-2.0-ml sterile 10% (v/v) solution of non-fat dry milk powder in water before transferring to sterilised and labelled lyophilisation tubes, approximately 200 µl each. The tubes were placed at -80 degrees Celsius overnight before placing in a lyophilisation machine. When the spore suspension was totally dry, the lyophilisation tubes were stored in plastic boxes at room temperature (25 degrees Celsius).

2.1.2 Inoculum Preparation

The inoculum for the whole project was prepared using the same procedure. The spores from a 7 days old mature culture plate were washed with sterile distilled water and transferred into 200 ml medium in 500-ml Erlenmeyer flasks. The final concentration of spores was around 10^5 spores/ml. The inoculum shake flasks were incubated at 28 degrees Celsius and 220 rpm in a rotary shaker incubator for 48 hours before inoculation. Shake flask experiments were inoculated with 20 ml of inoculum in 180 ml of medium, while for the small bioreactor, BiostatQ experiments, 75 ml of inoculum was added to inoculate with 675 ml of medium. In the scale up experiment with a Bioflo 110, the inoculums was prepared in 5L Erlenmeyer flasks containing 1L of medium, with 1L of inoculums used to inoculate 9L of fermentation medium (section 2.2.3.3).

2.2 Media composition and growth condition

PDA medium, Yeast extract, and Czapex-Dox medium were purchased from Oxoid, Basingstoke, UK. Malt extract and Bacto-peptone were purchased from Merck Chemicals Ltd., Nottingham, UK. PDB medium, glucose and dextrose were purchased from Sigma-Aldrich, Dorset, UK. Instant Ocean (Aquarium Systems, Cedex, France) was obtained from Aquapharm Biodiscovery Limited.

2.2.1 Plate culture and growth condition

2.2.1.1 Effect of salinity and light on sporulation of AQP4097

The effect of salinity on growth and sporulation of the fungus was carried out by culturing this strain in triplicate on PDA and PDA plus IO at 10, 20, and 33 g/L (the latter being the Aquapharm Biodiscovery Ltd. recommended

medium). Cultures on this media were divided into two sets to observe effects of light on sporulation; one set was incubated at room temperature under natural light (on a lab bench) and another set was also incubated at room temperature, but kept in the dark. Both sets were incubated for 7 days, and then the growth on the plate was observed by visual examination.

2.2.1.2 Metabolomic analysis of AQP 4097 cultured on PDA plates with Instant Ocean.

The effect of salinity on metabolomic production of the fungus was carried out by culturing this strain in triplicate on PDA without IO and PDA with IO 10, 20, and 33 g/L under natural light, and incubated for 7 days, followed by extraction and analysis using the methods as described in sections 2.6.3.1 and 2.6.4.1, respectively.

2.2.2 Shake flask culture and growth condition

2.2.2.1 Biomass production by AQP 4097 in shake flasks

In order to search for a suitable medium to scale up to fermenter production, four media were chosen comprising of Potato dextrose broth,PDB, (Potato Infusion from 200 g 4 g, Dextrose 20 g) plus Instant Ocean which was recommended by Aquapharm Biodiscovery Ltd, Malt yeast glucose peptone agar, MYGP, (malt extract 3 g/L, yeast extract 3 g/L, glucose 10 g/L, bacto-peptone 5 g/L), Czapex-Dox medium (sucrose 30.0 g, sodium nitrate 3.0 g, dipotassium phosphate 1.0 g, magnesium sulfate 0.5 g, potassium chloride 0.5 g, ferrous sulfate 0.01 g), and GY medium (glucose 10 g/L, yeast extract 5 g/L).

2.2.2.2 Effect of Carbon source on biomass and lovastatin derivative production

A shake flask experiment was performed as a preliminary experiment to compare the effect of carbon source on biomass and lovastatin derivative production by the fungus. The medium contained 30 g/L of three carbon sources including lactose, glycerol, and glucose (which was routinely used as the carbon source in previous experiments and by the industrial partner) and 5 g/L of yeast extract as a nitrogen source. The shake flasks were incubated at 26 degrees Celsius and 220 rpm in a rotary shaker incubator. Samples were collected for measuring biomass and for metabolite analysis every 24, 48, and 72 hours. Each carbon source was carried out in four sets of triplicate (including zero time).

2.2.3 Fermentation medium and growth condition

2.2.3.1 Effect of initial glucose concentration on biomass and lovastatin derivative production by AQP 4097

In order to examine the effects of initial glucose level upon growth and glucose consumption within batch fermentations in section 3.4 GY medium was used as a basal medium (according to the results from section 3.3) and glucose content was varied from 10, 20, up to 30 g/L. Temperature, pH, air flow rate were controlled at 26 degrees Celsius, 6.5, and 1 vvm respectively. The stirrer rate varied from 220 rpm to 900 rpm in order to control the level of Dissolved oxygen tension in the medium at 30 % of saturation. These conditions were chosen to promote biomass production by fungus. A 0.66L working volume Braun BiostatQ bioreactor (section 2.4.1) was operated in duplicate for each concentration of glucose examined.

2.2.3.2 Effect of salinity on biomass formation, gamma linoleneic acid and lovastatin derivative production in a bioreactor

Batch fermentations were established to observe the effect of salt on biomass and metabolite production by comparing GY medium plus two different concentrations of IO, 10 g/L and 20 g/L, GY medium without IO under dissolved oxygen tension (DOT)-controlled conditions at 30% of saturation, 26 degrees Celsius, 220-800 rpm, 1 vvm, pH 6.5 and initial glucose at 30 g/L. A 0.66L working volume fermentation was operated in duplicate in a BiostatQ bioreactor (section 2.4.1).

2.2.3.3 Process Scale-up: Effect of dissolved oxygen tension (DOT) control on biomass and lovastatin derivative production

Batch fermentations were established to study the aeration effect on growth, and lovastatin production by the fungus by comparing between controlled and uncontrolled dO_2 condition in GY medium with 30 g/L glucose, temperature 26 degrees Celsius, 80-350 rpm, 1 vvm, pH 6.5. A 10L working volume Bioflo110 bioreactor (Braun) was operated in duplicate (section 2.4.2)

2.2.3.4 Effect of carbon source on biomass and lovastatin derivative production

Batch fermentations were established to study the effect of carbon source on biomass and lovastatin derivative production using 30 g/L glycerol instead of glucose and 5 g/L of yeast extract as a nitrogen source under dO_2-controlled conditions at 30% of saturation, 26 degrees Celsius, 220-800 rpm, 1 vvm, pH 6.5. These conditions seemed suitable for biomass production of the fungus. A 0.66L working volume fermentation was operated in duplicate in a BiostatQ bioreactor (section 2.4.1).

2.3 Analytical Reagents and Kits

Gamma-linolenic acid standard was obtained from Acros Organic, Geel, Belgium and lovastatin standard was purchased from Merck Chemicals Ltd., Nottingham, UK.

Chloroform, methanol, acetronitrile, acetone, butanol were purchased from Merck Chemicals Ltd., Nottingham, UK.

YSI 2776 as a glucose-lactate standard and YSI 2357 System buffer were purchased from YSI Limited, Hampshire, UK. A glycerol measurement kit was purchased from RBiopharm Rhone Ltd., Glasgow, UK.

2.4 Bioreactors

Fermentation experiments were carried out in two different laboratory scale bioreactors. Multi-bioreactor system, Biostat Q (B. Braun Biotech International, Switzerland), was used in the initial step for optimising the culture conditions of the marine microorganism, and Bioflo 110 (B. Braun Biotech International, Switzerland) was used in the scale up step.

2.4.1 Biostat Q fermenter

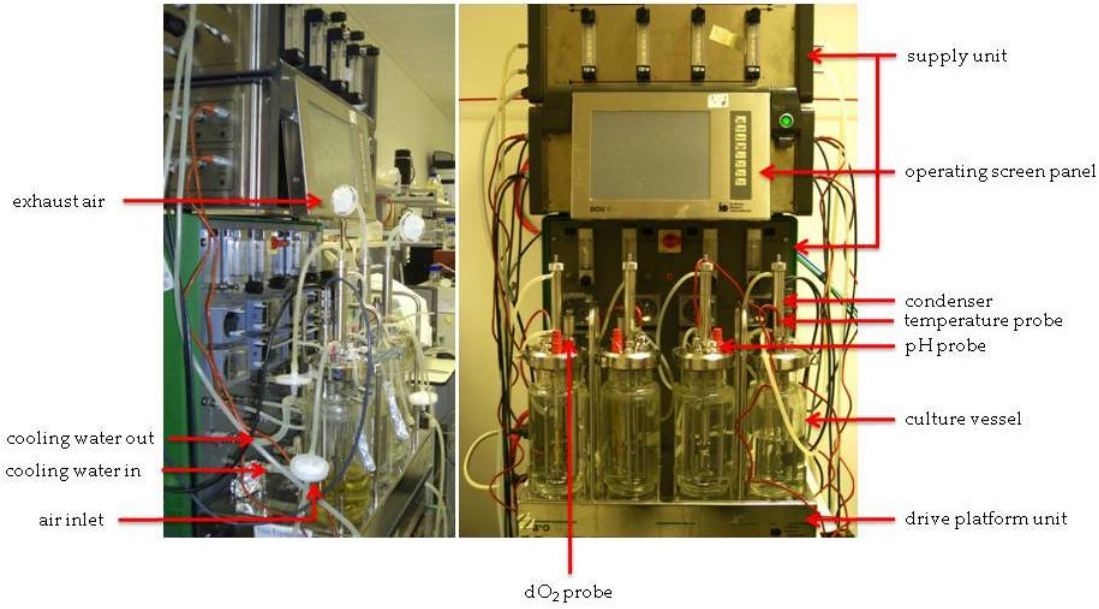

Figure 2.1 Operational configuration of Biostat Q during batch fermentation process.

Biostat Q is a multiple small volume fermenter designed for serial tests with measurement and control of important parameters in the reactor. It is an ideal tool for the investigation and optimisation of metabolism and productivity of microorganisms. In addition, it is also suitable for investigating the expression level of recombinant proteins by genetically modified microorganisms. Biostat Q consists of three basic elements including a compact supply unit, a drive platform unit with integrated magnetic stirrers and portable vessel holders, four-autoclavable culture vessels that have a 1L total volume (0.75L working volume) and a DCU3 digital instrument control system.

The supply unit contains an attached temperature control, gas supply and the addition agent pump. The culture temperature is controlled via a jacket

of the culture vessel, which is controlled by a thermostat unit heater and a circulation pump that supplies heated water (maximum temperature 60 degrees Celsius) allowing for separate control of each culture vessel. Aeration was controlled by four rotameters with a central pressure reducer installed in the supply unit. The flow rate was between 0.1 to 1L/min for each culture vessel connected. Exhaust humidity was minimised using an exhaust cooler at each of the culture vessels. The exhaust cooler supplied cooling water by extra cooling water connections at the supply unit.

Figure 2.2 Cooling unit use in cooling system control of the BiostatQ bioreactor.

The drive platform unit with integrated magnetic drive was separated from the supply unit for a flexible arrangement and to enable ease of transport. Brushless DC-motors and respective speed controller were used to control the speed of a magnetic stirrer from 50 to 1000 rpm. This unit is cable-connected to the supply unit. It has two transport trays for the culture vessels

together with two bottles of alkaline and acid solutions, which can be placed in autoclave.

The culture vessels are jacketed vessels made from borosilicate glass, which are resistant to thermal shock. The standard size of the vessel is 500 and 1000 ml total volume (330 ml and 750 ml working volume). A Rushton turbine-impeller is attached with a Teflon coated magnetic bar used as a stirrer. Stainless steel top plate includes three additional ports for acid, base agent and substrate supply, one rising pipe for sampling or connection of a bypass and one adapter for corrective agent supplies or the return of a bypass connection. The culture vessels are designed for measurement equipment including temperature sensor Pt 100, pH-electrode 12/120 mm (Mettler Toledo Ltd., Leicester, UK), pO2-electrode 12/120mm (Mettler Toledo Ltd., Leicester, UK), stainless steel sparger pipes with microporous frits of pore size 20 μm, air inlet sterile filter, and self-sealing membrane septum port.

The digital operating system DCU-3 was contained in a bench top cabinet, which was usually placed on top of the supply unit. The DCU-3 included the measurement amplifiers for parallel measurement of the process parameters controlled by an operating screen panel. The operating screen panel showed the main process including all important process data, calibration panel, control loops, displayed all controllers via bar chart, batch control, recipe setting up to 4 recipes, maintenance record, alarm monitoring, process record and password protection for all system critical parameters.

2.4.2 Bioflo 110

Bioflo 110 is a non-jacketed fermentation and cell culture vessel available to cover 0.4 through 14.0L. For temperature control, non-jacketed vessels use an external heating blanket and an internal cooling coil. The operator unit, the

primary control unit (PCU) served as the control center for all attached vessels and their associated loop controllers. A four-channel output to a strip-chart recorder is available from the PCU. It also provides power for liquid pumps and other control modules. The rotameter and cooling water valve are mounted on the outside of the power controller. Additional control modules and sensors enable expanding a basic temperature/agitation/ airflow fermentor to include control of pH, dO_2, antifoam addition, removal and addition of nutrients and other liquids, and blending inlet air with up to three other gases.

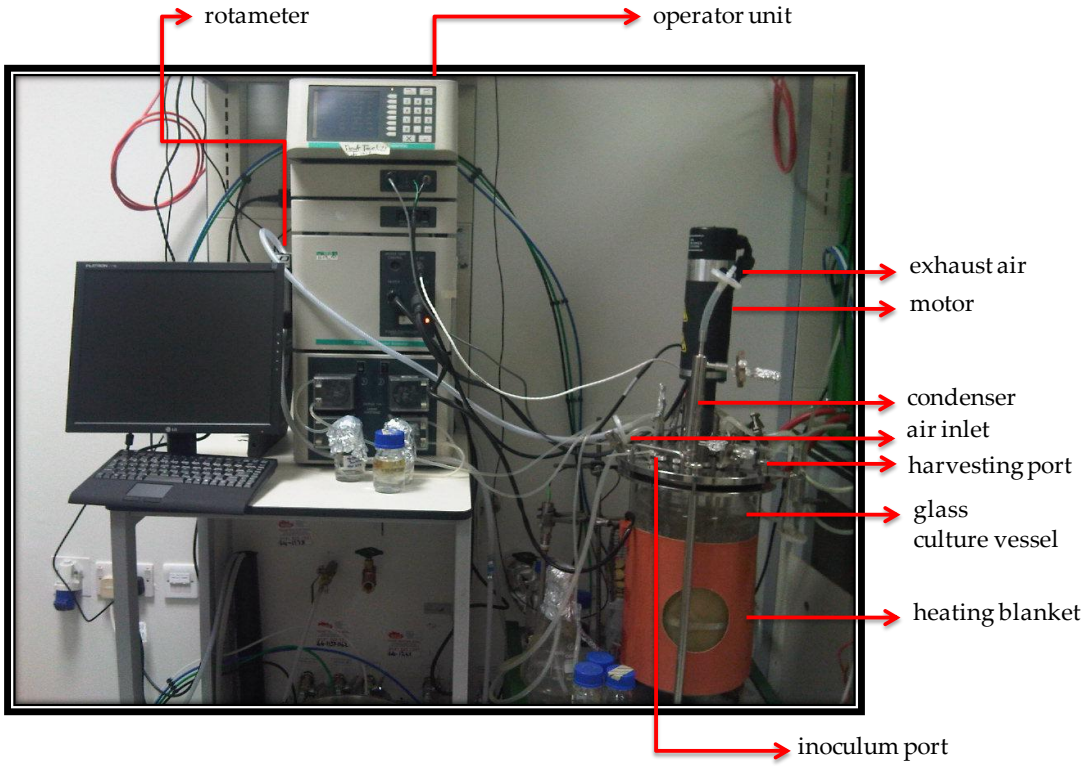

Figure 2.3 Operational configuration of a Bioflo 110 fermenter during batch fermentation process.

2.5 Analytical Equipment

2.5.1 YSI 2700 SELECT™ Biochemistry Analyzer

The YSI 2700 Analyzer (YSI Limited, Hampshire, UK) is a biochemistry analyser, which was used to analyse the concentration of D-glucose in this project using YSI 2776 as a glucose-lactate standard. The YSI is suitable for use in research, in food-processing and in bioprocessing applications. It can be set up to measure different analytes, for example, D-Glucose (Dextrose), L-Lactate, Sucrose, Lactose, Ethanol, L-Glutamate, Choline, L-Glutamine, Methanol, Galactose, and Hydrogen Peroxide. The advantages of the YSI on measurement process areis virtually unaffected by sample colour, turbidity, density, viscosity, pH, volatility, specific gravity, temperature, index of refraction, optical activity, or the presence of proteins and/or other biochemicals. In addition, the aspirated sample size can be adjusted from a minimum of 5 microliters to a maximum of 65 microliters.

2.5.2 Cell disruptor

The cell disruptor (Model 4000, Constant Systems Ltd., Warwick, UK) was used to disrupt the cells in metabolomic analysis. This cell disrupter has a mounted stainless steel disrupter head to avoid spoilage and allows loading of solid sample, cell paste, or suspended samples. The hydraulic operating system was performed at a pressure of 30 kpsi to disrupt the microorganism's cell structure. The homogeniser was washed twice using by distilled water between each sample to remove any remaining residue. Following the collection of the homogenised sample, the homogenate sample was collected; all samples would be then processed through the extraction protocol, and analysed by LC-MS. The remaining residues were also

eliminated by distilled water was passed twice through the homogeniser in each experiment between samples to remove any remaining residue.

2.5.3 Vacuum rotary evaporator

A Rotavapor® R-3 (BUCHI Labortechnik AG, Postfach, Switzerland) was used in this project in an extraction process to purify the metabolites and to elucidate the structure of the target compounds produced by the fungus in section 3.2. Rotavapor® R-3 is a modular rotary evaporator, which has more advanced features including digital heating bath, safety glass, and vapour duct with Combi-Clip (Clip for fixing the flask against loosening the flask during the rotation patented by BUCHI). Rotation speed can be adjusted from 20 to 280 rpm. A stainless steel heating bath can control temperature up to 95 degrees Celsius, but in this project, the temperature was set point at 50 degrees Celsius. The Rotavapor® R-3 can work with sample flask sizes from 50 ml to 4 L.

2.5.4 LTQ Obitrap

LTQ Obitrap was used to identify whole metabolomic compounds from extracted samples from fungus samples grown on PDA plates, shake-flask cultures, and submerge-fermentations. LTQ Obitrap is a type of liquid chromatography–mass spectrometry (LC-MS), which is based on the physical separation capabilities of liquid chromatography (or high-performance liquid chromatography, HPLC) combined with a specific mass-spectrophotometer (which has patented Orbitrap technology with the highly successful LTQ™ linear ion trap). LTQ Obitrap is widely used for metabolic compounds analysis because it helps to improve the detection process faster, more sensitive and more reliable than other analysis. It is also able to identify for complicated compound mixtures because of its advantages (faster, more

sensitive and more reliable detection) and can identify compounds in complex mixtures.

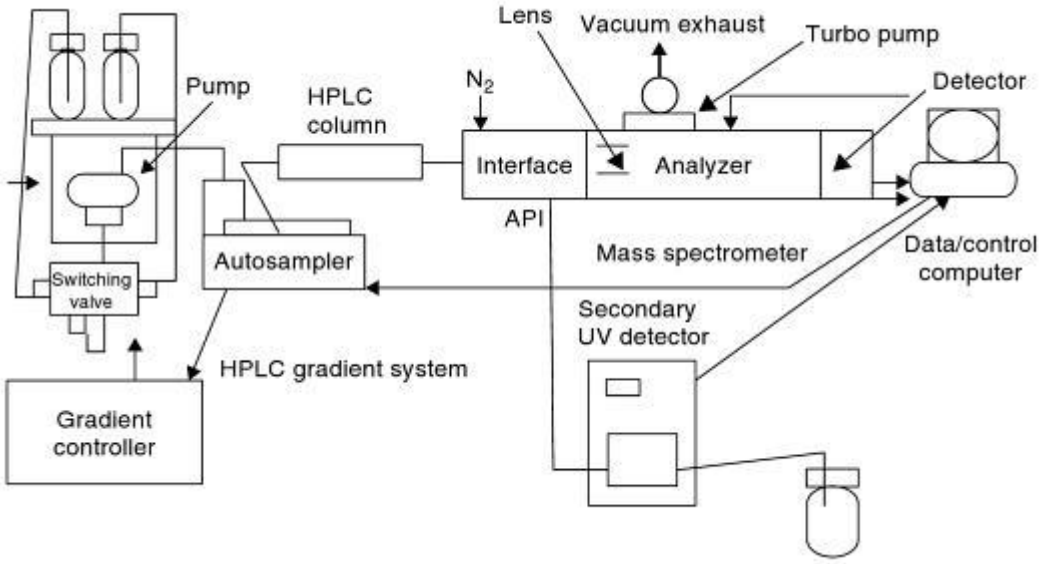

Figure 2.4 A basic system diagram of LC-MS. Adapted from McMaster (2005)

Ion source, ESI-MS, was performed on a Finnigan LCQ Deca mass spectrometer. HPLC analysis was carried out using an LTQ_Orbitrap_Discovery HPLC system (Thermo Fisher Scientific Inc., Waltham, MA). Detail of LC-MS experimentations were explained in section 2.6.4.1.

2.5.5 NMR

NMR is a spectroscopic technique that relies on the magnetic properties of the atomic nucleus used as a tool to elucidate the structure of a target compound. The variation of resonant frequency will give information to predict the molecular structure in which the atom resides (Neil, 2007). All

NMR experiments were carried out on a JEOL (JNM LA400) 400 MHz to identify the structure of purified compounds.

2.6 Analytical Methods

2.6.1 Biochemical assays

2.6.1.1 Dry cell weight measurement

The growth of fungus was assessed based on the biomass estimation of dry cell weight. After the sample was harvested from culture broth by filtration through a pre-weighed MF200 glass microfibre filter (particle retention size 1.6 um, Fisher Scientific, UK), cell dry weight was determined by washing the mycelium with distilled water twice, microwaving at defrost level for 20 minutes and allowing to dry overnight in a desiccator before weighing.

2.6.1.2 Glucose concentration

Glucose concentration was measured to observe the amount of D-glucose that the fungus consumed during batch fermentation. The measurement was determined by YSI 2700 SELECT™ Biochemistry Analyzer, which works as a direct reading of dextrose in solution through the enzyme sensor. The enzyme glucose oxidase is immobilised on a YSI Dextrose membrane. The detection range was from 0-9 g/L at 25-μL sample size, and from 0 - 25 g/L at 10 μL sample size. System buffer YSI 2357 and calibrator standard YSI 2776 were used in this measurement.

2.6.1.3 Glycerol concentration

Glycerol concentration was measured to observe the amount of D-glucose that the fungus consumed during the batch fermentation experiments using a commercial kit (RBiopharm Rhone Ltd., Glasgow, UK. ART number 10 148

270 035). For the glycerol measurement kit, 0.1 mL of harvested sample was mixed with the 3 kit solutions. To get a sufficient absorbance difference, suitable concentrations of sample were considered. The volume of water added must be reduced so as to obtain a suitable concentration. Following the reaction of glycerol, oxidized NADH was determined by UV-visible spectroscopy at wavelengths 334, 340 or 365 nm. The principle of glycerol reaction with the glycerol measurement kit in this study is shown below:

(1) Glycerol + ATP $\longrightarrow$ L-glycerol-3-phosphate + ADP

Glycerol is phosphorylated by adenosine-5′-triphosphate (ATP) to become an L-glycerol-3-phosphate in catalyzed reaction by glycerokinase (GK)

(2) ADP + PEP $\longrightarrow$ ATP + pyruvate

The Adenosine -5′-diphosphate (ADP) from step (1) is reconverted into ATP by phophoenolpyruvate (PEP) working with pyruvate kinase (PK) to form a pyruvate

(3) Pyruvate + NADPH +H+ $\longrightarrow$ L-lactate +NAD+

In the presence of enzyme L-lactate dehydrogenase (L-LDH), pyruvate was reduced to L- lactate by reduced nicotinamide adenine dinucleotide (NADH) with the oxidation of NADH to NAD. The amount of NADH oxidized from this reaction is stoichiometric to the amount of glycerol by UV-visible spectroscopy at wavelength 334, 340 or 365 nm.

2.6.2 Morphological characterisation

The morphological characteristics of the fungus were examined using light microscopy (Nikon Optiphot-2, Nikon, Japan) and images were captured through a colour video camera (JVC TK-C1381) with a total magnification of

x400. Samples were collected from the bioreactors every twelve hours to evaluate the changes in fungal morphology. An aliquot (50 µl) of each was transferred to a slide, covered with a cover slip and observed under the microscope.

2.6.3 Metabolomic assays

2.6.3.1 Extraction procedure

Fermentation samples were extracted to measure the concentration of gamma-linolenic acid and lovastatin produced by the fungus using the Bligh and Dyer method (Bligh and Dyer, 1959), while the Ebada method (Ebada, 2008) was used to prepare the sample for structure elucidation.

2.6.3.1.1 Bligh and Dyer method

Fermentation samples were collected every 24 hours to measure metabolic patterns following the procedure of Bligh and Dyer (1959). Five ml of sample was homogenised in a high-pressure homogeniser (Cell disruptor, Constant Systems Ltd., United Kingdom) under 30 kpsi pressures to disrupt the cell. Five ml of sample was extracted with chloroform: methanol (5 ml: 10 ml) for two min and then chloroform (100 µl) was added and mixed for 30s. Then, distilled water (100 µl) was added, and this was then mixed for 1 min. The homogenate was filtered through Whatman No. 1 filter paper, after allowing the filtrate to separate into two layers; the volume of the chloroform layer was measured. The chloroform fraction was determined by weighing a sample after evaporation to dryness at 40-50 degrees Celsius under a nitrogen stream. Extracted samples were re-suspended in 500 µl acetonitrile and kept in a freezer (-20 degrees Celsius) before analysis.

2.6.3.1.2 Ebada method

Fermentation samples were collected every 24 hours, then filtered through a pre-weighed MF200 glass microfibre filter (particle retention size 1.6 μm, Fisher Scientific), and kept at -80 degrees Celsius before freeze-drying. The freeze-dried sample was ground and extracted for 3 cycles, each with 1L acetone per 100 g of sample. After acetone extraction, the remaining residues were extracted with methanol 1 L per 100 g of sample, usually 3 cycles. The extract of acetone and methanol were combined together and evaporated with vacuum rotary evaporator (Rotavapor® R-3, BUCHI Labortechnik AG, Postfach, Switzerland) to get a solid residue. The rest of residue was dissolved with a small volume of 10% (v/v) methanol in water against ethyl acetate followed by butanol. Each fraction was dried using a vacuum rotary evaporator to get a solid residue. Then, purified via a SPE column (VersaPak® C18 Cartridge, Sigma-Aldrich, UK) to get a more pure compound and analysed by NMR (section 2.6.4.3).

2.6.4 Quantification and elucidation of metabolites

2.6.4.1 Metabolome quantification

The measurement of gamma-linolenic acid, and lovastatin concentration were performed using a LTQ Obitrap equipped with MS detectors (Finnigan LTQ, Thermo Fisher Scientific Inc, Waltham, MA). Extracted samples were separated on a 5μm C18 reverse phase column (75 × 3 mm, ACE, Berkshire, UK). A gradient solvent system consisting of acetonitrile and water was used: 0 min 5 % Acetonitrile+0.1% Formic acid; 30 min, 100% Acetonitrile+0.1% Formic acid; 35 min, 100% Acetonitrile+0.1% Formic acid; 45 min, 5% Acetonitrile+0.1% Formic acid. The flow rate of the mobile phase was 0.4 ml/min. Gamma-linolenic acid, and lovastatin were evaluated by an

automated label-free program (Sieve Fiona V1.2, Thermo Fisher Scientific Inc, Waltham, MA, and MZ mine 2.2) based on comparisons of LC/MS data. Concentration of both compounds was calculated by peak area comparison with external standards of known concentration (Appendix IV).

2.6.4.2 Sample and standard curve preparation

The standard curve samples were prepared by diluting standard gamma-linolenic (Acros Organic, Geel Belgium), and lovastatin (Merck Chemicals Ltd., Nottingham, UK) to generate a 10-fold serial dilution from 100 mg, to 1 μg in acetronitrile, which were then analysed by the method described in 2.6.4.1. Calibration curve of standard compounds are showed in Appendix IV.

2.6.4.3 Structure elucidation

NMR experiments were performed to compare and confirm the structure of gamma-linolenic acid and lovastatin produced by the fungus, with a standard.

Extracted samples using the Ebada method were dissolved in DMSO-d6 solvent (Euriso-Top SA, Paris, France). The experiment was carried out by three NMR experiments including: one dimensional ^{1}H and two dimensional correlation spectroscopy (COSY), and Heteronuclear Multiple Bond Coherence (HMBC) for identification of the structure of the purified compound. Spectral data was identified by comparison with standard spectral data.

The first experiment, one dimensional ^{1}H or Proton NMR, was used as an initial experiment to identify a structure of the expected signals of protons in the molecules; the chemical shifts in order from the range +14 to -4 ppm and

the integration curve for each proton reflects a position of functional group with proton attached with and the abundance of the individual protons within the molecule. The multiplicity and extent of coupling constant gives an idea of the adjacent protons and their spatial proximity (Claridge, 2006).

The second experiment, two dimensional correlation spectroscopy (COSY), is an experiment which is useful for identifying the correlation between protons. The proton shifts are plotted on both axes, the cross peaks occur when protons interact with each other through J-coupling. One proton can couple to another proton nearby, and give a diagonal peak which represents a resonance position of coupled protons (Claridge, 2006).

The third experiment, Heteronuclear Multiple Bond Coherence (HMBC), was used for identifying the correlation between carbon and neighbouring protons called long-range or multiple bond correlations. This experiment shows a proton-carbon atom bonding through couplings over two or three bonds, providing a useful approach to define organic compound structures (Claridge, 2006).

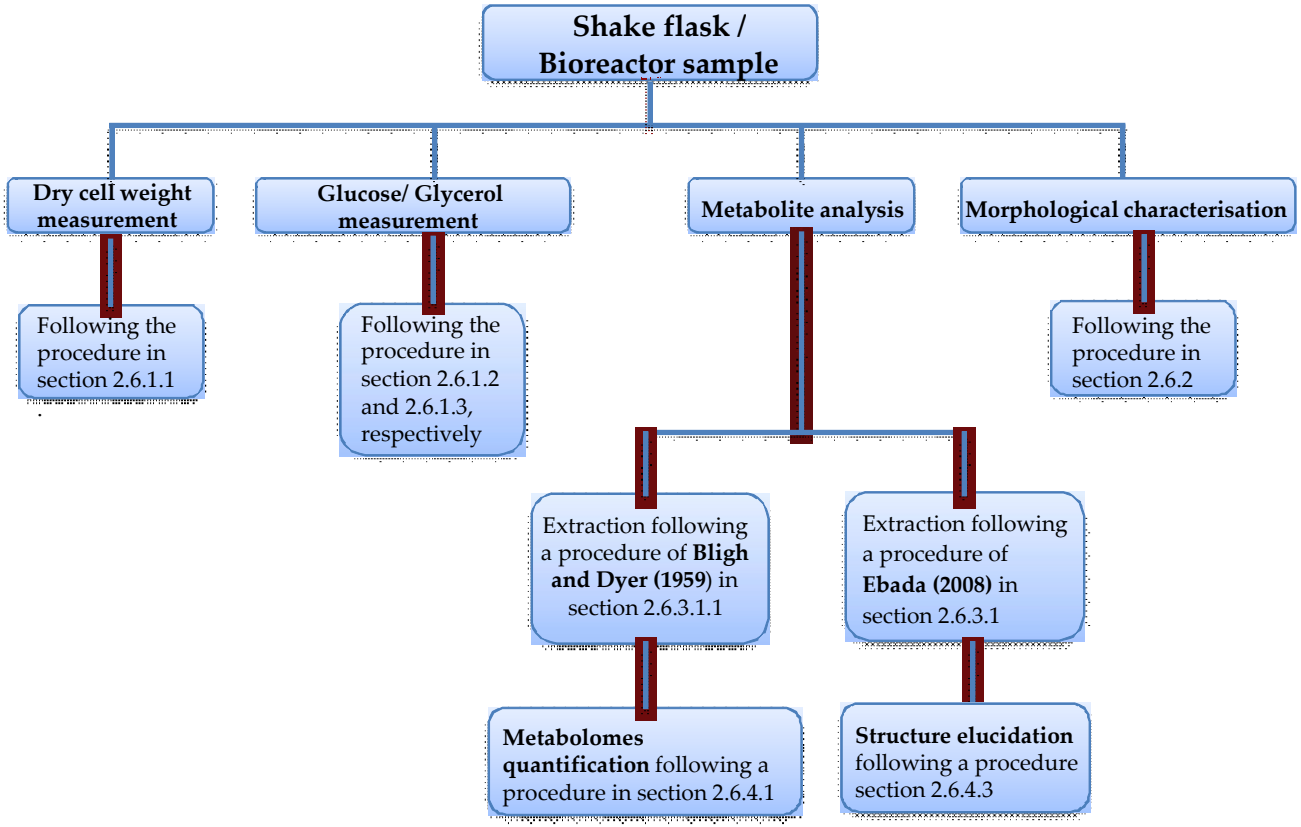

Figure 2.5 A diagram to show the analytical processes used to identify metabolomes and compounds produced by fungal isolate AQP 4097

2.7 Statistical analysis

The statistical analysis of the fungal growth was determined using One-way ANOVA and post-hoc methods (SPSS program, version 16.0) and tests of significant difference were determined by a Tukey's range test.

Chapter 3 Results

3. Results

3.1 Effect of salinity and light on sporulation of AQP4097

In the case of submerged fermentation, the inoculums preparation is an important step to control and define microbial performance in the fermenter, and to achieve reproducible processes. Broadly speaking, there are two types of inocula used as starters for fungal fermentations, spore and vegetative inocula.

The advantages of using spores as inocula are ease of inoculums preparation, prolonged storability for subsequent use (Khachatourians and Arora, 2001), and provision of good reproducibility in inoculums performance in terms of uniformity of the product (Kubicek and Druzhinina, 2007). Due to the poor sporulation of this fungal isolate, in this experiment the aim was to investigate the factors that might influence sporulation by changing the salinity, achieved by varying the concentration of salt in the medium, and assessing the effect of light on sporulation (Leach, 1964; Miller and Reid, 1961; Kheng (1973).

Besides its influence on sporulation, light has also been reported to stimulate the production of some Fusarium metabolites, such as carotenoids. In terms of how these effects are mediated, as in other fungi with well-known photoresponses, the Fusarium genome contains several genes for photoreceptors, among them a set of White Collar (WC) proteins, a cryptochrome, a photolyase, a phytochrome and two presumably photoactive opsins (Avalos, 2010).

Water is another factor that is necessary for the growth of fungi, and its availability is linked to efficiency of uptake of nutrients, and release of

extracellular enzymes by the fungi. Even water moulds need water to increase cell turgidity in order to penetrate solid surfaces (Harold *et al.* 1996; Money, 2001). However, this does not mean that fungi can use all water that is present in an environment because some is bound by external forces. The term water potential means the sum of all the forces that act on water and tend to restrict its availability to cells, denoted by φ and defined in terms of energy (negative MegaPascals). Ultra-pure water has the highest potential equal to 0 MPa, and water potential will decrease when pure water is mixed with other solutes (such as salts and sugars) (Deacon, 2006).

$$\varphi \text{ (water potential)} = \varphi\pi + \varphi m + \varphi p + \varphi g$$

where φπ is osmotic potential (solute binding forces), φm is matric potential (physical binding forces), φp is turgor potential, and φg is gravimetric potential.

There are some reports on the relationship between water potential and growth and sporulation of both terrestrial and marine fungi. Suleman *et al.* (2001) studied the effect of solute potential on the growth and sporulation of two pathogenic fungi of the Date palm tree, *Chalara radicicola* and *Chalara* (*Thielaviopsis*) *paradoxa*, and discovered that adding glycerol, NaCl, and KCl to potato dextrose agar to decrease the osmotic matrix-based water potential of the medium up to –4.25 MPa decreased the radial growth, biomass, and sporulation of both *C. radicicola* and *T. paradoxa*. While Giorni *et al.* (2008) investigated the effect of temperature, different solutes (ψs) and matrix potentials (ψm) on growth and sporulation of three aflatoxigenic strains of *A. flavus* and found that faster growth occurred at 30 degrees Celsius and -1.4 and -2.8 MPa. *A. flavus* strains were more sensitive to ψm than ψs stress with limits of -9.8 MPa and -14 to -18 MPa, respectively. It can be concluded that

both temperature and ψs/ψm stress had statistically significant effects on growth rates of the three strains, while sporulation was significantly influenced by ψs potential, solute type and temperature, as shown by sporulation decreasing significantly at each ψs variation, with a complete inhibition with ionic solute at -14.0 MPa and decreased down to 4.7×10^5 conidia at -21 MPa in glycerol modified medium. This result is consistent with the study of Samapundo *et al.* (2010) which examined the effect of four different concentrations (0-6.4 %) of NaCl and various NaCl replacers ($CaCl_2$, $MgCl_2$, KCl and $MgSO_4$) on the growth of *P. roqueforti* and *A. niger*. The study showed that the higher concentrations of NaCl and various NaCl replacers inhibited the growth of *P. roqueforti* and *A. niger*, and also increased the lag phase durations of both fungi.

By contrast to marine fungi, growth increased as the concentration of sea water increased as did the production of antimicrobial agents (Masuma *et al.*, 2001). On the other hand, Kerzaona *et al.* (2008) concluded that seawater salinity significantly reduced the rate of growth of marine-derived *A. fumigatus* strains, but the gliotoxin excretion in marine strains seemed to be less influenced by seawater salinity than the terrestrial strains. In addition, Byrne (2009) stated that terrestrial ascomycetes and appendaged fresh-water hyphomycetes showed limited tolerance to high salinity, while appendaged marine hyphomycetes were intolerant to extreme low-salinity conditions. Moreover, marine ascomycetes have a wide tolerance to low-salinity conditions and sporulation of the majority of the imperfect fungi also showed a broad tolerance to high and low-salinity conditions.

Due to the lesser spore production by this fungus, the following study the effect of different IO concentrations was carried out using PDA medium and the effects of light upon sporulation were examined.

3.1.1 Results and Discussion

For those cultures incubated in the dark, the most rapid growth was seen on the cultures on PDA alone which completely covered the medium surface within 6 days, followed by the cultures grown on PDA mixed with IO 10 g/L, 20 g/L and 33 g/L, respectively. In terms of sporulation as can be seen Figures 3.2 A-D, fungi grown on PDA with IO 10 g/L (Figure 3.1 B) and 20 g/L (Figure 3.1 C) produced spores most rapidly (within 7 days) after inoculation, while fungi grown on PDA (Figure 3.1 A) and PDA mixed with IO 33 g/L (Figure 3.1 D) barely produced any spores.

The results of culturing fungi isolate AQP 4097 under natural light were broadly similar to the above in that fungal growth was most rapid on PDA and PDA with IO 10 g/L in which the medium surface was fully colonized within 4 days. Cultures on PDA with IO 20 g/L and 33 g/L, took longer to fully cover the plate surface. As the results show in Figures 3.1 E-H, cultures grown on PDA with IO 10 g/L (Figure 3.1 F) followed by PDA with IO 20 g/L (Figure 3.1 G) produced spores fastest within 7 days, while fungi grown on PDA (Figure 3.1 E) and PDA with IO 33 g/L (Figure 3.1 H) produced almost no spores at all.

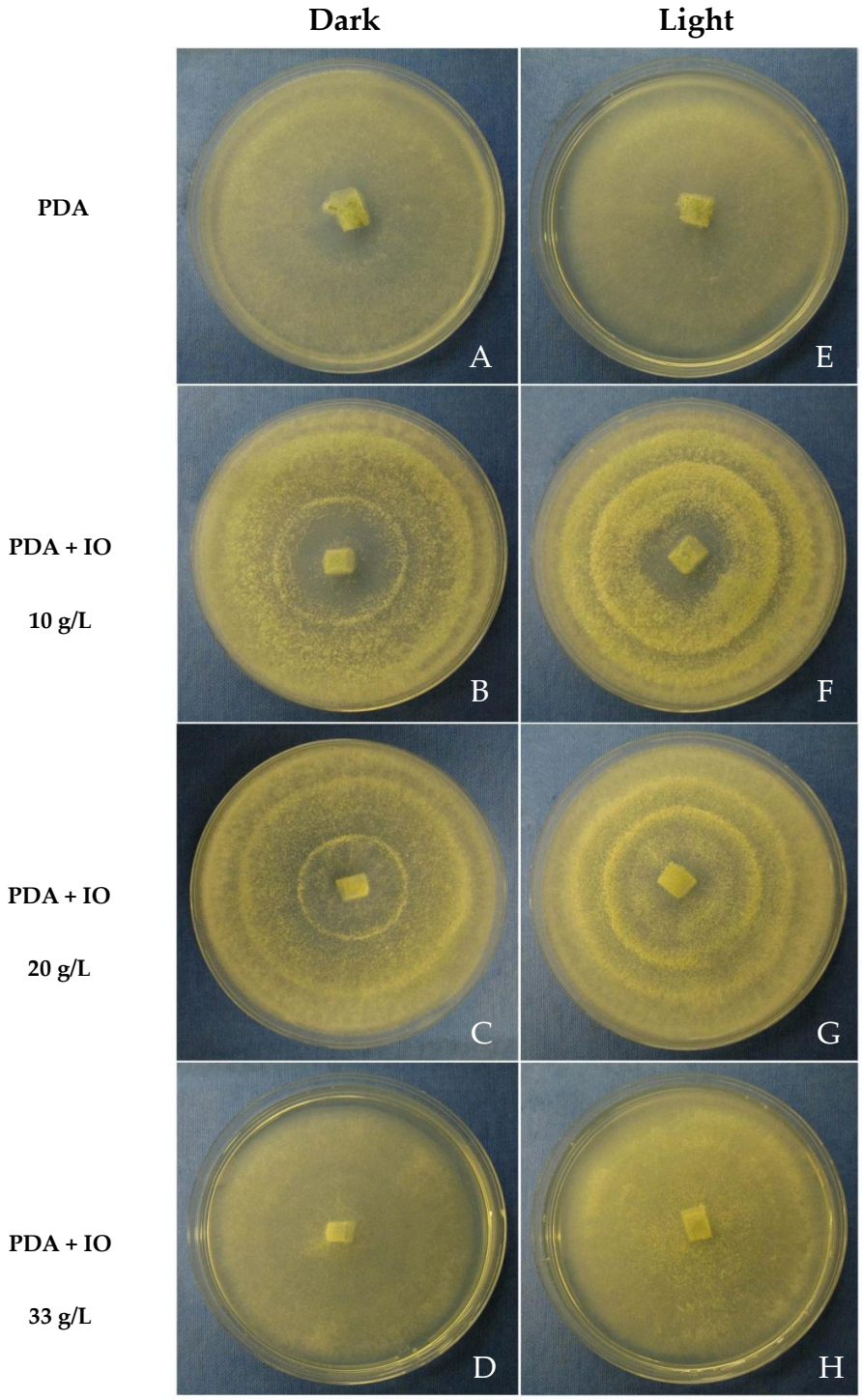

Figure 3.1 The effect of light and salinity on growth and sporulation of fungal isolate AQP 4097. PDA (A,E), PDA plus 10 g/L IO (B,F), PDA plus 20 g/L IO (C,G) and PDA plus 33 g/L IO (D,H) (company's preferred medium). Plates A-D were incubated in an enclosed incubator while plates E-H were incubated under natural light

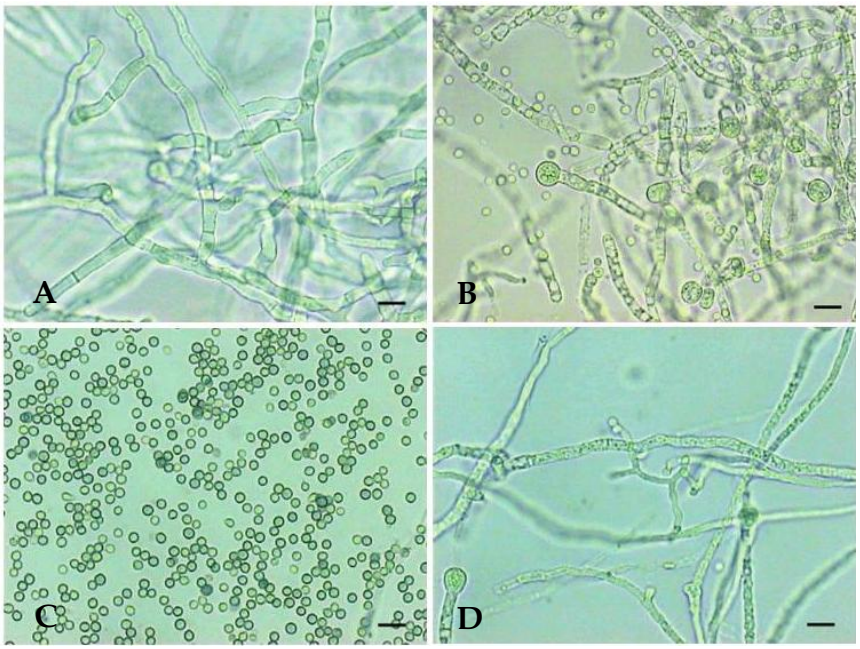

Figure 3.2 Morphology of *Trichoderma pseudokoningii* isolate AQP 4097 cultured in PDA medium plus 10g/L IO under microscope, including conidiophores (A), chlamydospore (B), conidia (C), and phialides (D). Magnification = 20x, Bar = 1μm.

The morphology of *T. pseudokoningii* under the microscope is shown in Figure 3.2. *T. pseudokoningii* produced long branched conidiophores; branches arose at or near 90° with respect to the main conidiophores. Primary branches re-branched to form secondary branches. Secondary branches followed the same pattern of branching as the primary branches with longer side branches closer to the main axis and short branches more distal (Figure 3.2A). A phialide shape was more irregularly disposed toward the apex of the conidiophore, lageniform, 0.3 × 1-1.2 μm, terminal phialides narrowly conidial (Figure 3.2 D). Conidia were ellipsoidal or ovoidal and smooth, 2.5–4.5 × 1.7–2.6 μm (Figure 3.2 C). Chlamydospores were produced terminal or intercalary within hyphae, and globose to subglobose, 0.1-0.3 × 0.3μm (Figure 3.2 B).

These results show that isolate AQP 4097 can grow in PDA which has various salt concentrations, but grows faster either in low concentrations of salt or with no salt in the medium; moreover, this isolate produced abundant spores when the salt concentration was decreased. Broadly similar results have been noted in a number of studies where the growth of fungi decreased when water potential in the medium decreased, while the lag phase duration increased in these circumstances (Gindrat, 1977, Suleman *et al.,* 2001, Giorni *et al.,* 2008, Samapundo *et al.,* 2010). However, surprisingly sporulation was poorest in the medium formulation adopted by Aquapharm Biodiscovery Ltd. as optimal for this isolate. In addition, those cultures grown in a low salt concentration medium which were incubated under natural light produced much more spores than those incubated in the dark. This can be correlated to the study of Gao *et al.* (2009) which demonstrated that light also enhances the sporulation of biocontrol fungi, including *Paecilomyces lilacinus* M-14, *Pochonia chlamydosporia* HSY-12-14, and *Lecanicillium lecanii* CA-1-G. Ghajara *et al.* (2006) also demonstrated that near ultraviolet light enhanced sporulation of *Drechslera avenacea* on agar medium. It is clear that light has a very clear influence upon growth and sporulation of this isolate in low salinity medium. This is broadly in agreement with the findings of Byrne (1975) and Kerzaona *et al.* (2008), in which marine ascomycetes were found to have a wide tolerance to low-salinity conditions and sporulation of the majority of imperfect fungi also showed a broad tolerance to high and low-salinity conditions. By contrast Masuma *et al.* (2001) reported that the growth of marine fungi increased when the concentration of salt increased. Also, the present results are not in accordance with that of Miller and Reid (1961), in which white light only caused subsequent formation of a ring of conidia-

bearing mycelium, but even if incubated in dark condition fungi isolate AQP 4097 also formed a ring of conidial-bearing mycelia on the plate.

3.1.2 Conclusions

In conclusion, related to the results, growing fungal isolate AQP4097 in PDA with 10 g/L IO and incubating under natural light is the best set of conditions for generating spore inocula for subsequent studies.

3.2 Metabolomics analysis of AQP 4097 cultured on PDA plate with Instant Ocean.

From the results presented in section 3.1, PDA with 10 g/L IO medium incubated under natural light seemed to be the most suitable set of conditions for generating spore inocula from this isolate. The industrial partner, Aquapharm Biodiscovery Ltd., also reported that this isolate was capable of producing two unsaturated fatty acids, oleic acid (47.69%, w/v) and gamma-linolenic acid (2.76%, w/v) when cultured in PDA plus IO 33 g/L. However, the major problem of marine microorganism fermentation is the high concentration of chloride ion (> 500ppm) in medium induced pitting corrosion on a stainless steel bioreactor. The recommendation to solve the problem was to use of non-chloride sodium salts, using of ceramic or silicon coatings to provide a protective film for the stainless steel, or using specialized stainless steel alloys having enhanced corrosion resistance in the bioreactor; however these alternatives are prohibitive and not applicable to saline fermenters in an industrial scale (Reader *et al*., 2007).

Therefore the aim of this experiment was to reduced the concentration of IO in the medium and measure the levels of both fatty acids and other compounds which AQP 4097 produced, and to assess the effect of changes in the amount of IO in the medium upon the metabolome. The details of inoculums preparation, culture conditions, and extraction by the Bligh and Dyer method are described in section 2.1.2. The culture conditions were described in section 2.2.1.2. The extraction procedure for the sample was followed Bligh and dyer methods in section 2.6.3.1.1., the metabolomics quantification was performed as described in section 2.6.4.1., and calculated the concentration of interesting compounds by comparing with calibration of

standard compound a standard curve (section 2.6.4.2). Structure elucidation was performed as described in section 2.6.4.3.

3.2.1 Results and Discussion

Metabolic analysis of AQP 4097 cultured on PDA plate with IO 10, 20 and 33 g/L compared with PDA without IO was carried out using a LTQ-Orbitrap and raw data were analysed using Automated Analysis Software; Sieve Fiona (v.1.2) and MZMine (v.2.2) program. From the analysis, four compounds were identified, virescenoside B, gemfibrozil, γ-linolenic acid, and a derivative of lovastatin.

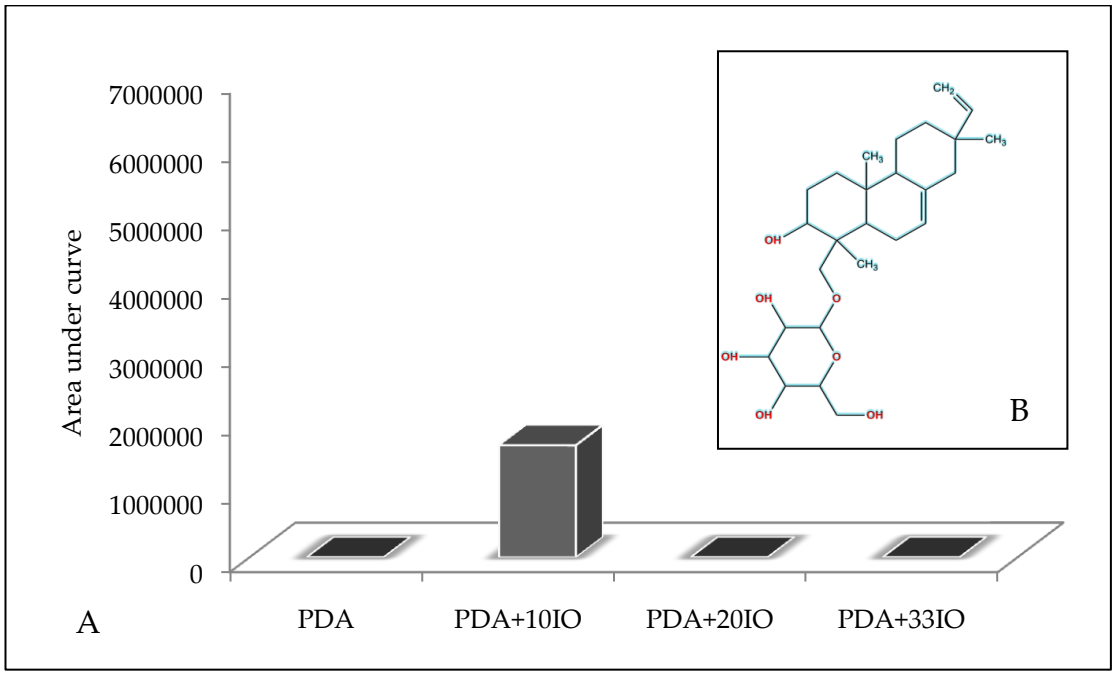

Figure 3.3 Virescenoside B ($C_{26}H_{42}O_7$) produced by 7 days old AQP 4097 cultured on PDA with IO 10, 20, and 33 g/L compared with PDA without IO (A = Area under curve, and B = Molecular structure).

From Figure 3.3A, it can be clearly seen that virescenoside B was produced by AQP 4097 cultured in PDA plates with IO 10 g/L, while barely detected in

PDA with other concentrations of IO. Virescenoside B is a diterpenoid, which was previously found in terrestrial strains of *Oospora virescens* (Cagnoli-Bella *et al.*, 1969**).** This compound was reported in the database of NCI Yeast Anti-Cancer Drug Screen that it has activity in anti-cancer assays (http://pubchem.ncbi.nlm.nih.gov/summary/summary.cgi?cid=280575#x299).

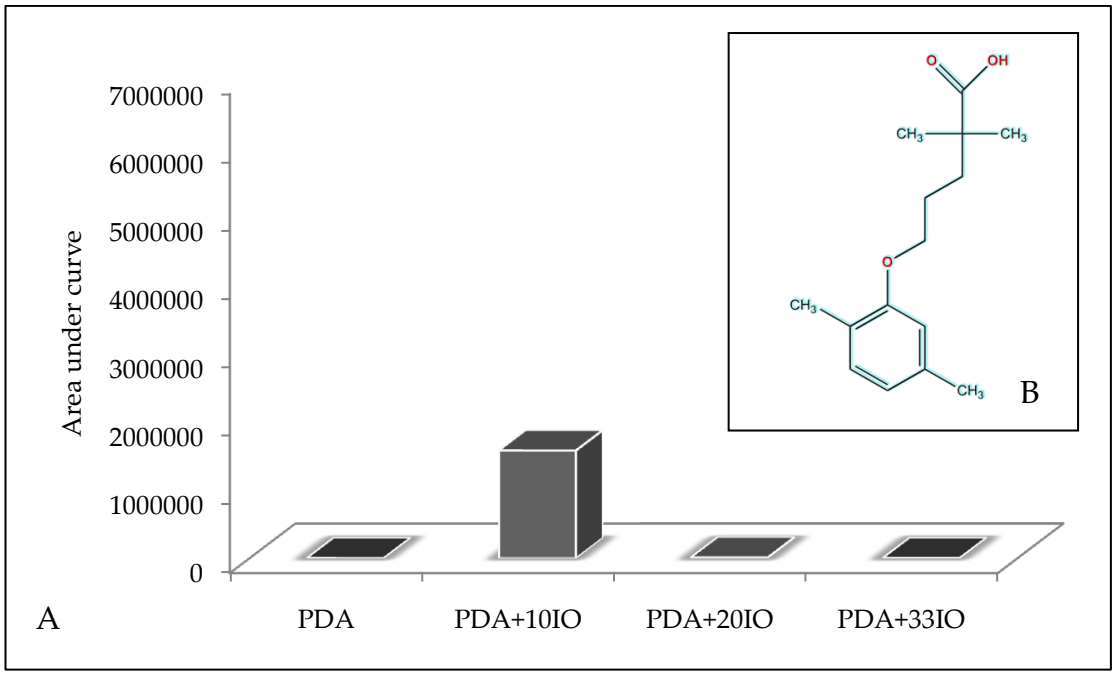

Figure 3.4 Gemfibrozil ($C_{15}H_{22}O_3$) produced by 7 days old AQP 4097 cultured on PDA with IO 10, 20, and 33 g/L compared with PDA without IO (A = Area under curve, and B = Molecular structure).

As can be seen from Figure 3.4A, gemfibrozil, another compound produced by AQP 4097 was also detected only in PDA plate with IO 10 g/L. Gemfibrozil was classified as a fibric acid derivative (http://www.drugbank.ca), and previously described in the terrestrial fungus, *Cunninghamella elegans* (Kang *et al.*, 2009). It is known as a

hypolipidemic agents, commonly sold as an oral drug under the brand names; Lopid, Jezil (Australia), and Gemfibrozil.

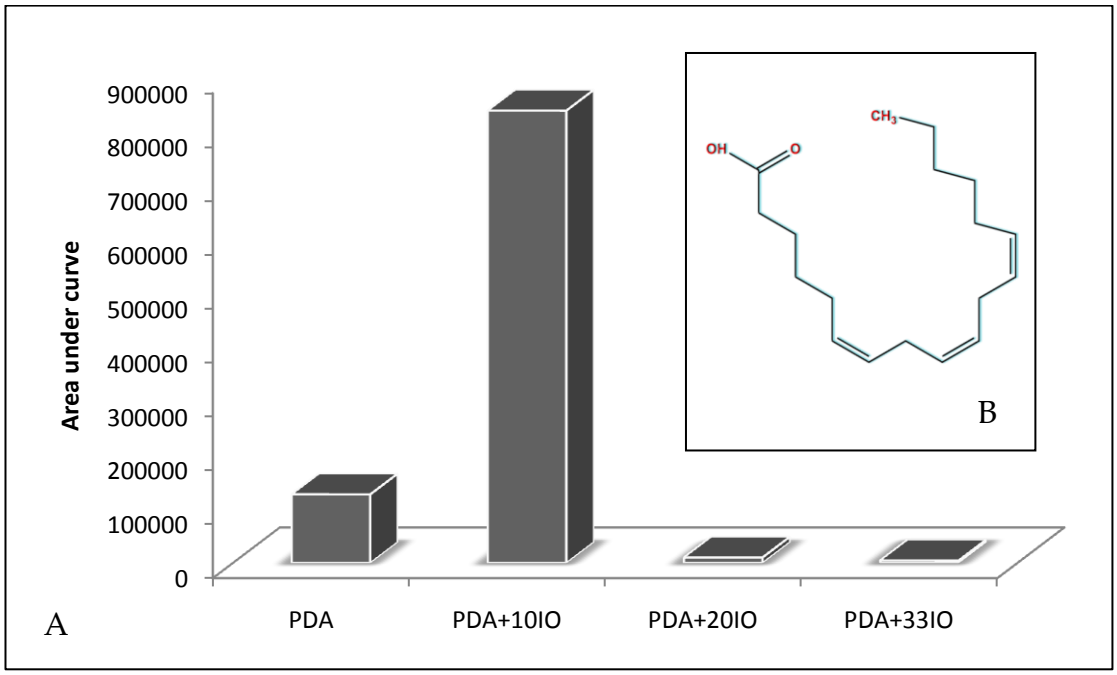

Figure 3.5 γ-linolenic acid ($C_{18}H_{30}O_2$) produced by 7 days old AQP 4097 cultured on PDA with IO 10, 20, and 33 g/L compared with PDA without IO (A = Area under curve, and B = Molecular structure).

The analysis confirmed the presence of a third compound, γ-linolenic acid, as shown in Figure 3.5A. It was observed that γ-linolenic acid was detected in PDA with IO 10 g/L and PDA without IO, whereas it was barely detected in PDA with 20 and 33 g/L. The level of γ-linolenic acid produced by AQP 4097 in PDA with IO 10 g/L was 8 fold higher compared with that of PDA without IO. From previous studies, several fungal species are usually described as γ-linolenic acid producers which include *M. ruber* (Endo, 1979), *A. terreus* (Alberts, 1980), *Mucor rouxii* (Hansson *et al.*, 1989), *Circenella simplex*, *M.*

indicus, Syzygites megalocarpus (ATCC 18025), *Zygorhynchus moellierie A* (UMH 1556) (Weete *et.al.,* 1998**),** *Mortierella sp*. (Higashiyama *et al.,* 2002**),** and *Cunninghamella echinulata* (Chen and Chang, 1996). The production of γ-linolenic acid has been reported to be related to the survival mechanism of fungi in marine ecology (Raghukumar, 2008).

Finally, mass spectral analysis of AQP 4097 demonstrated the production of a lovastatin derivative, as shown in Figure 3.6A. It can be clearly seen that the lovastatin derivative was detected in all media; the highest yield was derived from PDA without IO. Various fungi genera were previously reported to yield lovastatin including *Aspergillus*, *Penicillium*, *Monascus*, *Paecilomyces*, *Trichoderma*, *Scopolariopsis*, *Doratomyces*, *Phoma*, *Pytium*, *Gymnoascus*, *Hypomyces*, as well as the higher fungus, *Plurotus* (Samiee *et al.,* 2003). Nowadays, a commercial strain of *A. terreus* is utilized for lovastatin production. The high yield of γ-linolenic acid confirms its involvement in maintaining osmotic pressure in culture (Raghukumar, 2008).

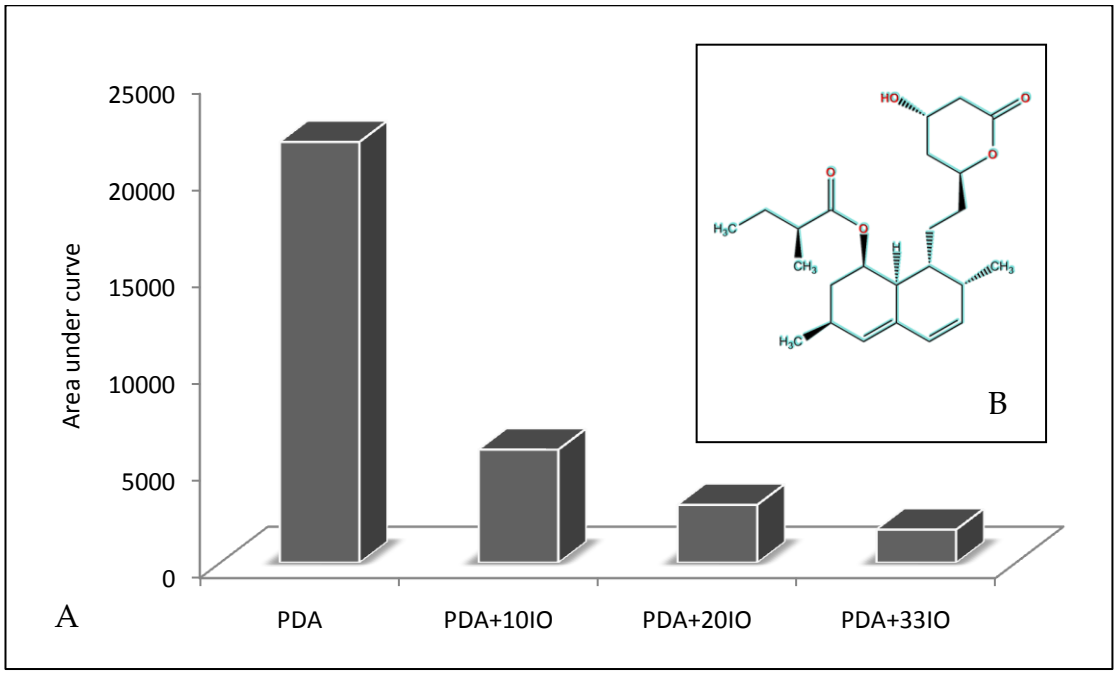

Figure 3.6 Lovastatin derivative ($C_{24}H_{36}O_5$) produced by 7 days old AQP 4097 cultured on PDA with IO 10, 20, and 33 g/L compared with PDA without IO (A = Area under curve, and B = Molecular structure).

Therefore, since the lovastatin derivative was found in all PDA at various concentrations of IO this compound was chosen to be the target compound to study the effect of fermentation and scale up process on its production.

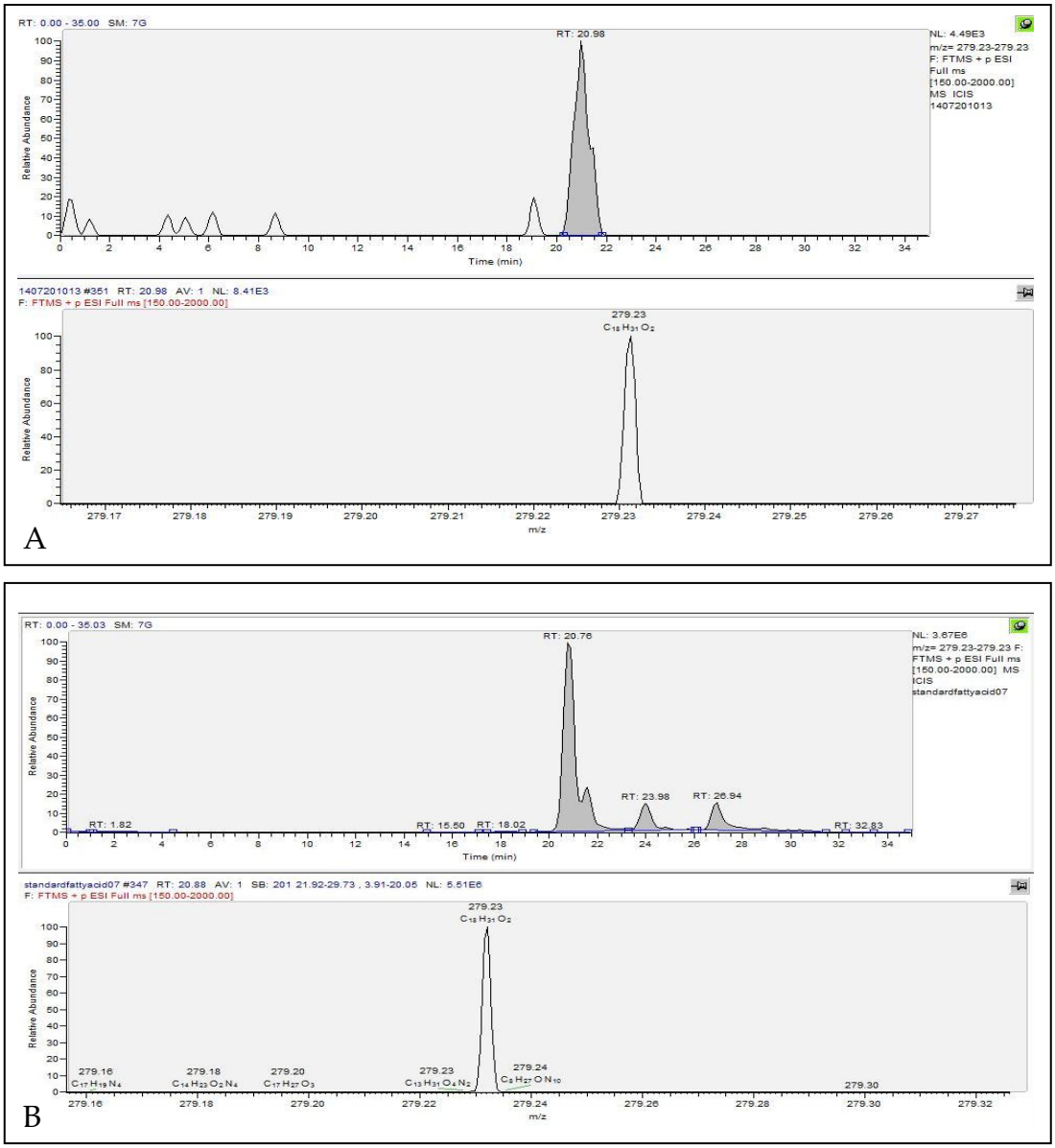

Figure 3.7 Chromatographic chemical profiling of standard γ-linolenic acid at 100 µg (A) and extracted sample of AQP 4097 cultured on PDA plate (B)

The concentrations of lovastatin derivative and γ-linolenic acid extracted from PDA plates were calculated by comparison with a calibration of standard compounds (Appendix IV) and the molecular structure of both compounds were studied using NMR.

Figure 3.7 shows that γ-linolenic acid from the sample (B) was indicated by the molecular ion peak at m/z 279.23 $[M+H]^+$ and eluted at 20.98 min using an HPLC solvent gradient of acetonitrile: water commencing at a ratio of 95:5 and finishing with 100% acetonitrile in 30 min., which is similar to that of standard γ-linolenic acid which has a retention time at 20.76 min (A).

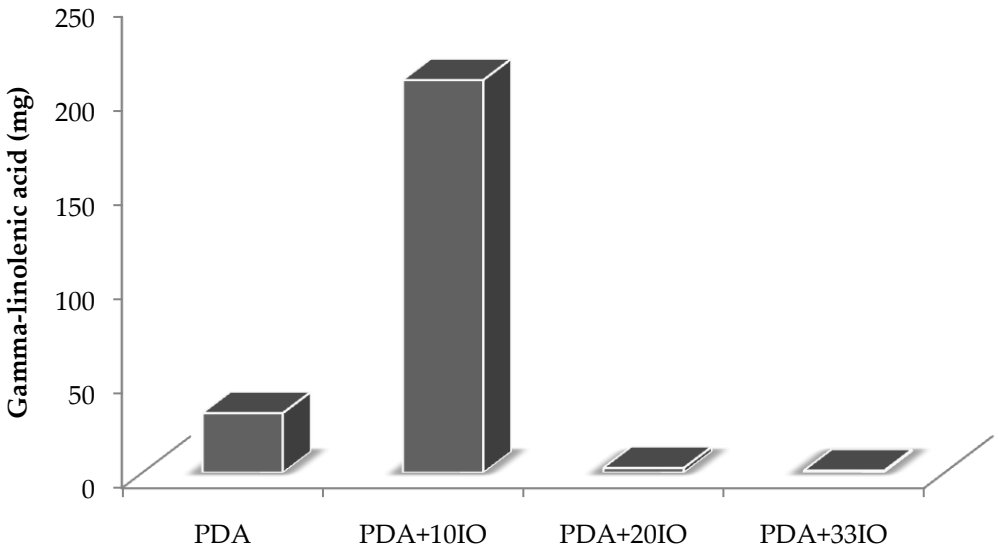

Figure 3.8 The concentration (in mg) of detected γ-linolenic acid from PDA plate varying IO concentration.

The γ-linolenic acid detected from PDA plates with IO compared with PDA without IO as shown in Figure 3.8 was calculated by employing a calibration curve of standard γ-linolenic acid. It can be seen that the maximum yield of γ-linolenic acid was achieved from PDA plates with IO 10 g/L, followed by PDA without IO; whereas it was barely detected in the other two

concentrations of IO. The maximum γ-linolenic acid derived was 208 mg/plate, 6 fold higher compared to that of PDA without IO.

The molecular structure of γ-linolenic acid produced by AQP 4097 was determined by NMR with ^{1}H and HMQC experiments which showed a unique correlation pattern between directly-bonded protons and carbons atom in a molecular structure of compound. As shown in Figure 3.9, the NMR spectral data of the sample matches with that of the gamma-linolenic acid standard.

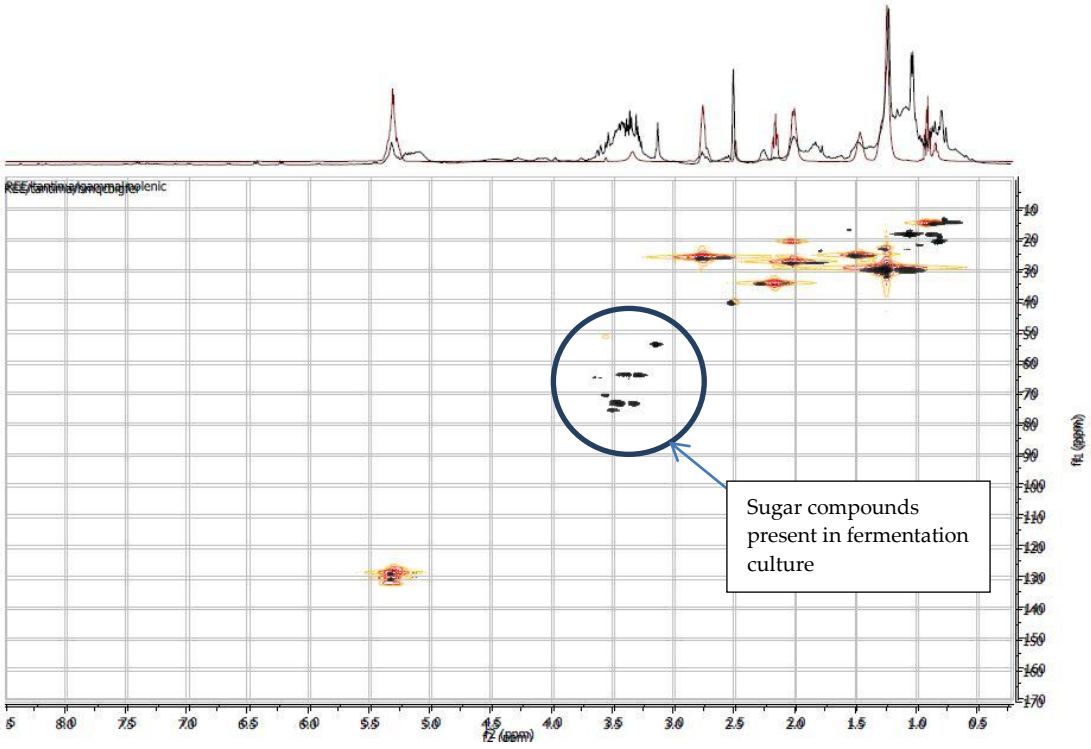

Figure 3.2 NMR: ^{1}H, Heteronuclear Multiple Quantum Coherence (HMQC) experiment. The red dot is gamma-linolenic and the dark dot is ethyl acetate fraction of a sample from Bioflo 110 (Braun).

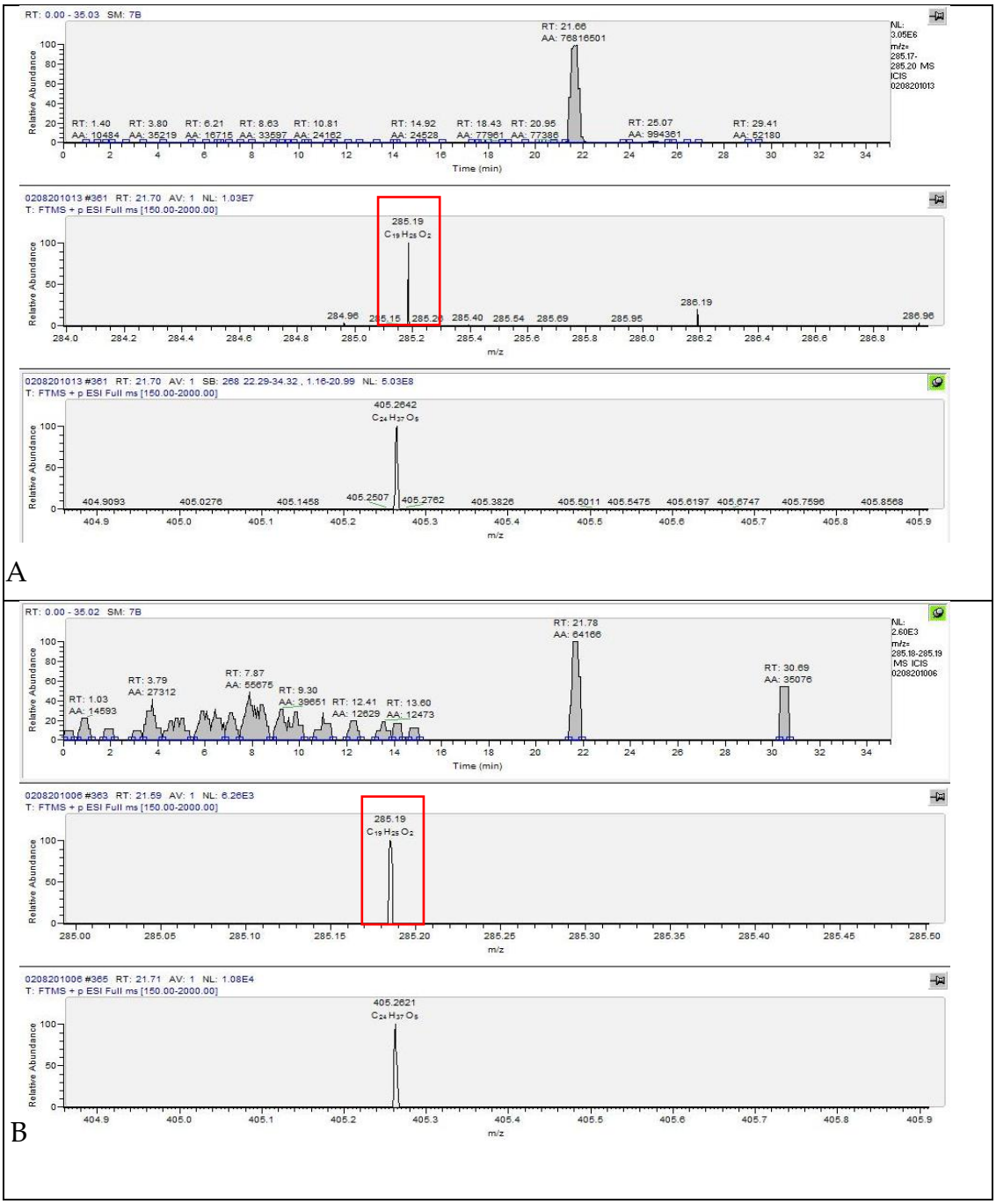

Figure 3.30 Chromatographic chemical profiling of lovastatin standard at a concentration of 100 µg/mL (A) and extracted sample of AQP 4097 cultured on PDA plate (B). Both were injected at a volume of 20uL. The red square show identical ion peak of lovastatin standard compared with lovastatin derivative represented in sample.

Figures 3.10 shows that the lovastatin derivative had a retention time of 21.78 min in liquid chromatography, with a molecular ion peak at m/z 405.26 $[M+H]^+$(Figure 3.10 B). This was similar to that of the lovastatin standard dissolved in the same solute which has a retention time at 21.66 min (Figure 3.10A). From the fragmentation experiment, the detected lovastatin derivative from the sample had the same fragment (ms/ms) peak with an ion peak at m/z 285.18 $[M+H]^+$ which is identical to the lovastatin standard.

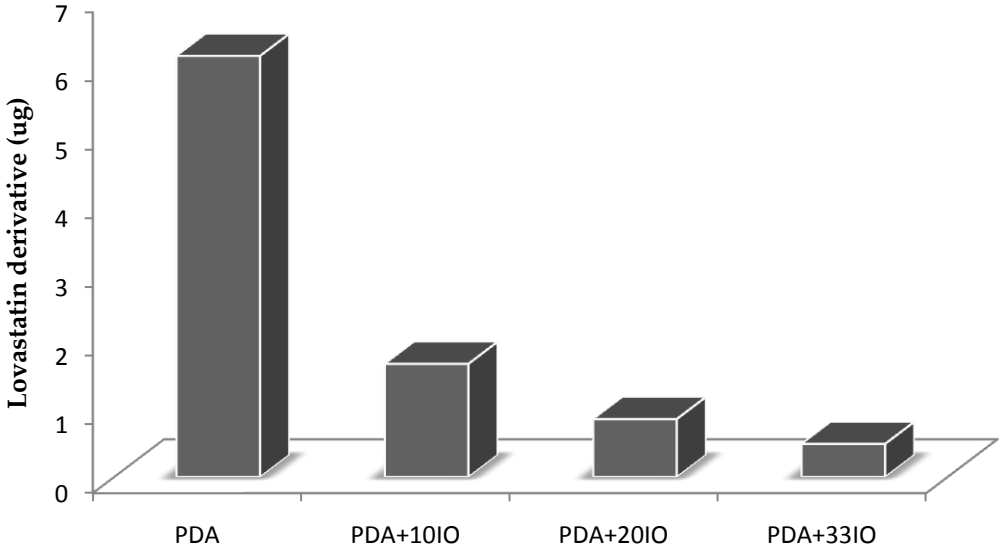

Figure 3.11 The concentration (in μg) of detected lovastatin derivative from PDA plate in various IO concentrations.

The extracted lovastatin derivative from the PDA plate with IO compared with PDA without IO was calculated by comparison with a calibration curve of standard lovastatin as shown in Figure 3.11. It can be seen that the lovastatin derivative was found in AQP 4097 cultured in all media, the maximum yield for the lovastatin derivative was achieved from PDA

without IO; followed by PDA with IO 10, 20, and 33 g/L respectively. The maximum lovastatin derivative produced was 6.132 µg/plate.

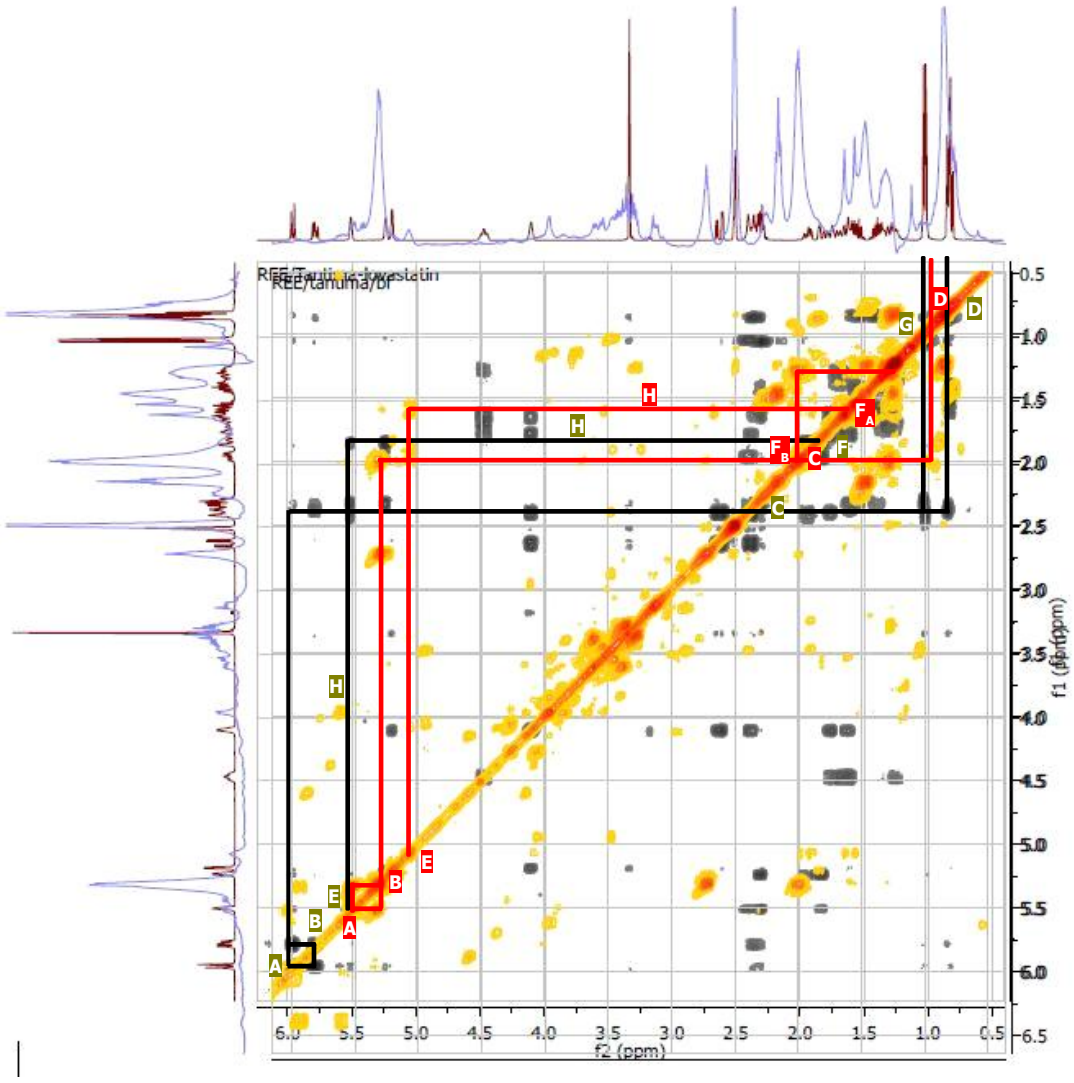

Figure 3.4 NMR: ^{1}H and ^{1}H Correlation spectroscopy (COSY) experiment. The black cross peaks are the lovastatin standard and the orange-red cross peaks belong to the ethyl acetate fraction of the sample from Bioflo 110 (Braun).

From the COSY correlation it can be confirmed that the compound with an identical molecular weight and fragment ion as lovastatin is its isomer. However, to further explore and elucidate its structure, a scale up will be needed to increase its yield. The presence of the olefinic system as in lovastatin (as shown by the red line) can still be observed in the ethyl acetate fraction of the sample from Bioflo 110 as represented by the black line. The differences in chemical shifts of the olefinic protons maybe due to a change in stereochemistry of one the methyl groups and/or migration of the second methyl group on ring B as illustrated in Figure 3.13

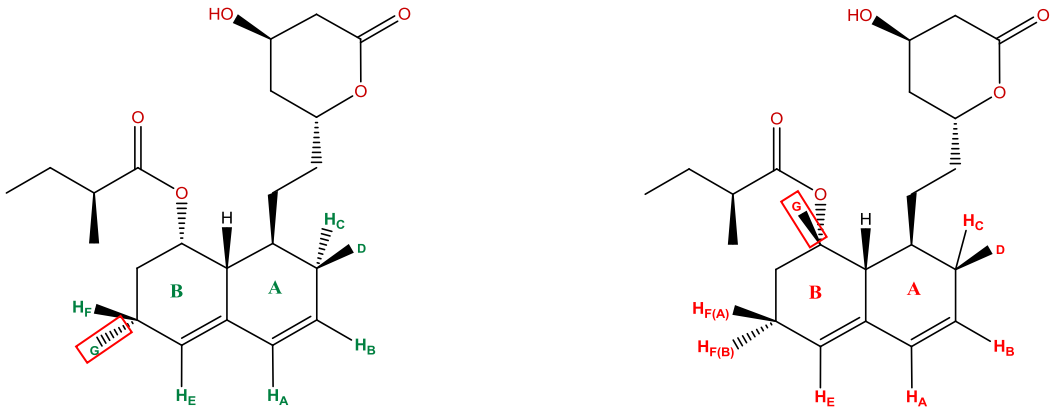

Lovastatin

Lovastatin derivative

Figure 3.5 Conformation of lovastatin derivative produced by AQP 4097 compared with lovastatin standard. The red square shows the different position of chemical shifts compared between lovastatin standard and lovastatin derivative produced by the fungus.

3.2.2 Conclusions

In summary, four compounds were produced by AQP 4097 cultured in PDA with varying concentrations of IO, which included virescenoside B,

gemfibrozil, γ-linolenic acid, and a derivative of lovastatin. Due to commercial interest, the lovastatin derivative was chosen as the target compound for further study in optimizing the fermentation conditions for scale up.

From LC-MS analysis, a derivative of lovastatin was found in AQP 4097 cultured in all PDA medium with and without IO; PDA without IO gave the maximum concentration achieved (6.13 μg/plate). NMR experiments confirmed the presence of a structure related to lovastatin produced in cultures of AQP 4097. The highest concentration of γ-linolenic acid was achieved in PDA with IO 10 g/L (208.46 mg/plate).

3.3 Biomass production by AQP 4097 in shake flasks

Supplying the correct nutrients in the culture medium is the key to supporting the growth of fungi. There is a need to supply a range of nutrients such as a carbon source and energy source, nitrogen source, other macro nutrients such as sulphur and phosphorus, and trace elements which are usually regarded as micronutrients, being required only in tiny amounts. Regarding the carbon and nitrogen content in the cells of fungi, bacteria, and yeast, it is often noted that the carbon content within the three different groups is broadly similar around 48% (w/v), but the nitrogen content of fungi is sometimes much less than in yeasts or bacteria owing to the fact that fungi having a large areas of hyphae that are empty and are no longer involved in biochemical activities, and which may contain no nucleic acids or proteins, thus they require considerably less nitrogen than yeasts or bacteria (McNeil and Harvey, 2008).

The largest contributor to growth found in a fungal medium is usually the carbon source. The carbon source for fungal culture includes simple sugars, (monosaccharide, and disaccharides), common alcohols (methanol, ethanol), polysaccharides, and oils. Within the bioprocessing industry the commonest nitrogen source regularly chosen is ammonia, in the form of its salts, either ammonium sulfate ($(NH_4)_2SO_4$), or ammonium chloride (NH_4Cl), and complex nitrogen sources such as yeast extract, soya bean meal (8% w/w nitrogen), and corn steep liquor (4% w/w nitrogen). However, the best type of carbon and nitrogen source depends on the type and the utilisable capacity of the microorganisms.

The aim of this part of the study was to assess the growth of fungal isolate AQP 4097 in three media with described composition as detailed in section

2.2.2.1 including MYGP medium, Czapek-Dox medium, and Glucose–Yeast extract medium in comparison to growth in PDB plus IO (33 g/L) in shake flask cultures. This will also give insights into the appropriate incubation times and medium composition for inocula for further experiments, including fermenter batch cultures.

The details of inoculums preparation, the culture conditions, dry cell weight measurement, and the statistical analysis of the fungal growth compare in each media was described in section 2.12, 2.2.2.1, 2.6.1.1, and 2.7, respectively.

3.3.1 Results and Discussion

3.3.1.1 Growth of AQP4097 in shake flasks

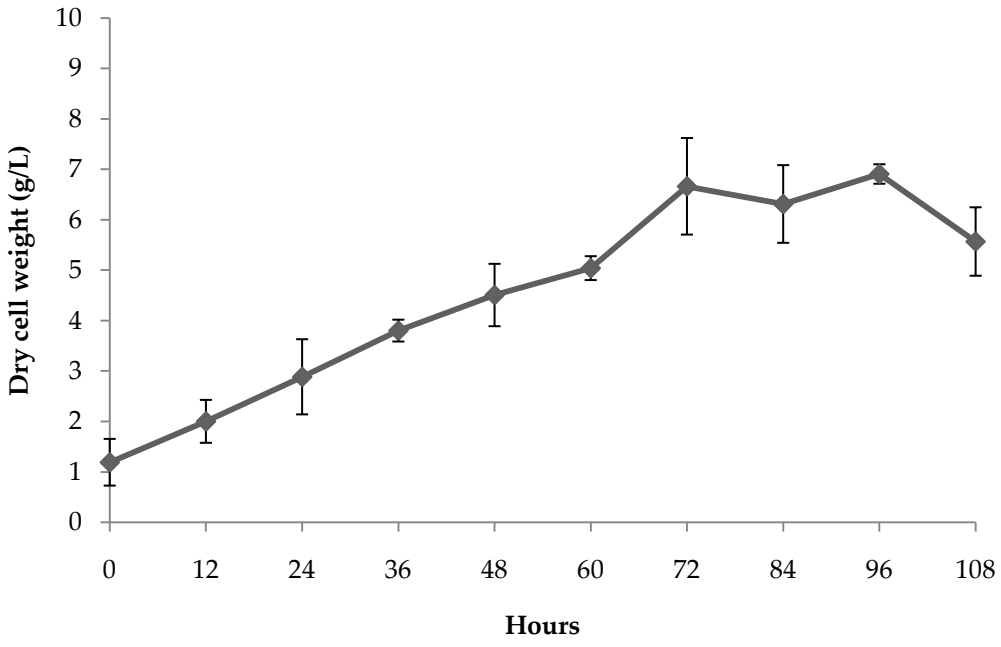

Figure 3.14 The growth (g/L) of fungal isolate AQP 4097 cultured in PDB medium plus 33g/L IO at 26◦C, rotary shaker speed 220 rpm in a 250 ml shake flask.

The growth of AQP 4097 cultured in PDB medium with added IO 33 g/L can be seen in Figure 3.14. The growth was assessed based on the biomass estimation by dry cell weight measurement. As can be seen, the growth gradually increased from zero time to 72 hours, and slightly fluctuated until reaching a peak at 96 hours. The biomass then decreased sharply until the process ended at 108 hours. The maximum dry cell weight achieved was 6.9 g/L at 96 hours. From the trend of AQP 4097 growth curve, it can be clearly seen that this fungus showed no significant lag phase before growth commenced, and growth continued for around 72 hours before entering a brief stationary phase founded by a decline phase.

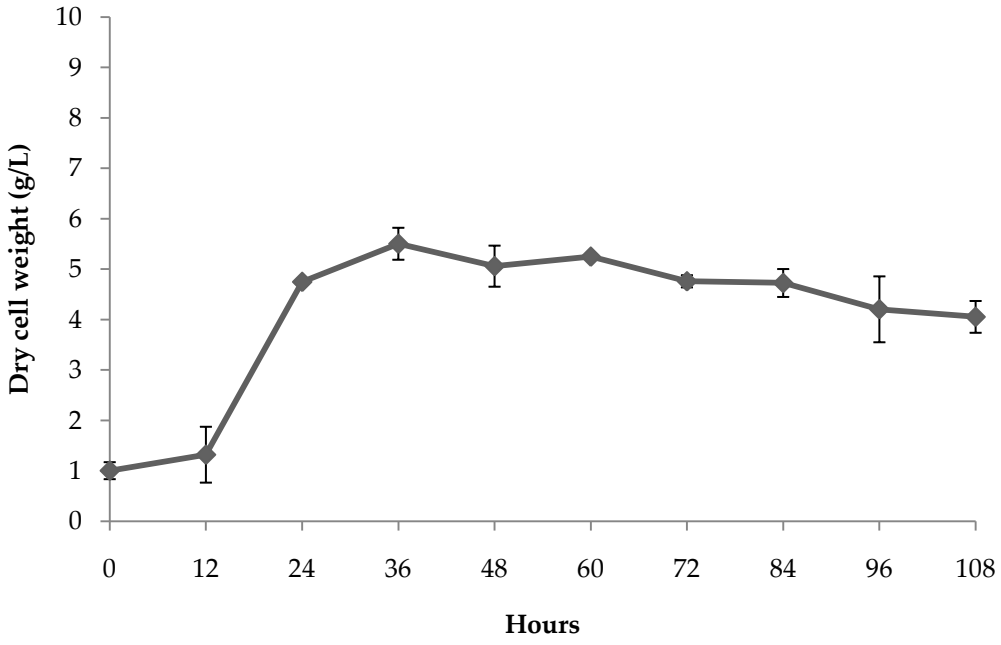

Figure 3.65 Growth of fungal isolate AQP 4097 in MYGP medium at 26◦C, rotary shaker speed 220 rpm in a 250 ml shake flask.

The growth of AQP 4097 in MYGP medium is shown in Figure 3.15. It can be seen that there was a short lag phase until 12 hours, and then the biomass

rose sharply by 4-fold between 12 hours and 24 hours. Afterwards, the growth continually increased until of reached the highest level at 36 hours, and gradually decreased thereafter. The maximum dry cell weight derived was 5.5 g/L at 36 hours. It is clear that although there is a short (12 hour) lag in this medium thereafter growth is more rapid than in PDB/IO 33 g/L and biomass peaked within 36 hours.

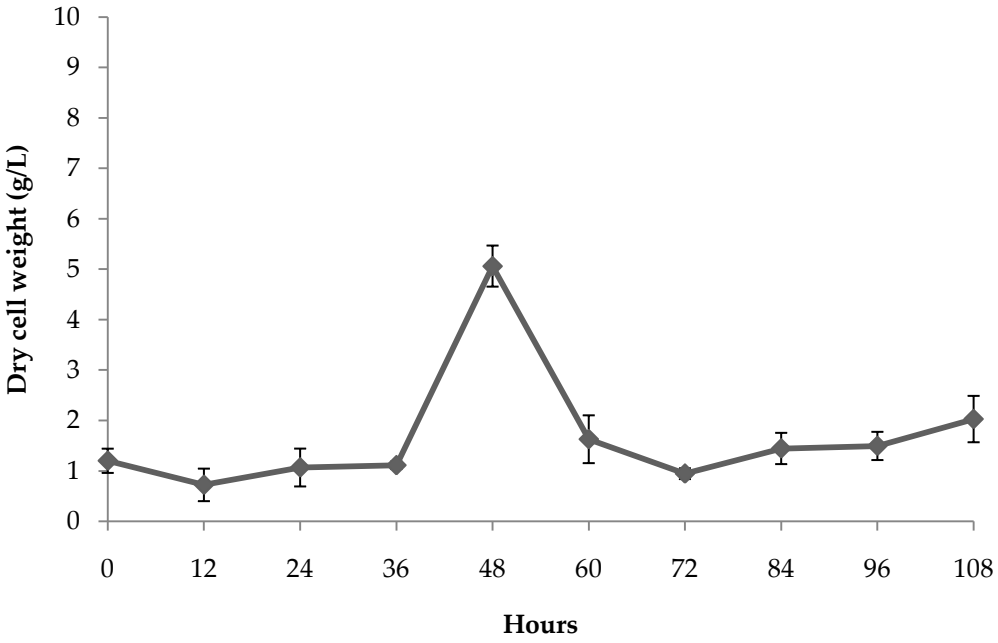

Figure 3.76 Growth of fungal isolate AQP 4097 culture in Czapex-Dox medium at 26◦C, rotary shaker speed 220 rpm in a 250 ml shake flask.

Figure 3.16 shows the growth of AQP 4097 cultured in Czapex -Dox medium. From zero time to 36 hours, there was a lengthy lag phase. After this lag, cell dry weight suddenly increased 5-fold between 36 hours and 48 hours. Consequently, it reached a peak at 48 hours and then the biomass decreased

to nearly the same level it had reached at 48 hours. It can be clearly seen that in this medium AQP 4097 showed a lengthy lag phase and barely grew over the first 36 hours. Thereafter, there was a brief, but very rapid growth phase where a maximum biomass of 5 g/L was achieved within the space of a day. Following the growth phase was a very rapid decline phase, perhaps suggesting that a key nutrient in the medium had been exhausted, or that conditions in the culture fluid had become unsuitable or inhibitory to fungal culture. Clearly Czapek-Dox medium is far from ideal for culturing this isolate routinely, as shown by the long lag phase and rapid culture decline. Both would make preparation of inocula from this medium challenging.

The growth of AQP 4097 cultured in GY medium is presented in Figure 3.17. The growth increased by 4-fold within 24 hours after inoculation, broadly similar to that achieved in MYGP medium (Figure 3.15). It reached the highest level at 48 hours, and then gradually declined until the process end. It can be seen that in this medium again there was no clear lag phase present, and that the culture grew to a maximum biomass of 4.9 g/L within 48 hours after inoculation. Thereafter culture biomass declined slowly over the remaining culture period.

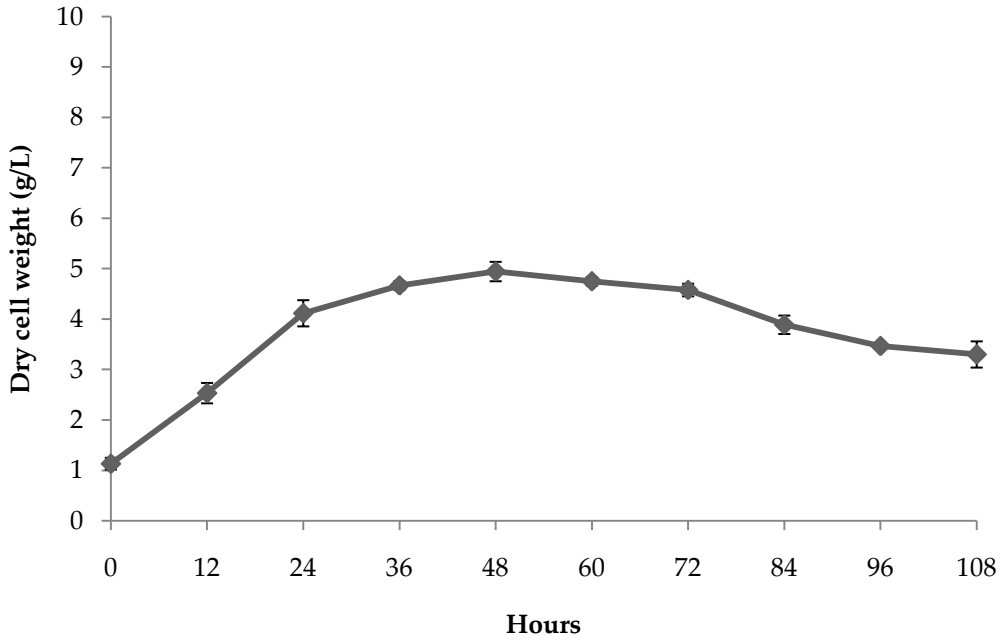

Figure 3.8 Growth of fungal isolate AQP 4097 culture in GY medium at 26◦C, rotary shaker speed 220 rpm in a 250 ml shake flask.

3.3.1.2 Statistical analysis

Statistical analysis of growth based on maximum biomass achieved AQP 4097 is shown in Table 3.1. There was no significant different between PDB plus IO 33 g/L, MYGP and GY media. By contrast, growth in Czapek-Dox medium was significantly different from growth in the other three media. From these results it is clear that this fungal isolate actually grows faster and reaches maximal cell dry weight more quickly on simple media which includes a rapidly utilized carbon source such as MYGP and GY, than on the recommended medium used by the company.

Table 3.1 Statistical analysis of the influence of growth medium upon fungal growth (AQP 4097) comparing 4 media with culturing in shake flask experiments using One-way ANOVA and post-hoc methods (SPSS program, version 16.0)

ANOVA

growthrate

			Sum of Squares	df	Mean Square	F	Sig.
Between Groups	(Combined)		140.257	3	46.752	20.330	.000
	Linear Term	Contrast	34.197	1	34.197	14.871	.000
		Deviation	106.059	2	53.030	23.060	.000
Within Groups			266.756	116	2.300		
Total			407.013	119			

Multiple Comparisons

growthrate
Tukey HSD

(I) variable	(J) variable	Mean Difference (I-J)	Std. Error	Sig.	95% Confidence Interval	
					Lower Bound	Upper Bound
pda	mgyp	.42171	.39155	.704	-.5989	1.4423
	czapek	2.81615*	.39155	.000	1.7955	3.8368
	gy	.79344	.39155	.184	-.2272	1.8141
mgyp	pda	-.42171	.39155	.704	-1.4423	.5989
	czapek	2.39443*	.39155	.000	1.3738	3.4151
	gy	.37173	.39155	.778	-.6489	1.3924
czapek	pda	-2.81615*	.39155	.000	-3.8368	-1.7955
	mgyp	-2.39443*	.39155	.000	-3.4151	-1.3738
	gy	-2.02271*	.39155	.000	-3.0433	-1.0021
gy	pda	-.79344	.39155	.184	-1.8141	.2272
	mgyp	-.37173	.39155	.778	-1.3924	.6489
	czapek	2.02271*	.39155	.000	1.0021	3.0433

*. The mean difference is significant at the 0.05 level.

This finding is in agreement with the report of Adejoye and Fasidi (2009) which stated that using glucose as a sole carbon source supported the highest biomass yield of the fungus *Schizophyllum commune* (FR.), and the study by Gbolagade *et al.* (2006) which compared the effects of types of monosaccharides upon biomass production of *Pleurotus florida* (mont.), reported that glucose stimulated the highest biomass production (6.22 g/L)

followed by fructose mannose, and sorbose (P 0.05). In addition, Mojsov (2010) reported that glucose stimulated the highest biomass production by *A. niger* compared with fructose, pressed apple pulp, galactose, lactose, and apple pectin. Feeding glucose at 24 hours after inoculation also stimulated both biomass and enzyme production by the white-rot fungus *Phanerochaete chrysosporium* (Xiaoyan *et al.*, 2007). Moreover, using a combination of glucose, a rapidly utilized sugar, together with a slow release carbon source such as rice bran also stimulated biomass production in *A. niger* (Oshoma & Ikenebomeh, 2005).

3.3.2 Conclusions

Overall, it can be clearly seen that Czapek-Dox is not suitable as a growth medium for this isolate, due to sodium nitrate which is the sole source of nitrogen in the composition of this medium and which cannot be utilised by some species of bacteria and some classes of fungi such as Chytridiomycetes, Oomycetes, and Basidiomycetes (Garraway and Evans, 1984). The simple medium, GY, was chosen for future cultivation of this fungus for studying the growth and metabolome development in fermenter cultures. In addition to the good growth in GY, this medium has only one major C and energy source and one N source, allowing easy optimization of the ratio of C to N source in subsequent research.

3.4 The effect of initial glucose concentration on biomass and lovastatin derivative production of AQP 4097

In the previous experiments, GY medium was chosen for studying the growth and metabolome evolution of isolate AQP 4097 due to the consistency with which it promoted growth in shake flask experiments. In this next part of the project, the effect of initial glucose concentration on biomass and the production of the target compound, a derivative of lovastatin, by AQP 4097 cultured in batch cultures in a fermenter vessel was investigated. Batch processes for each concentration of glucose were carried out in a 1L Braun Biostat Q bioreactor in duplicate.

Inoculums preparation, culture conditions, dry cell weight measurement, statistical analysis of the fungal growth compare in each media, extraction procedure using Bligh and Dyer method, and the metabolomics quantification was performed as described in section 2.12, 2.2.3, 2.6.1.1, and 2.6.4.1., respectively.

3.4.1 Results and Discussion

3.4.1.1 Growth of AQP 4097 cultured in GY with 10 g/L glucose in a BiostatQ bioreactor

Figure 3.18 shows the relationship between the growth and glucose consumption by isolate AQP 4097 cultured in GY medium with 10 g/L glucose. As can be seen from the Figure, the growth increased gradually from zero time, and reached a peak within 48 hours, while glucose in the medium was completely consumed by that point. From 48 hours to 120 hours, the biomass slowly declined until the process ended. It can be seen that this isolate grew rapidly under these operational conditions until

biomass reached a peak at 48 hours after inoculation. This cell growth was associated with consumption of all the glucose in the medium, after which the cell mass gradually decreased until the process end. The maximum biomass derived from AQP 4097 was 4.73 g/L at 48 hours. However, despite cultivation in the fermenter the growth of this fungus was broadly similar in pattern compared with the same medium in shake flasks (Figure 3.17)

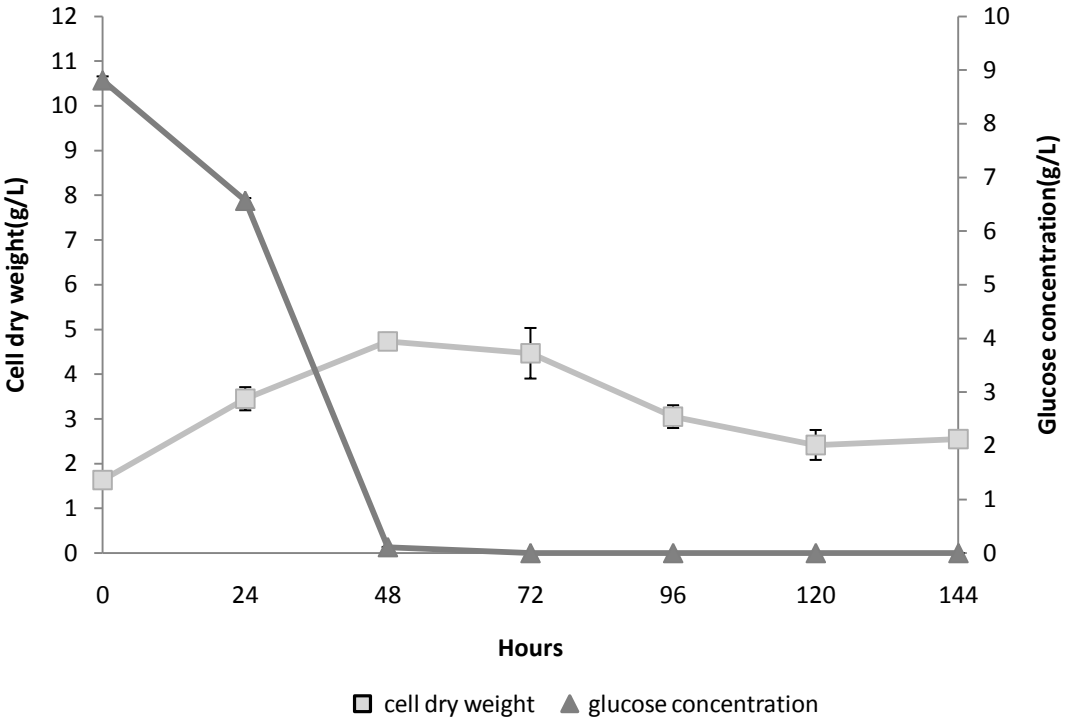

Figure 3.98 The growth and glucose concentration of fungal isolate AQP 4097 cultured in GY medium with 10 g/L glucose in a BiostatQ bioreactor.

The relationship between dissolved oxygen tension (DOT) and stirrer rate in batch cultures of fungal isolate AQP 4097 cultured in GY medium with 10 g/L glucose in the bioreactor is shown in Figure 3.19. DOT rapidly decreased to around 40% saturation within 48 hours, and this was closely associated with the culture growth which was rapid in this phase (as shown in Figure 3.18). After 48 hours, DOT gradually increased till the process end. This was probably due to the cessation of growth due to glucose exhaustion.

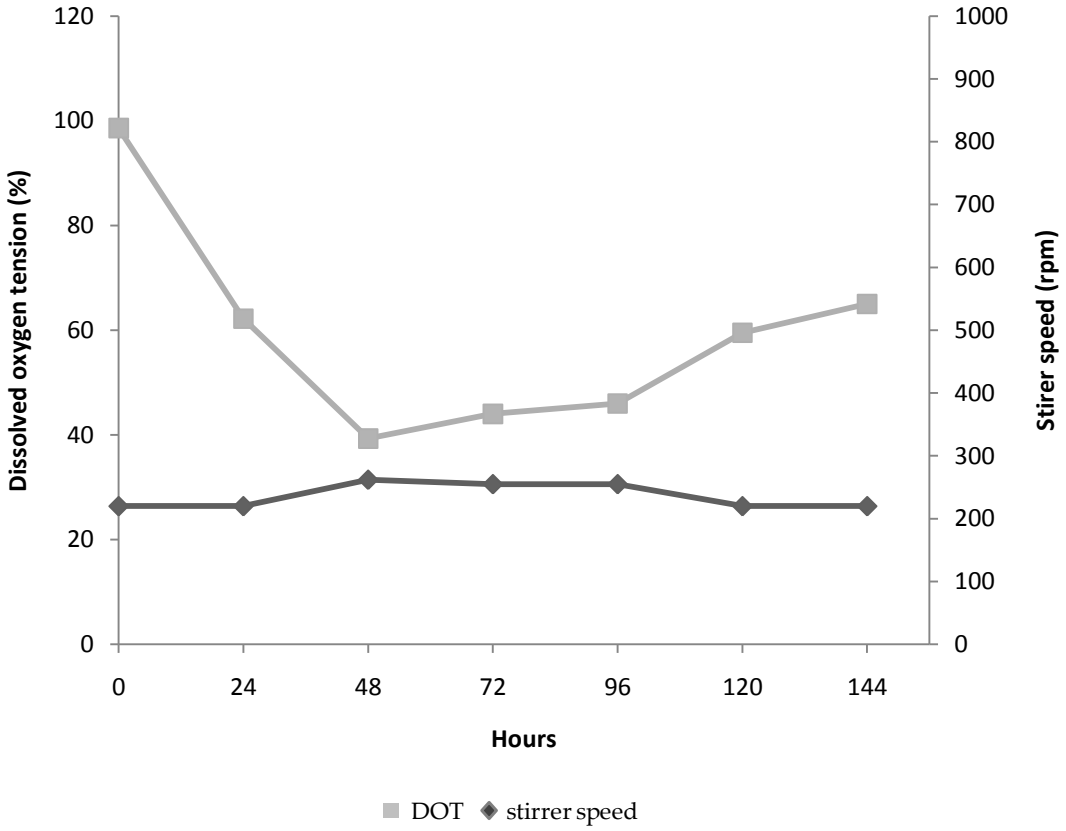

Figure 3.10 Dissolved oxygen tension and stirrer speed of fungal isolate AQP 4097 cultured in GY medium with 10 g/L glucose in a BiostatQ bioreactor.

3.4.1.2 Growth of AQP 4097 cultured in GY with 20 g/L glucose in a BiostatQ bioreactor

Figure 3.20, shows the relationship between growth and glucose consumption of AQP 4097 cultured in GY medium with glucose 20 g/L; biomass increased rapidly by six fold from zero time to 48 hours, reached its peak at 72 hours and this was associated with a decrease in glucose from zero time, leading to glucose exhaustion by 72 hours. After 72 hours, the growth declined until the end of the process. It may be that this medium is not entirely suitable for culturing this organism because although the growth was rapid in the early process phase after inoculation, biomass levels fell very rapidly after 72 hours presumably due to glucose exhaustion again. The maximum biomass achieved was 9 g/L at 72 hours; double that of GY with 10 g/L glucose.

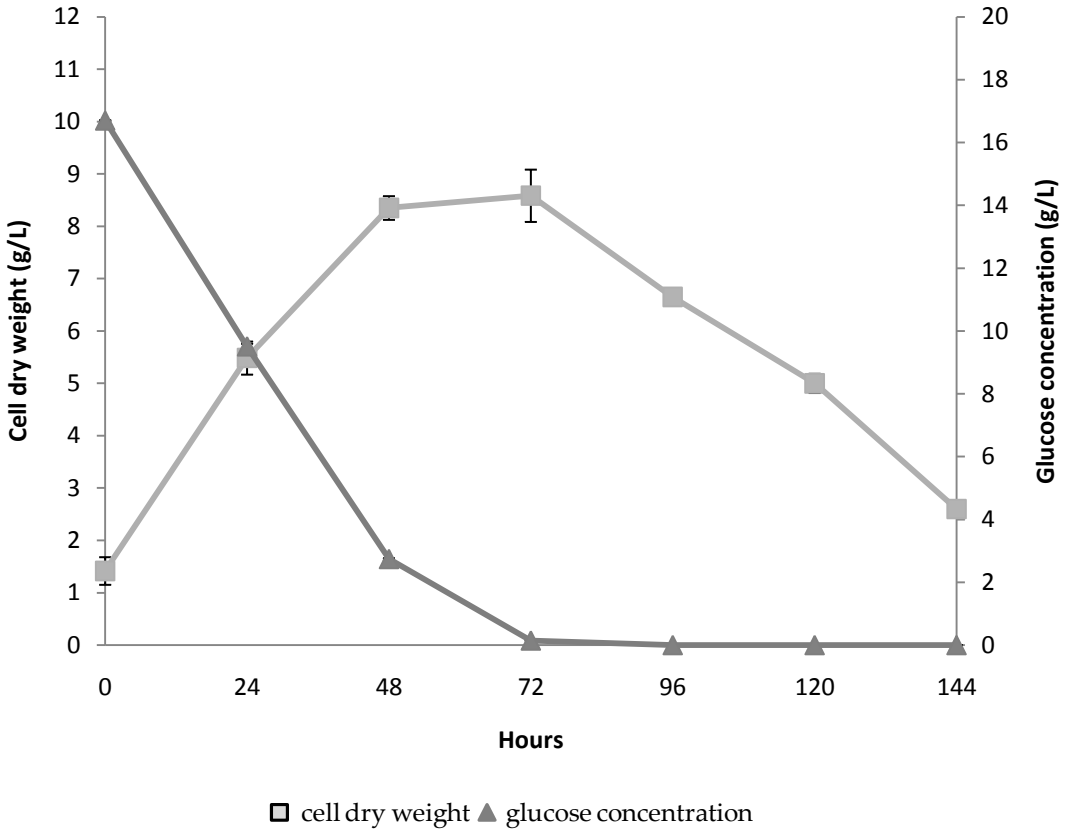

Figure 3.11 The growth and glucose concentration of fungal isolate AQP 4097 cultured in GY medium with 20 g/L glucose in a BiostatQ bioreactor.

The relationship between DOT and stirrer rate in batch cultures of AQP 4097 cultured in GY medium with 20 g/L glucose in the bioreactor is shown in Figure 3.21. The level of DOT in the medium dropped sharply to zero within 24 hours leading to an increased stirrer speed rate of 800 rpm. Then DOT was gradually increased due to the depletion of glucose and associated reduction in cell mass (Figure 3.20). It is worth noting that these cultures became oxygen limited early in the process and that this led to a reduced growth rate after the onset of oxygen limitation. The short stationary phase could have clear implications for secondary metabolite synthesis.

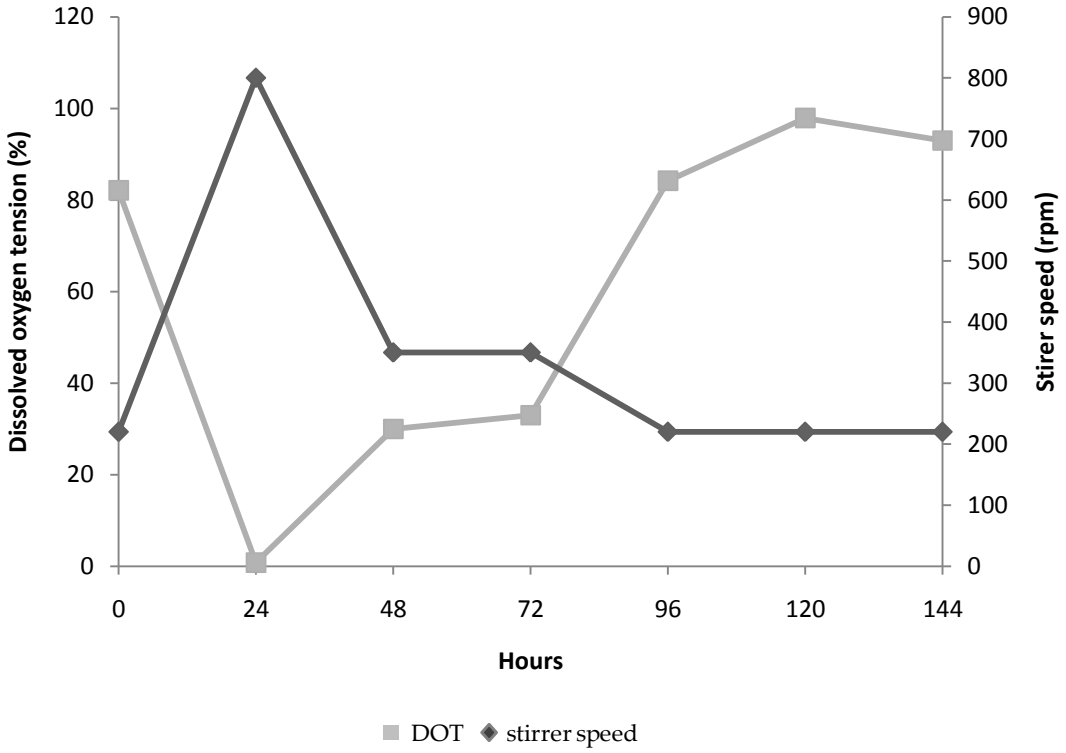

Figure 3.12 Dissolved oxygen tension and stirrer speed of fungal isolate AQP 4097 cultured in GY medium with 20 g/L glucose in a BiostatQ bioreactor.

3.4.1.3 Growth of AQP 4097 cultured in GY with 30 g/L glucose in BiostatQ bioreactor

The relationship between the growth of AQP 4097 and glucose concentration in GY medium with 30 g/L glucose is shown in Figure 3.22. From Figure 3.22 it can be seen that growth commenced rapidly in this medium and the biomass maximum was achieved at 72 hours after inoculation. Biomass entered a stationary phase after that with no significant decline in cell mass noted in the experimental period.

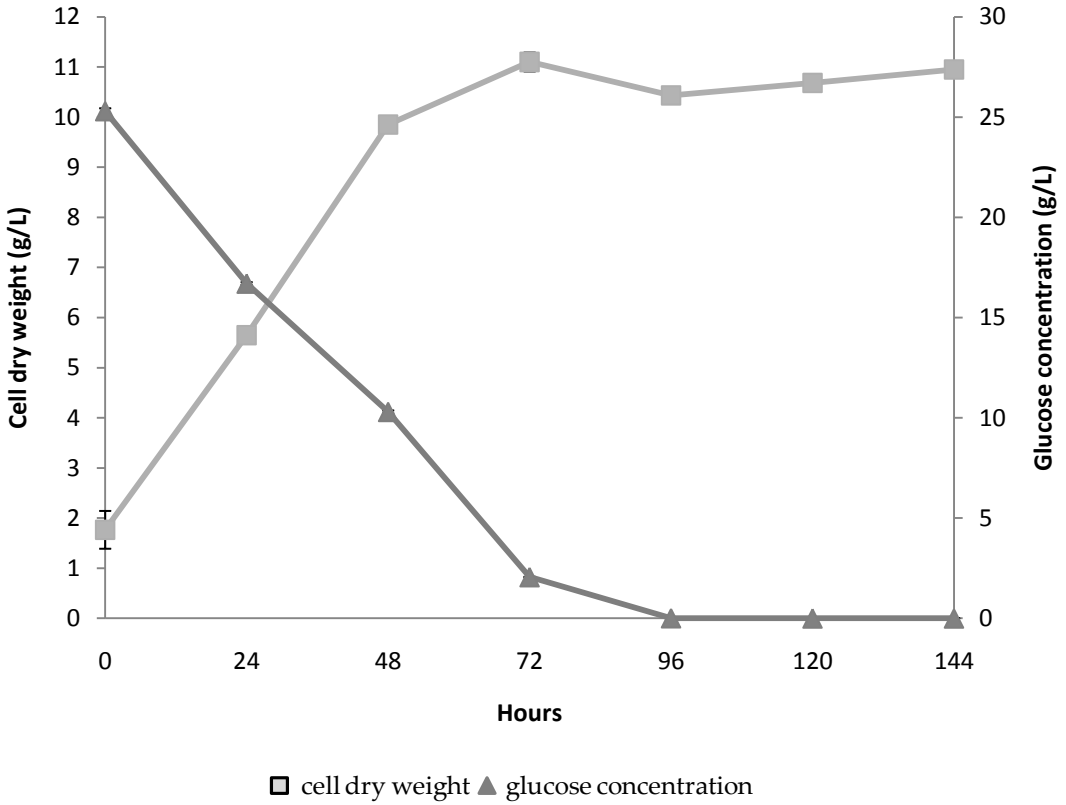

Figure 3.13 The growth and glucose consumption of fungal isolate AQP 4097 cultured in GY medium with 30 g/L glucose in a BiostatQ bioreactor.

The higher initial glucose level resulted in a lengthier period of glucose consumption of up to 96 hours. The maximum biomass achieved in these processes was around 11 g/L at 72 hours after inoculation, higher than that with GY with 20 g/L glucose which was 9 g/L (Figure 3.20), and GY medium containing 10 g/L glucose which was 4.73 g/L (Figure 3.18).

The changes in DOT and stirrer rate in batch cultures of AQP 4097 cultured in GY medium containing 30 g/L glucose in a bioreactor is shown in Figure 3.23.

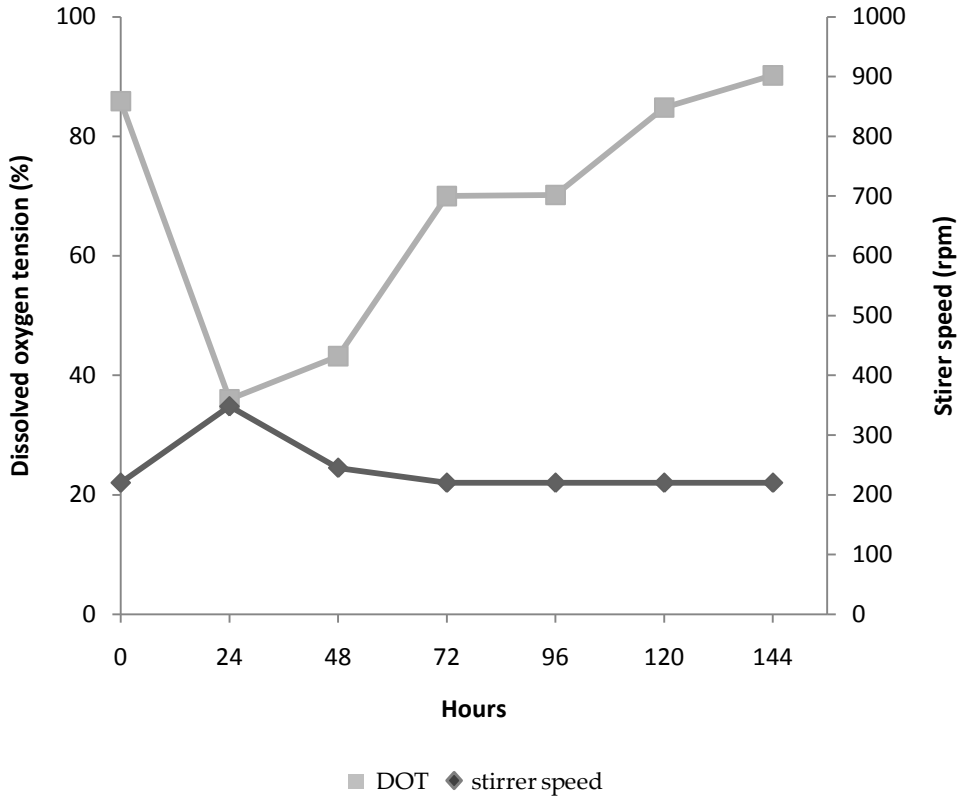

Figure 3.14 Dissolved oxygen tension and stirrer speed of fungal isolate AQP 4097 cultured in GY medium with 30 g/L glucose in a BiostatQ bioreactor.

It can be seen from Figure 3.23 that the DOT in the medium dropped sharply to below 40% saturation within 24 hours, afterwards gradually increasing until the end of the process. The stirrer speed slightly increased at 24 hours, but afterwards remained constant as the level of DOT was above the set point of 30% saturation.

3.4.1.4 Statistical analysis of the effects of glucose concentration on growth of AQP4097

Statistical analysis of growth based on maximum biomass achieved by AQP 4097 from Table 3.2 indicates that there were no significant differences

between the growth of AQP4097 cultured in GY medium containing 20 g/L and 30 g/L glucose. While growth in GY medium containing 10 g/L glucose is significantly different from growth in the other two media. However, GY medium containing 20 g/L glucose is not entirely suitable for culture of this fungus due to the short stationary phase which is an important phase during which it would be expected that secondary metabolite formation would occur.

Table 3.2 Statistical analysis of the influence of growth medium upon fungal growth (AQP 4097) used One-way ANOVA and post-hoc methods (SPSS program, version 16.0)

ANOVA

growthrate

			Sum of Squares	df	Mean Square	F	Sig.
Between Groups	(Combined)		101.058	2	50.529	9.756	.000
	Linear Term	Contrast	99.803	1	99.803	19.270	.000
		Deviation	1.255	1	1.255	.242	.625
Within Groups			201.993	39	5.179		
Total			303.052	41			

Multiple Comparisons

growthrate
Tukey HSD

(I) variable	(J) variable	Mean Difference (I-J)	Std. Error	Sig.	95% Confidence Interval	
					Lower Bound	Upper Bound
glucose 10g	glucose20g	-2.25464*	.86018	.033	-4.3503	-.1590
	glucose30g	-3.77593*	.86018	.000	-5.8716	-1.6803
glucose20g	glucose 10g	2.25464*	.86018	.033	.1590	4.3503
	glucose30g	-1.52129	.86018	.193	-3.6169	.5744
glucose30g	glucose 10g	3.77593*	.86018	.000	1.6803	5.8716
	glucose20g	1.52129	.86018	.193	-.5744	3.6169

*. The mean difference is significant at the 0.05 level.

3.4.1.5 Effect of initial glucose on Lovastatin derivative production

The production of a lovastatin derivative by AQP 4097 in GY medium with differing initial glucose concentrations is shown in Figure 3.24. It can be seen that with the 30 g/L initial glucose which gave the highest lovastatin

derivative concentration, the concentration of this analyte was fairly steady up to 96 hours but rose to its maximum of 1.89 mg/L at 120 hours, while glucose completely ran out in the medium by 96 hours (as shown in Figure 3.22). By contrast in the medium with 10 g/L glucose no lovastatin derivative production was seen before 48 hours, thereafter the concentration rose steadily to reach a maximum of 1.63 mg/L.

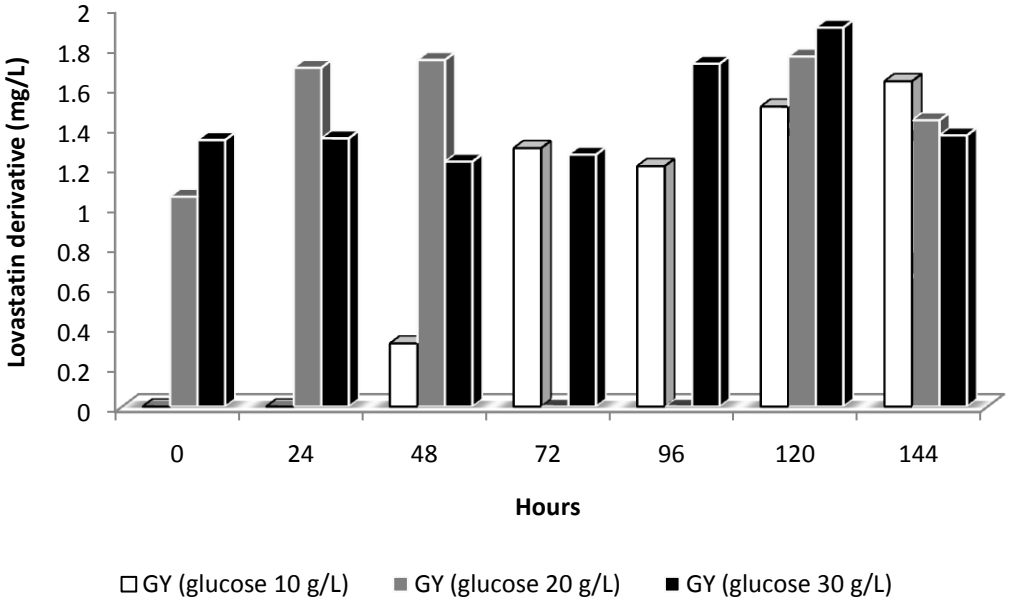

Figure 3.15 Lovastatin derivative production by fungal isolate AQP 4097 cultured in GY medium with 10 g/L, 20 g/L, and 30 g/L glucose in a Biostat Q bioreactor.

As shown in Table 3.2 although there were no significant differences in growth between the cultures in 20 and 30 g/L media, in terms of lovastatin derivative production there were major differences. In the 20 g/L medium, the concentration of this analyte increased between 0 and 48 hours then remained high with a small decline towards the process end. The maximum target compound concentration derived from this isolate was 1.75 mg/L. The

undetectable production during 72 to 96 hours in GY medium with 20 g/L initial glucose (as shown in Figure 3.24), and the short stationary phase (as shown in Figure 3.20) may also have arisen from the steep increase in the stirrer rate speed up to 800 rpm (as shown in Figure 3.21) which might have caused mycelial damage. Overall, increasing initial glucose, promoted biomass and lovastatin derivative production by AQP 4097, which is broadly similar to the findings of Liu *et al.* (2010) who reported that an increase in initial glucose concentration within the range of 40 - 60 g/L led to enhancement of either biomass or lipid yield in *Thamnidium ctenidium*, whereas higher levels of glucose above this range did not increase the lipid and biomass production. Moreover, Rojas *et al.* (2008) reported that increasing the initial glucose concentration in the medium enhanced biomass production of *Geotrichum klebahnii* up to 2.5 fold. C:N ratio is the main factor affecting the growth of fungi such as ectomycorrhizal fungi, e.g. *Pisolithus microcarpus*; Rossi and Oliveira (2011) reported that increasing the glucose concentration in these cultures promoted biomass production by up to 40%. In addition, increasing the stirrer rate led to extensive damage to the mycelium leading to decreased biomass and lovastatin derivative production. These findings were supported by the study of Higashiyama (2002) which reported a decrease of arachidonic acid in *Mortierella sp.* derived from mycelial damage due to shear stress in the bioreactor. In addition Xu *et al.* (2006) compared the production of exopolysaccharides (EPS) of *Paecilomyces tenuipes* strain C240 in two types of bioreactor, stirred-tank (STR) and airlift reactors, and reported that STR bioreactor gave the higher biomass production, while specific production rate of EPS was significantly higher in the airlift reactor than that achieved in the STR. In spite of high agitation rates (> 400 rpm) causing severe mycelial damage due to shear stress, and

reducing biomass production in a recombinant *A. niger* strain AB4, by contrast high agitation rates in these cultures led to a beneficial decrease in protease activity, which in turn led to increased Green Fluorescent Protein (GFP) production (Wang *et al.*, 2003)

3.4.2 Conclusions

In summary, increasing the initial glucose up to 30 g/L promoted the highest biomass (11 g/L at 72 hours) and lovastatin derivative production (1.89 mg/L at 120 hours) in AQP 4097. Increased stirrer rate seemed to impact upon both biomass and lovastatin derivative production, possibly owing to damage to the mycelium. The 20 g/L glucose overall seemed to be poorer for lovastatin derivative production when compared to 30 g/L glucose medium.

3.5 Effect of salinity on biomass formation, gamma linoleneic acid and Lovastatin derivative production in a bioreactor

This experiment was conducted using the study by Adebayo *et al.* (1971) which showed variation in growth or stress in microorganisms was related to nutritional imbalances and that dissolution of nutrients in each environment varied due to water activity also known as water potential. Nevertheless, each microorganism has a specific optimal water potential for growth and sporulation, in general, the range of water activity that is suitable for growth of fungi is 0.55 to 1.00 or solute potential equal to -81 – 0 MPa (Griffin, 1996) is a more solid substrate is better for fungal growth.

In this experiment, the effect of different IO concentrations on growth of the fungus was investigated in a 1L Bioreactor (Biostat Q, Braun) and biomass, metabolomics analysis, and morphological characteristics were observed and measured.

Inoculums preparation, culture conditions, dry cell weight measurement, statistical analysis of the fungal growth compare in each media, extraction procedure using Bligh and Dyer method, and the metabolomics quantification was performed as described in section 2.12, 2.2.3, 2.6.1.1, and 2.6.4.1., respectively.

3.5.1 Results and Discussion

3.5.1.1 Growth of AQP 4097 cultured in GY without IO in BiostatQ bioreactor

Figure 3.26 shows the relationship between the growth of AQP 4097 cultured in GY medium without IO and the consumption of glucose by the fungus in this medium. The growth was assessed based on the biomass estimation by dry cell weight measurement. It can be seen that fungal growth gradually rose after inoculation and increased eight fold from 24 hours to 72 hours and around half the glucose was consumed by this stage.

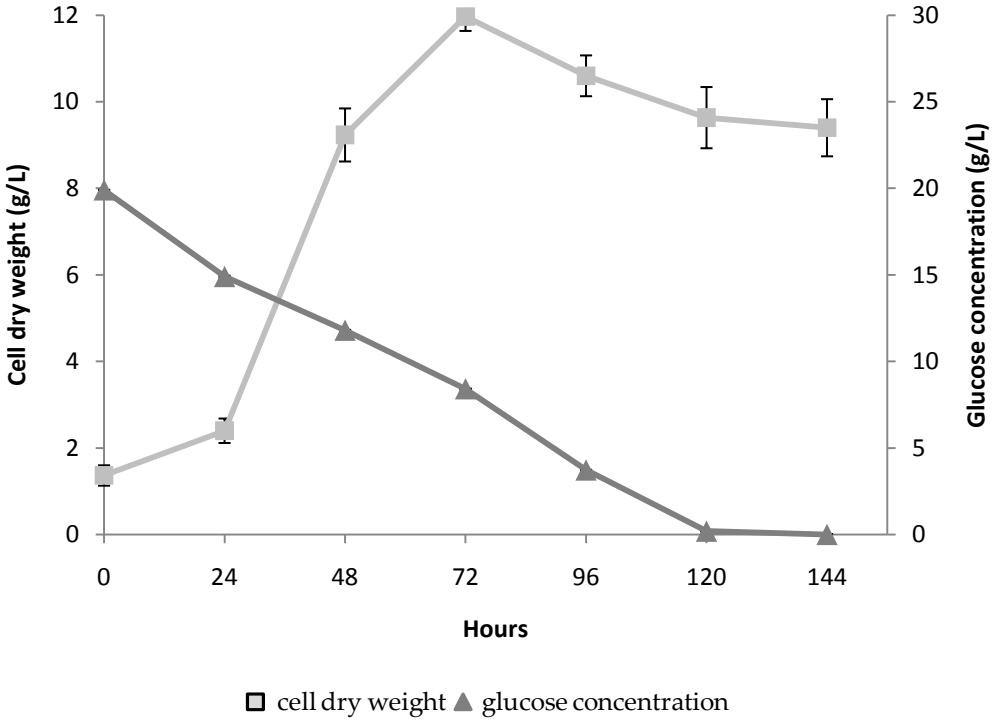

Figure 3.16 The growth and glucose concentration of fungal isolate AQP 4097 culture in GY medium without IO in the a BiostatQ bioreactor.

From 72 hours to 144 hours, the biomass slowly declined, while glucose levels decreased gradually and ran out at 120 hours. The maximum cell dry weight achieved was 11.9 g/L.

The changes with time in DOT in the medium and stirrer speed are shown for this fermentation process in Figure 3.26. As can be seen from Figure 3.26, DOT decreased rapidly from time zero and reached zero by 72 hours, at this point, as shown in Figure 3.25, the culture was rapidly growing and maximum dry cell weight was achieved. After 72 hours, the DOT remained unchanged till the end of the fermentation process.

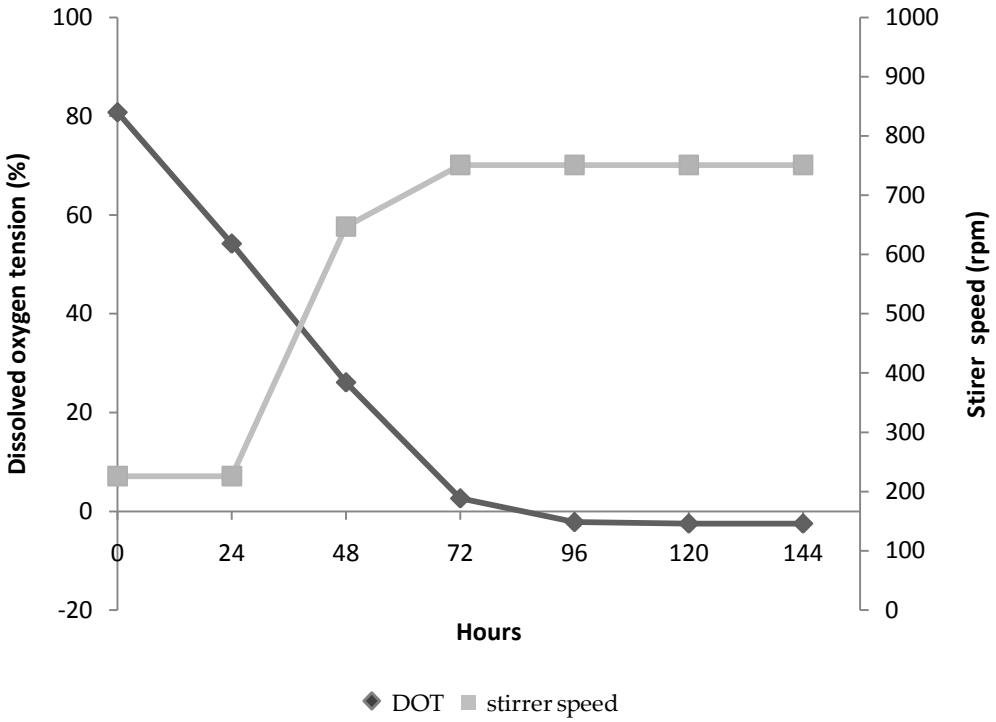

Figure 3.17 Dissolved oxygen tension and stirrer speed of fungus isolate AQP 4097 cultured in GY medium without IO in a BiostatQ bioreactor.

It is noticeable that despite the early onset of growth, the stirrer speed did not increase until after 24 hours by which time the concentration of biomass had slightly increased. In combination with presumably an increased metabolic activity level, led to an increased oxygen demand by the culture met by increased agitator speed until the agitator speed reached its maximum setting for this fermenter. This was maintained until the process

end despite biomass actually decreasing during this period, perhaps indicating continued metabolic activity in the culture to process end.

3.5.1.2 AQP 4097 cultured in GY with IO10 g/L

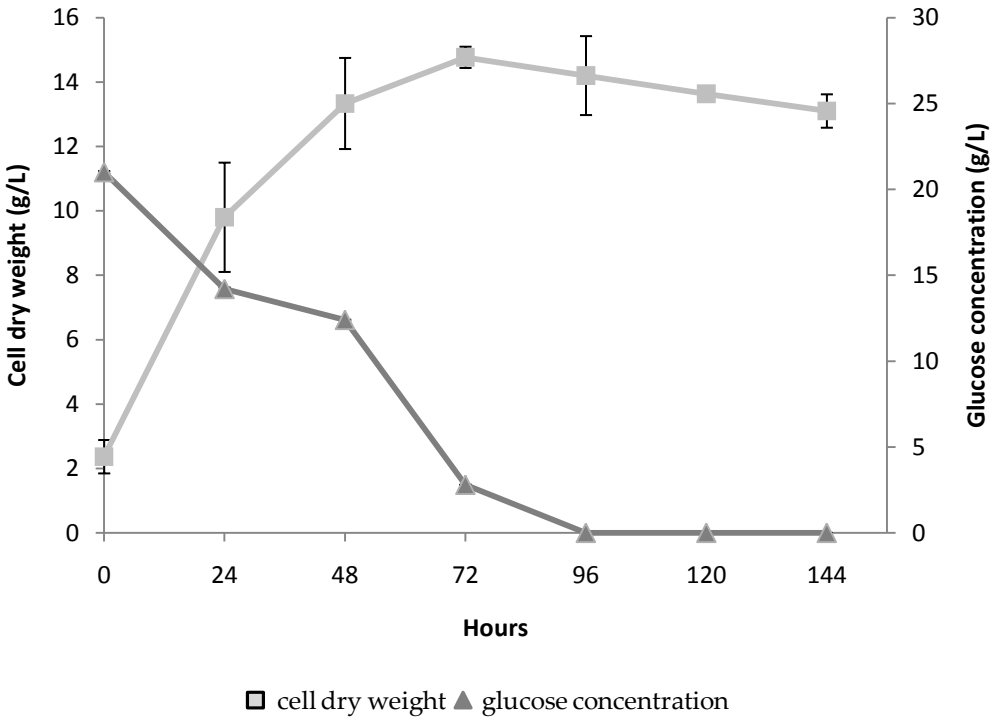

Figure 3.18 The growth and glucose consumption of fungal isolate AQP 4097 cultured in GY medium with IO 10 g/L in a BiostatQ bioreactor.

The relation between the growth of the fungus cultured in GY medium with 10 g/L IO and the consumption of glucose in this medium can be seen in Figure 3.27.

It can be seen that the growth increased rapidly seven fold from zero time to 72 hours and almost all of the glucose was consumed by the culture by this stage. Afterwards, the growth slightly declined while glucose dropped and was fully utilized by 96 hours. This medium gave a higher maximum dry cell

weight of around 14.8 g/L, and also a shorter lag phase when compared with GY medium without IO (Figure 3.25).

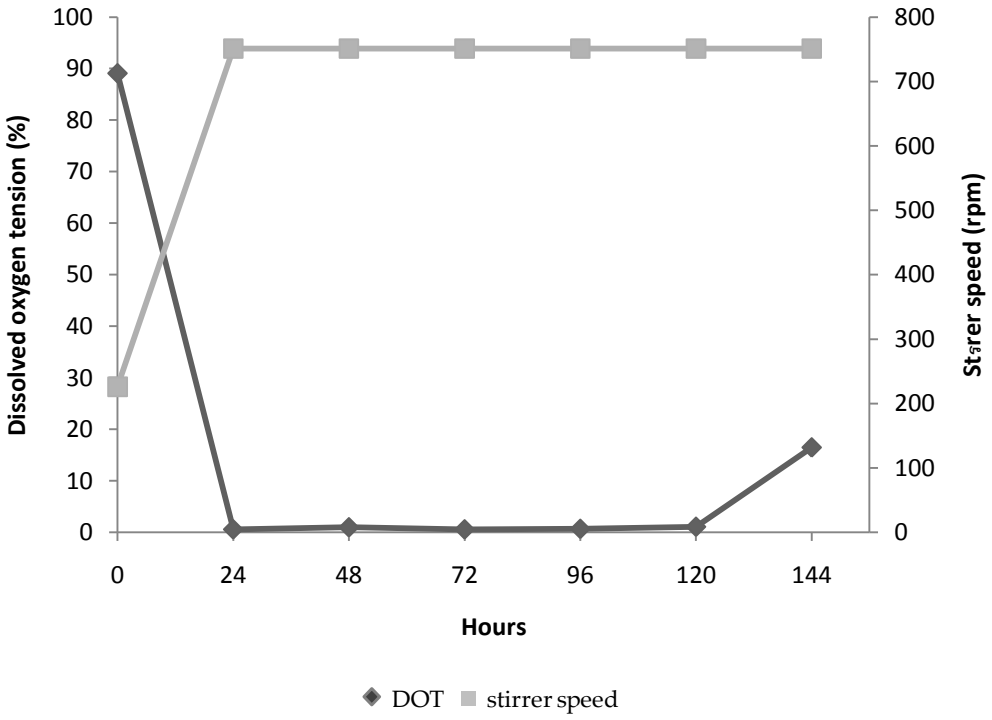

Figure 3.19 Dissolved oxygen tension and stirrer speed of fungus isolate AQP 4097 cultured in GY medium with IO 10 g/L in a BiostatQ bioreactor.

It can be seen from Figure 3.28 that DOT in the medium decreased rapidly to zero percent within 24 hours, owing to the fast growth of fungus (Figure 3.27); which led the agitator speed to increase up to 750 rpm to try to keep DOT at the set point. From 24 hours to 120 hours, it remained constant, and increased slightly in the last 24 hours of the experiment, due to the decline in cell mass and associated decrease in metabolism.

3.5.1.3 AQP 4097 cultured in GY with IO20 g/L

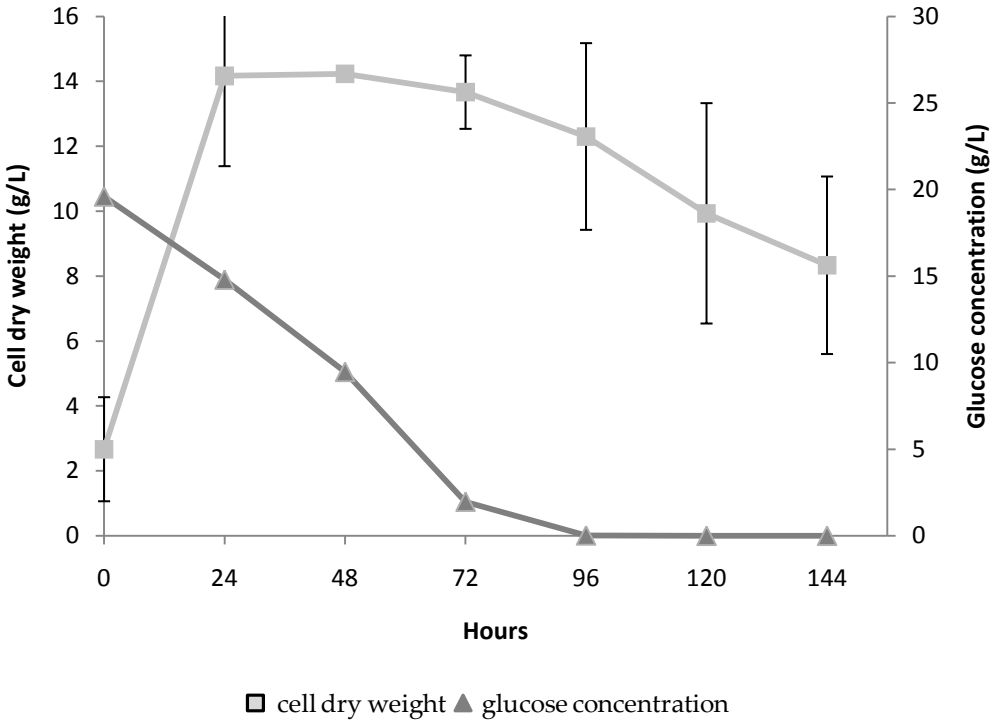

Figure 3.20 The growth and glucose concentration of fungal isolate AQP 4097 cultured in GY medium with IO 20 g/L in a BiostatQ bioreactor.

Figure 3.29 shows the relationship between growth of AQP 4097 cultured in GY medium with IO 20 g/L and the concentration of glucose in this medium. Fungal growth increased rapidly and reached the highest level within 48 hours, earlier than GY medium without IO, and GY medium with IO 10 g/L as shown in Figure 3.25 and Figure 3.27. This rapid growth was associated with a rapid decrease in glucose concentration and glucose was completely consumed by 96 hours. After 48 hours, the growth gradually declined till the end of the batch culture. The maximum dry cell weight achieved was 14.23 g/L at 48 hours.

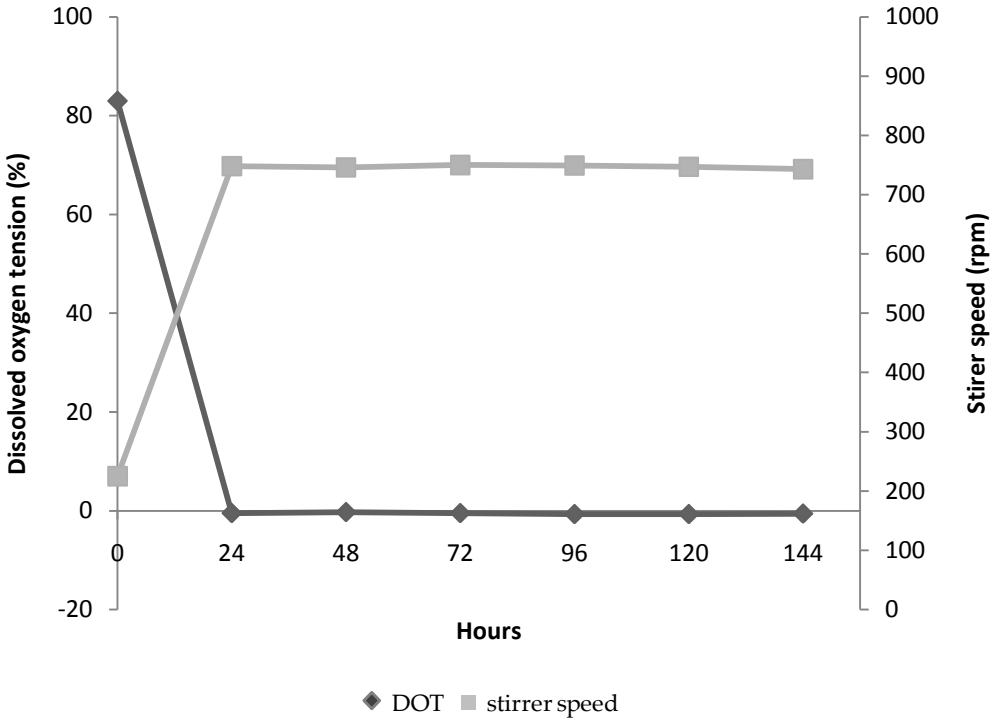

Figure 3.21 Dissolved oxygen tension and stirrer speed of fungus isolate AQP 4097 cultured in GY medium with IO 20 g/L in a BiostatQ bioreactor.

It can be seen in Figure 3.30 that DOT in the medium decreased sharply to zero percent within 24 hours in this medium, consequent upon the rapid culture growth (Figure 3.29) and the stirrer speed rose to 750 rpm at 24 hours to keep the DOT under controlled conditions as far as possible. After this it remained constant at near zero from 24 hours to 144 hours.

3.5.1.4 Statistical analysis

From Table 3.3, it can be seen that there were no significant differences between the growth of AQP4097 cultured in GY medium with the other two IO concentrations, 10 and 20 g/L based upon maximum cell dry weight achieved in each process. However, AQP 4097 grew fastest in GY medium

with 10 g/L IO and achieved a maximum cell dry weight around 14.8 g/L, which was slightly higher than when cultured in GY medium alone.

Table 3.3 Statistical analysis of the influence of salinity upon fungal growth (AQP 4097) using One-way ANOVA and post-hoc methods (SPSS program, version 16.0).

ANOVA

growthrate

	Sum of Squares	df	Mean Square	F	Sig.
Between Groups	54.182	2	27.091	3.492	.039
Within Groups	349.112	45	7.758		
Total	403.294	47			

Multiple Comparisons

growthrate
Tukey HSD

(I) variable	(J) variable	Mean Difference (I-J)	Std. Error	Sig.	95% Confidence Interval	
					Lower Bound	Upper Bound
GY	GY+10IO	-3.11454	1.56370	.126	-6.9043	.6753
	GY+20IO	-2.41048	1.56370	.282	-6.2003	1.3793
GY+10IO	GY	3.11454	1.56370	.126	-.6753	6.9043
	GY+20IO	.70406	1.56370	.895	-3.0857	4.4939
GY+20IO	GY	2.41048	1.56370	.282	-1.3793	6.2003
	GY+10IO	-.70406	1.56370	.895	-4.4939	3.0857

In accordance with the result of previous work, Kogej *et al.* (2006) reported that the growth of two species of yeast in the genus *Trimmatostroma* (*T. abietis* and *T. salinum*) isolated from extreme environments increased up to 16 and 26 percent, respectively, in sodium chloride amended media, and also growth of both species was slower and more restricted on the medium without added sodium chloride. Surprisingly, some marine-derived fungi

such as *Arthrinium c.f. saccharicolawere* grew faster in freshwater medium at 30°C, at pH 6.5, however, antibiotic productivity was higher in 34 ppt (parts per thousand) seawater (Miao *et al.*, 2006). From the present study, it is possible to conclude that the composition of the medium with for example sodium chloride, IO etc. has to be carefully considered and the culture conditions depends on the species of microorganism used. The effects of salt on the growth seem to vary markedly from species to species.

3.5.1.5 The effect of salinity upon the morphology of AQP 4097 in a bioreactor

A medium of higher osmotic potential can lead to changes in fungal morphology and spore pigmentation. However, one other response to such media involves the accumulation of compatible solutes inside the cells of marine microorganisms in order to protect against cell damage from high osmotic potential in the marine environment. The term compatible solute was introduced by Brown and Simpson (1972). They defined compatible solute as a solute which has a high concentration, and one which increases in concentration in the cell in response to increased salinity, and which has no significant effect on enzymic activity *in vitro.* Such compounds include glycerol (Beever and Laracy, 1986; Burke and Jennings, 1990; Ellis *et al.* 1991; Hernández-Saavedra *et al.*, 1995; Ramos *et al.*, 1999; Davis *et al.*, 2000, Ramirez and Chulze, 2004; Ruijter *et al.* 2004), mannitol (Ellis *et al.* 1991; Ramos *et al.* , 1999; Ruijter *et al.* 2004), sorbitol (Ruijter *et al.* 2004), arabitol (Ramos *et al.* , 1999; Ramirez and Chulze, 2004; Ruijter *et al.* 2004), erythritol (Beever and Laracy, 1986; Ramos *et al.*, 1999; Ruijter *et al.* 2004), trehalose (Davis *et al.*, 2000), proline (Luard,1982), and fatty acids (Raghukumar, 2008).

Davis *et al.* (2000) found that microorganisms can produce a cocktail of osmolytes rather than a single compound. In addition, at high concentrations larger compatible solutes generated higher osmotic pressures than smaller ones, though differences between the osmotic effects of compatible solute with three, four, five and six carbon atoms were not pronounced at lower (physiological) concentrations. In 1984, Jennings reported that these compounds act as physiological buffering agents, and function: (i) as carbohydrate reserves, (ii) as translocated compounds, (iii) in helping to generate the appropriate internal solute potential and (iv) in coenzyme regulation.

In the present study, the influence of salinity on the morphology of AQP 4097 was observed using light microscopy as shown in Figure 3.22, 3.33, 3.34.

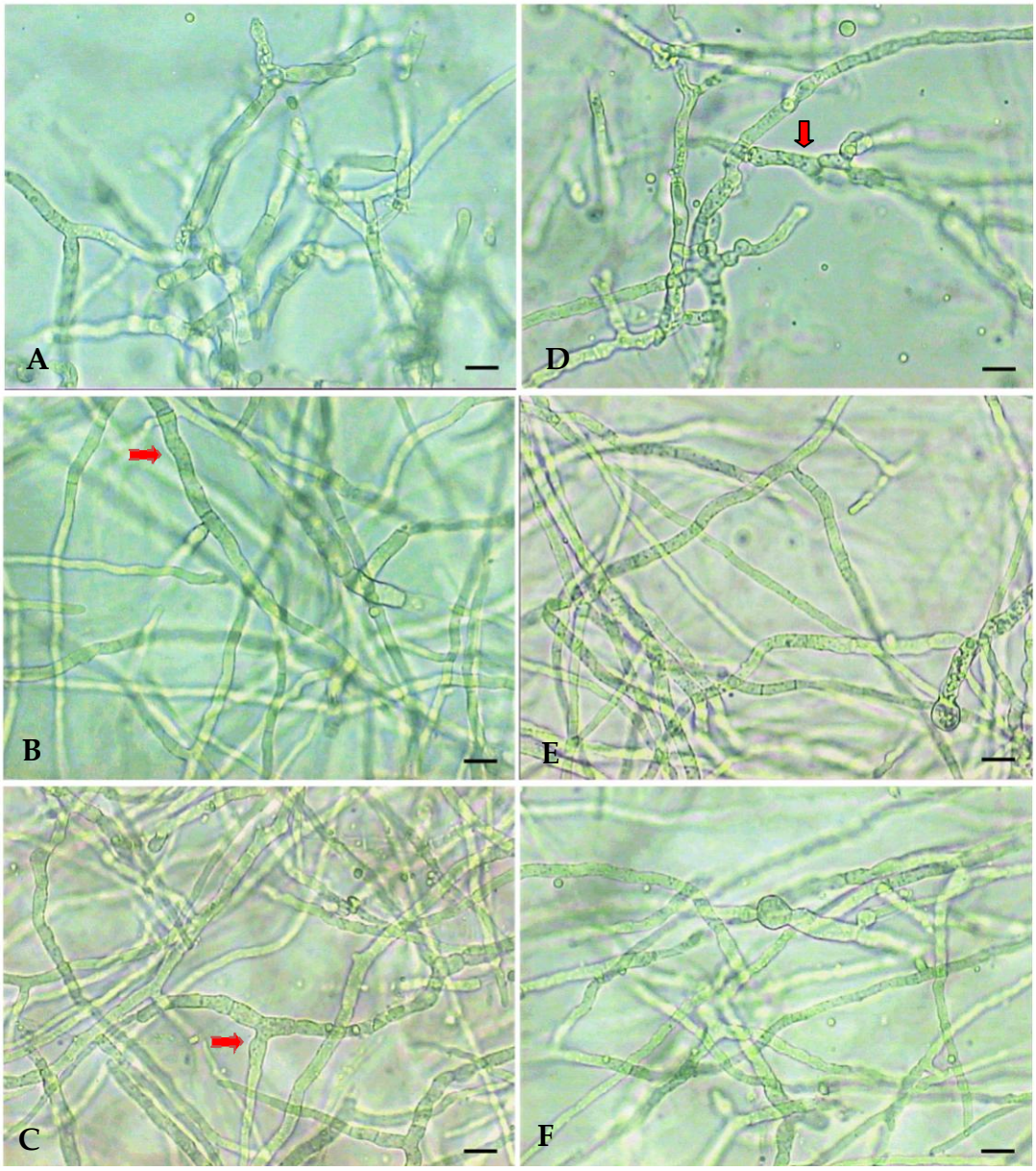

Figure 3.22 Morphological changes in mycelia of AQP4097 during batch fermentation at 36 hours (A-C) and 48 hours (D-F) of AQP 4097 with varying IO concentrations, 0 (A,D), 10 (B,E) and 20 g/L (C,F). Magnification = 20x, Bar = 1 μm The red arrows show the storage vacuoles produced in mycelium of fungus.

As can be clearly seen in Figures 3.31, AQP 4097 cultured in GY medium with IO 10 g/L (Figure 3.31 B) and 20 g/L (Figure 3.31C) started to produce

storage vacuoles, within 36 hours after inoculation. Whereas when AQP 4097 was cultured in GY medium (Figure 3.31 D) these were only apparent 12 hours later. At 48 hours, in GY medium plus IO 10 and 20 g/L some damage to the mycelium (Figure 3.32 A) possibly due to an increase in the stirrer speed was noted (Figure 3.28, and 3.30), and some hyphal lysis appeared, the damage was seen clearly at 96 hours (Figure 3.32 B).

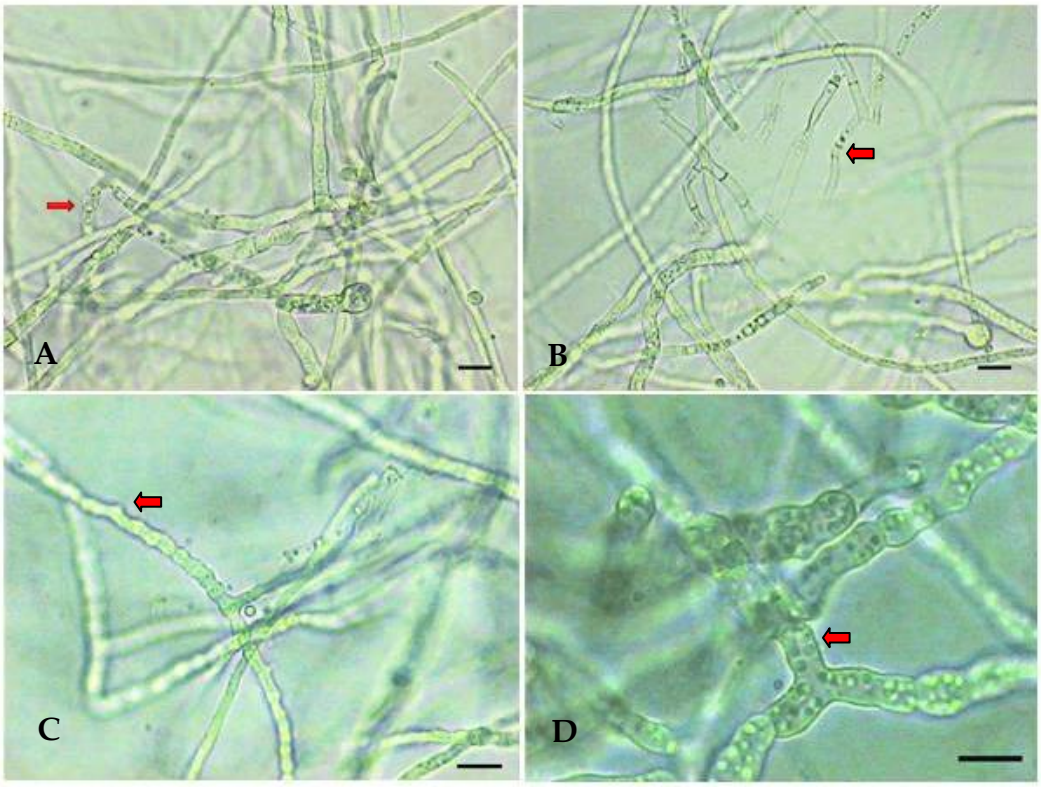

Figure 3.23 Morphological changes in mycelia during batch fermentation at 48 hours (A) and 96 hours (B) of fungus isolate AQP 4097 cultured in GY medium with IO 10 g/L at 84 hours (C) and with IO 20 g/L at 96 hours. Magnification = 20 (A-C), 40x (D), Bar = 1 μm. The red arrow indicates a damaged mycelium due to an increased stirrer speed (A), lysis hypha (B), swollen hyphae (c) and storage vacuoles (D).

In addition, the morphology of the culture which grew in GY medium with 20 g/L IO was different from that in other media, with short swollen sections

and smaller hyphae as shown in Figure 3.32 C, similar to a report by Kogej *et al.* (2006) that noted swollen round hyphae of *Trimmatostroma salinum* produced under lower osmotic potential. Apart from that characteristic, under these conditions there was also a vast amount of spherical storage vacuoles present (Figure 3.32 D).

Surprisingly, only GY medium with 20 g/L IO showed clear sporulation which began at 108 hours after inoculation as shown in Figure 3.33 A and by 144 hours a vast amount of conidia had been produced (Figure 3.33 B). This was in contrast with the result from experiment 3.1 (the effect of salinity and light on sporulation of AQP4097 on PDA plate) where 10 and 20 g/L of IO had resulted in sporulation. Perhaps the controlled conditions, in this fermenter batch culture such as pH and dissolved oxygen tension, also affected sporulation of this fungus.

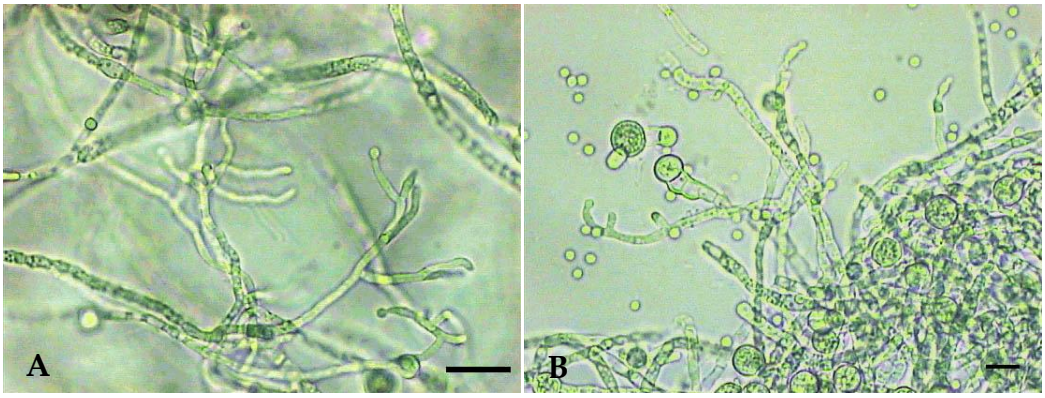

Figure 3.24 Morphological changes in mycelia during batch fermentation at 108 hours (A) and 144 hours (B) of fungus isolate AQP 4097 cultured in GY medium with 20 g/L IO. Magnification = 20x, Bar = 1 μm

Figure 3.34 illustrates the level of gamma-linoleic acid produced by AQP 4097 when cultured in two different concentrations of IO; GY medium plus

IO 10 g/L, and 20 g/L compared with GY medium without IO. At 72 hours after inoculation, gamma linolenic acid was initially detected in GY medium without IO, while in the other two media it was found 24 hours later. The amount of gamma-linolenic acid increased sharply (5-fold) from 72 hours to 96 hours, and suddenly dropped by more than half at the end of experiment. In GY medium with added IO 10 g/L and 20 g/L, the gamma-linolenic acids was initially detected at 96 hours, and it slightly fluctuated over the experiment (Figure 3.34).

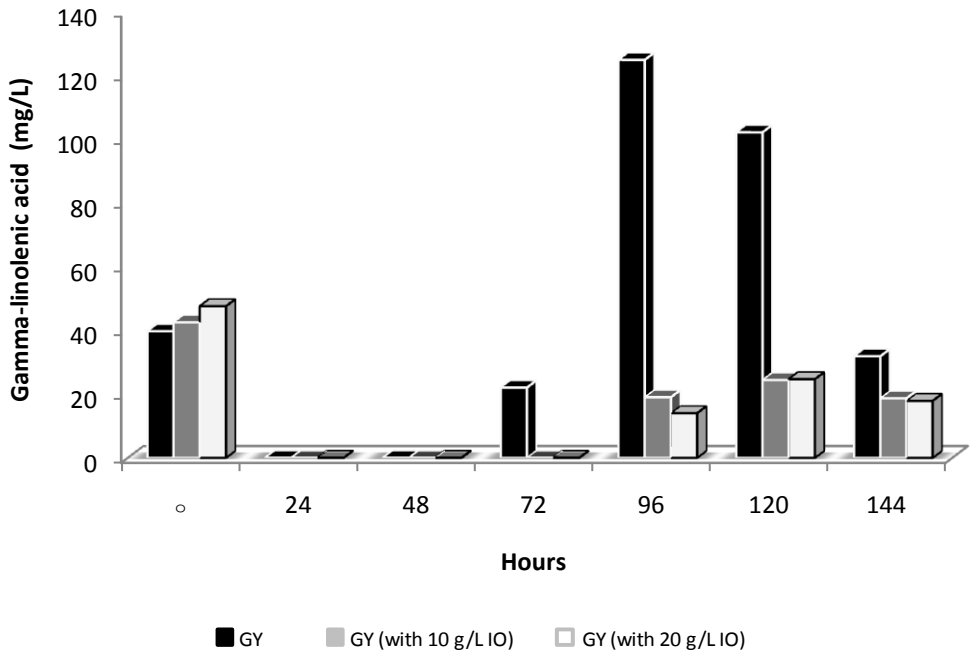

Figure 3.25 Time profile of gamma-linolenic acid produced by AQP 4097 during batch fermentation in GY medium plus two different concentrations of IO, 10 g/L and 20 g/L in a BiostatQ fermenter.

The highest gamma linolenic acid concentration achieved in GY medium was approximately 125 mg/L at 96 hours, higher than GY plus 10 g/L IO and GY plus 20 g/L IO by around five-fold. As can be clearly seen from Figure 3.34,

the culture started to produce gamma-linolenic acid at 72 hours in GY medium, and 96 hours in GY plus IO (10 and 20 g/L), at the same time as DOT in all media decreased to zero (as shown in Figures 3.26, 3.28, and 3.30). Chen and Liu (1997) stated that production of gamma-linolenic acid in the fungus *Cunninghamella echinulata* increased when DOT decreased, and nutrient transfer in the medium was limited. In addition, Yen and Zhang (2011) demonstrated that low DOT enhanced the accumulation of lipid in *Rhodotorula glutinis.* In case of fungus cultured in GY medium plus IO (10 and 20 g/L), some mycelial damage was found from 48 hours after inoculation and this damage increased by 96 hours. It is possible this damage may have affected gamma-linolenic acid production by the culture. This is broadly similar to the study of Higashiyama *et al.* (2002) who reported a decrease of arachidonic acid in *Mortierella sp.* caused by mycelial damage due to shear stress in the bioreactor. Thus, it is clear that DO and agitation speed affect the morphology and production of gamma-linolenic acid for AQP 4097.

The production of the lovastatin derivative by AQP 4097 in GY medium plus IO 10 g/L, and plus IO 20 g/L compared with GY medium without IO can be seen in Figure 3.35. The amount of lovastatin derivative produced in GY medium without IO increased gradually by 1.8 fold from time zero to 24 hours, and reached a peak at 96 hours. Thereafter, it fluctuated slightly for the rest of the batch. While the amount of lovastatin derivative in GY medium plus 10 g/L IO slightly decreased from zero time to 48 hours, this was followed by an increase and lovastatin derivative reached a peak at 72 hours. Between 96 hours and 144 hours, lovastatin derivative levels declined

by half, whereas the amount of lovastatin derivative in GY medium plus 20 g/L IO remained relatively constant throughout the batch.

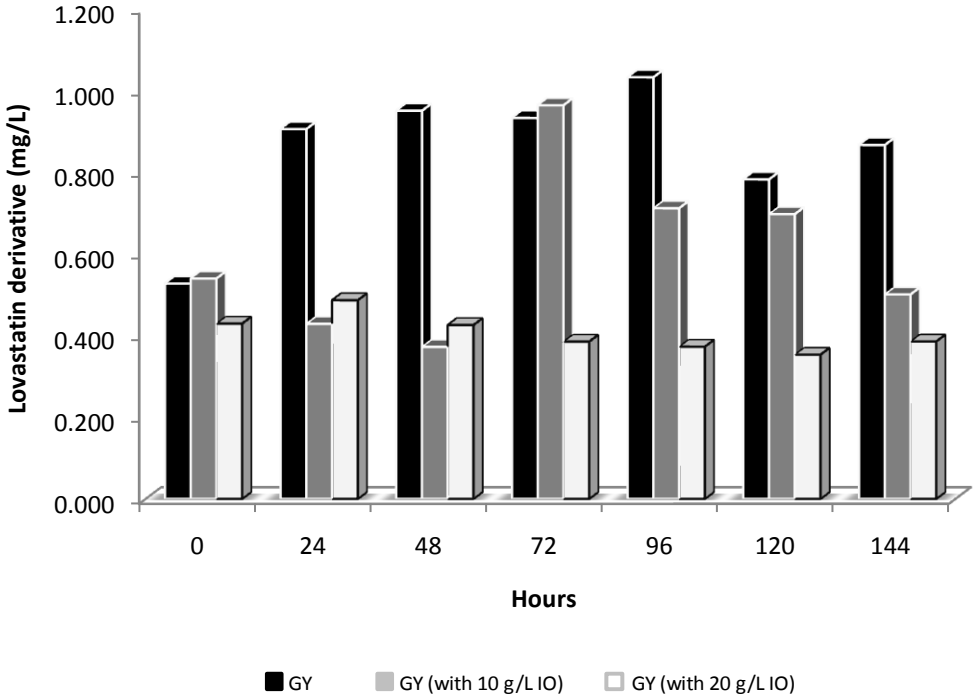

Figure 3.26 Time profile of lovastatin derivative produced by AQP 4097 during batch fermentation in GY medium without IO plus two different concentration of IO, 10 g/L and 20 g/L in a BiostatQ fermenter.

The maximum lovastatin derivative achieved from GY medium without IO was 1.032 mg/L at 96 hours in, more than double that achieved in GY medium plus IO 10 g/L and 20 g/L. From Figure 3.35, the production of lovastatin derivative in GY medium without IO increased after the glucose in the medium was depleted, and this is similar to the effect noted by Barbesgaard *et al.* (1992) which showed that glucose and acetate caused repression of α-amylase production in the filamentous fungus *A. oryzae*, while the biosynthesis of the β-lactam antibiotic cephalosporin C in the filamentous fungus *A. chrysogenum* was also repressed by glucose (Jekosch

and Kück, 2000). In the case of lovastatin production by *A. terreus,* López *et al.* (2003) stated that use of a slowly metabolized carbon source (lactose) in combination with either soybean meal or yeast extract under N-limited conditions stimulated higher productivity. By contrast the production of lovastatin derivative in GY medium with IO 10 g/L and 20 g/L did not increase following glucose depletion. This may well have been due to severe damage to the mycelium as shown in Figure 3.32 B. It may be that shear stress induced hyphal damage which may be one of the limiting factors in lovastatin derivative production in this culture. It may also be possible that hyphal differentiation may also be necessary before lovastatin derivative production occurs (Atalla *et al.*, 2008).

3.5.2 Conclusions

Over all, salinity had a pronounced effect on both gamma linoleneic acid and lovastatin derivative production in this culture. It also influenced culture morphology perhaps indirectly due to impeller speed changes.

3.6 Process Scale-up: Effect of dissolved oxygen tension (DOT) control on biomass and lovastatin derivative production

In previous experiments (Section 3.5) when AQP 4097 was cultured in a 1L bioreactor (Biostat Q, Braun Biotech International) when DOT was not controlled the culture faced limited DOT for much of the process. By contrast, if the DOT was controlled at a pre-set non-limiting level (30% saturation) by increasing stirrer speed this led to cause a damage to the mycelium and also affected biomass formation or target compound production. In this experiment, a larger volume fermenter which had better mixing was used.

Average shear rates can either change during fermentation, if the organism produces a viscous compound such as xanthan gum (Pipe *et al.*, 2008) or produces enzymes which can degrade viscous substrates e.g. pectinases from some filamentous fungi such as *Cochliobolus sativus* (Boothby and Magreola, 1984), or the organism goes through changes in submerged morphology, e.g. moving from a pelleted growth to a more filamentous growth form (Lai *et al.*, 2005).

In this experiment, the effect of DOT on biomass and formation of the target compound, a derivative of lovastatin, production by AQP 4097 cultured in batch cultures in a fermenter vessel was investigated. The batch cultures involving both controlled and uncontrolled DOT conditions were carried out in 14L Bioflo110 bioreactor (Braun) in duplicate; a constant impeller tip speed criteria (as described in section 1.4) was chosen in the scale-up process of this experiment. The geometric details of the fermentation process are shown in Table 3.4. In order to control a constant impeller tip speed similar

to a small fermenter (Biostat Q, Braun Biotech International); the agitation speed was calculated using the following equation:

$$\text{Impeller tip speed } (m/s) = \frac{\pi ND}{60}$$

where $\pi = 3.142$

N = Agitation speed (rpm)

D = Impeller diameter (m)

Table 3.4 Geometric details and operating conditions of a 1L (BiostatQ, Braun) and 14-L (Bioflo110, Braun) stirred tank fermenter.

Dimension/operating condition	**1 L**	**14 L**
Impeller tip speed (m/s)	0.3	0.3
Agitation speed (rpm)	220	80
Working volume (L)	0.75	10.5
Number of impeller (Rushton turbine)	2	2
Vessel diameter, Dt (m)	0.118	0.29
Impeller diameter, Di (m)	0.029	0.074

This study also forms a useful comparison with the batch fermentation carried out in the 1L system (section 3.6).

Inoculums preparation, culture conditions, dry cell weight measurement, statistical analysis of the fungal growth compare in each media, extraction

procedure using Bligh and Dyer method, and the metabolomics quantification was performed as described in section 2.12, 2.2.3.3, 2.6.1.1, and 2.6.4.1., respectively.

3.6.1 Results and Discussion

3.6.1.1 Growth of AQP 4097 cultured under DOT controlled conditions in Bioflo 110 bioreactor

The relationship between the growth of AQP 4097 cultured in GY medium and the consumption of glucose by the fungus can be seen in Figure 3.36. The DOT set point was 30%, and control was by means of automatic stirrer speed adjustment. The growth was assessed based on the biomass estimation by dry cell weight measurement. The biomass of AQP 4097 gradually increased within 48 hours after inoculation, while glucose concentration decreased by half by this stage. After 48 hours, biomass remained roughly constant until the process end, whereas glucose consumption continued at the same rate until the process end by which time it was exhausted. The maximum biomass derived from this isolate was 6.84 g/L at 96 hours. It is noticeable that the biomass cultured in the larger fermenter in these experiments was lower by half when compared to the previous experiments using the 1L Braun bioreactor, Biostat Q.

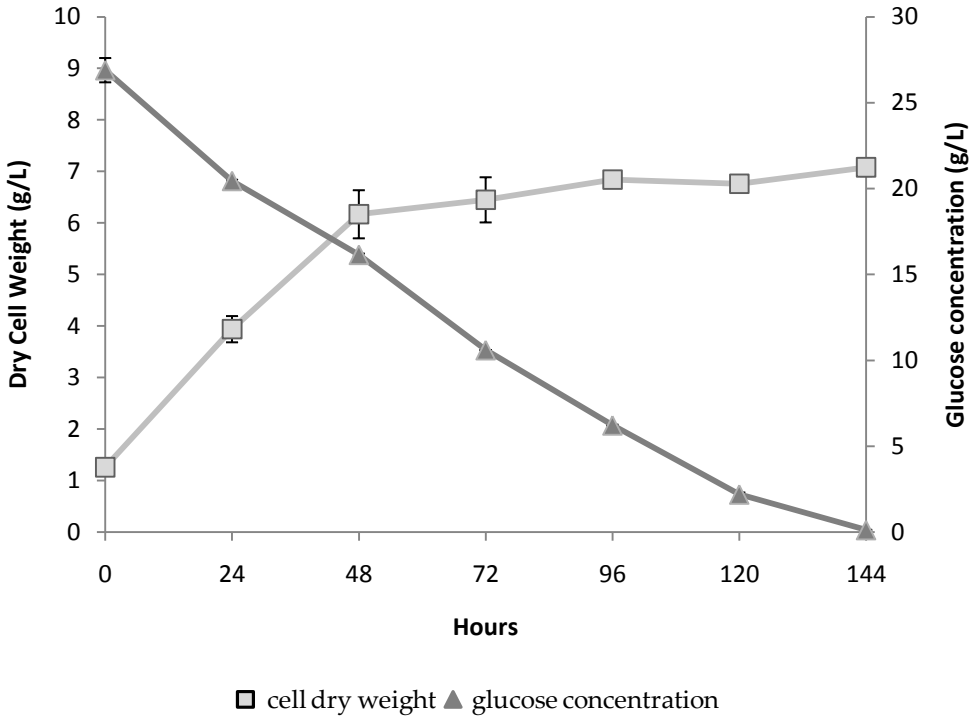

Figure 3.27 The growth and glucose concentration of AQP 4097 cultured in medium, used 30 g/L glucose as a carbon source under DOT controlled conditions in 14L bioreactor (Bioflo110, Braun).

The relationship of Bioreactor behaviour between stirrer speed and DOT level in medium is shown in Table 3.5. It can be seen that DOT level in medium from 24 to 72 hours plunged to 10 % of saturation, which led to the stirrer rate to increase to over 350 rpm (propeller tip speed ±1.3 m/s). Although this helped keep the DOT above the set-point, DOT fluctuated widely as the controller took action to increase impeller speed when DOT fell to the set point leading to an over shoot in the opposite direction. It is noticeable that the propeller tip speed of the Bioflo 110 is slightly higher than the maximum tip speed (1.1 m/s) in the Biostat Q bioreactor at a stirrer rate of 750 rpm which caused severe mycelial damage to this isolate (Section 3.6).

Table 3.5 Dissolved oxygen tension and stirrer speed during batch culture of isolate AQP 4097 cultured in medium, used 30 g/L glucose as a carbon source under DOT controlled conditions in 14L bioreactor (Bioflo110, Braun).

Hours	**Stirrer rate (rpm)** **Min and max**	**Dissolved oxygen tension (DOT, %)** **Min and max**
0	80	54.2
24	80-350	10-60
48	80-350	10-65
72	80-307	10-65
96	80-348	14.5-50
120	80-354	19.8-55.9
144	80-318	19.8-52.1

The lovastatin derivative production of AQP 4097 was cultured in a 14L Bioflo 110 under the same conditions as in 1L. BiostatQ using constant impeller tip speed as the scale-up criterion propeller tip speed constant can be seen from Figure 3.37. At 72 hours which culture was in stationary phase (Figure 3.36), and at this point the concentration of lovastatin derivative plunged to the lowest value then subsequently rapidly increased at 96 hours.

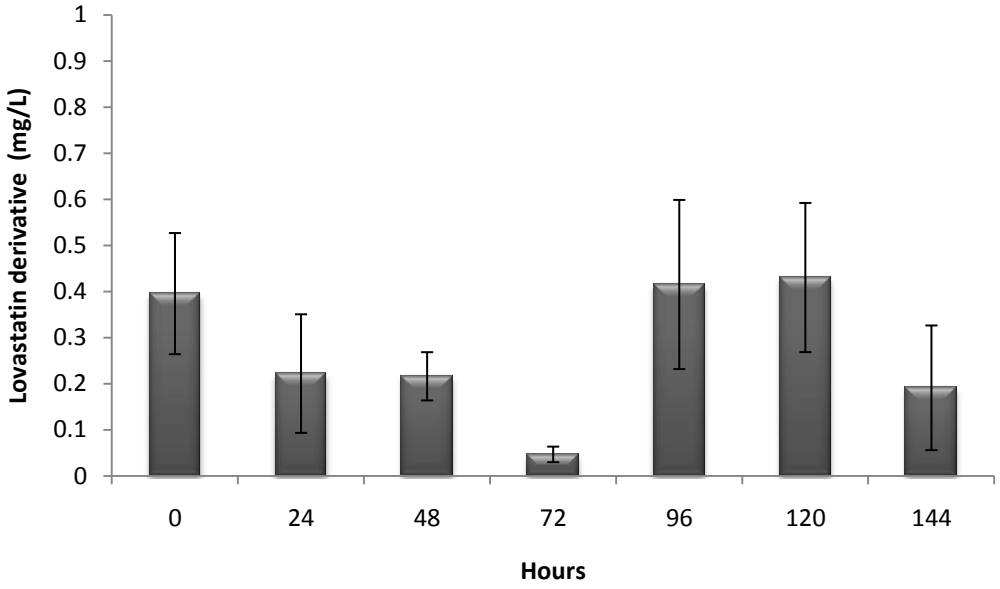

Figure 3.28 Lovastatin derivative concentration versus time in AQP 4097 during batch fermentations, used 30 g/L glucose as a carbon source under DOT-controlled conditions in 14L bioreactor (Bioflo110, Braun).

The maximum lovastatin derivative achieved from this isolate was 0.43 mg/L at 120 hours, lower by half when compared with production from a Biostat Q bioreactor (Figure 3.24, 3.35). It is possible the greater turbulence or wildly fluctuating DOT values either caused physical damage to the mycelium or led to inhibition or suppression of metabolite formation.

The relationship between the growth and the consumption of glucose of AQP 4097 cultured in GY medium under uncontrolled DOT in Bioflo 110 can be seen in Figure 3.38.

3.6.1.2 Growth of AQP 4097 cultured under uncontrolled DOT conditions in Bioflo 110 bioreactor

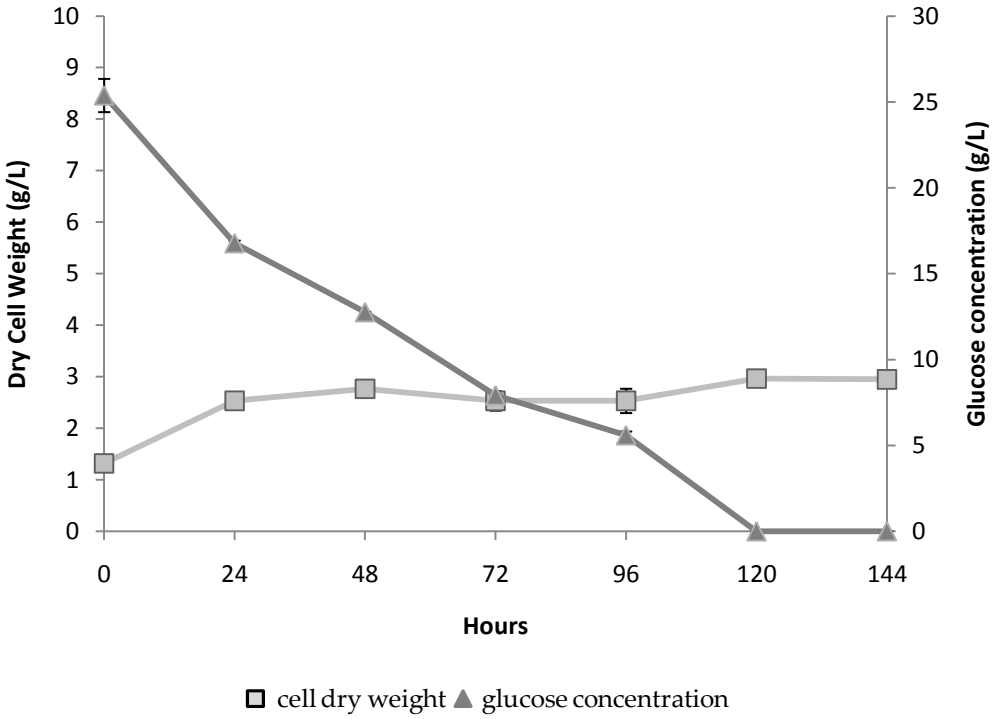

Figure 3.29 The growth and glucose concentration of AQP 4097 cultured in medium, used 30 g/L glucose as a carbon source under uncontrolled DOT conditions in 14L bioreactor (Bioflo110, Braun).

Growth of AQP 4097 increased slightly from time zero roughly doubling within 48 hours after inoculation. After that point it was constant over the process, while glucose consumption continued despite the cessation of growth until it eventually ran out at 120 hours. The highest biomass derived from AQP 4097 was 2.96 g/L at 120 hours after inoculation much lower when compared to the process with controlled DOT (Figure 3.36).

The relationship between stirrer speed and DOT for AQP 4097 cultured in the Bioflo 110 under uncontrolled DOT is shown in Figure 3.39. DOT level in

the fermenter decreased to zero within 24 hours, associated with growth of AQP 4097 (Figure 3.38), and slightly increased from 96 hours to 120 hours. The stirrer speed was kept constant at 80 rpm throughout the process which gave a tip speed equal to 0.3 m/s.

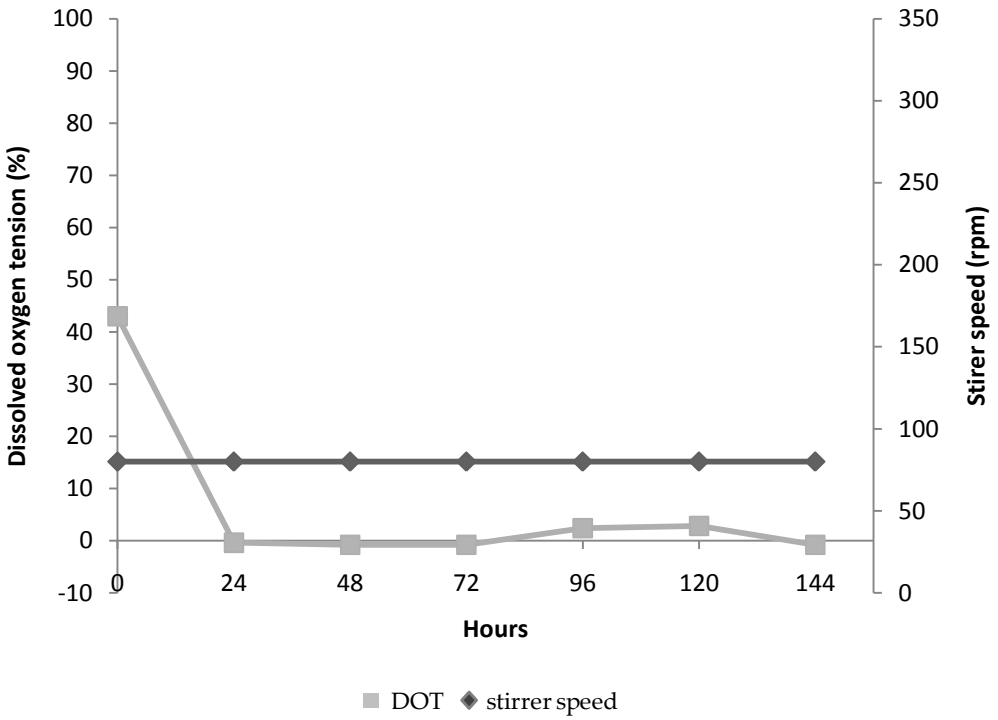

Figure 3.30 Dissolved oxygen tension and stirrer speed of AQP 4097 cultured in GY medium, used 30 g/L glucose as a carbon source under uncontrolled DOT in a 14L bioreactor (Bioflo110, Braun).

Lovastatin derivative production by AQP 4097 cultured in the Bioflo 110 bioreactor under the same conditions as in the Biostat Q using constant impeller tip speed as the scale-up criterion can be seen in Figure 3.40. It can be clearly seen that at 120 hours the production of lovastatin derivative sharply increased, at this stage glucose in medium was exhausted. When

compared with the other batch process with controlled DOT level, the production is far higher in this process (17-fold) as shown in Figure 3.37 even though the biomass production is much lower.

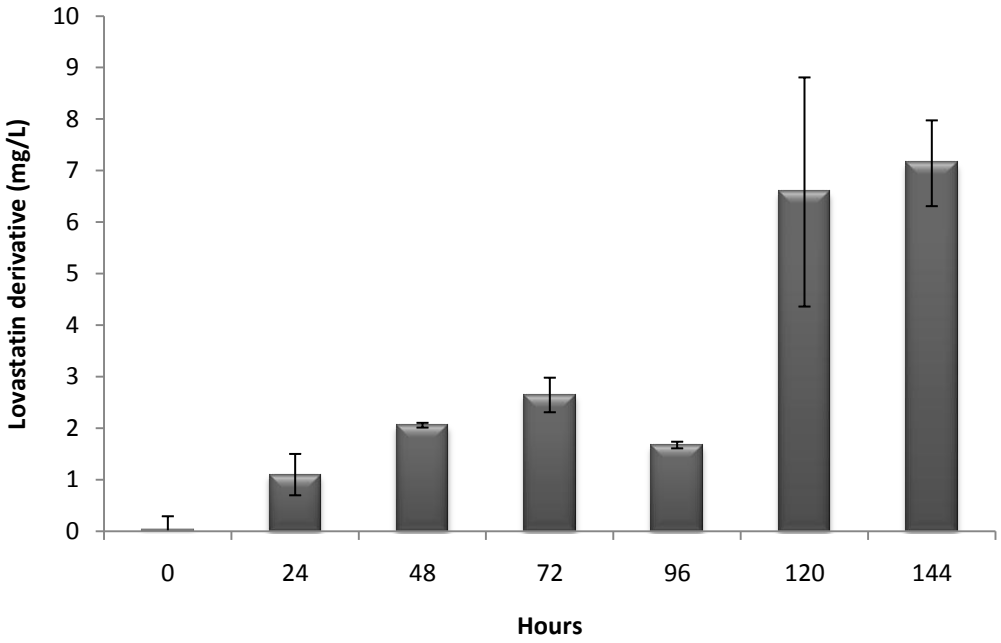

Figure 3.31 Lovastatin derivative concentration versus time produced by AQP 4097 during batch fermentation, used 30 g/L glucose as a carbon source uncontrolled DOT in a 14L bioreactor (Bioflo110, Braun).

.

To summarise, these findings show that in the early process phase when the culture is growing most rapidly this leads to a higher of broth viscosity in the fermenter in turn causing an oxygen mass–transfer limitation in both DOT controlled and uncontrolled DOT saturation. Where DOT level was controlled by increased agitator speed, this led to fragmentation of the mycelium, even though biomass production higher by twice than fermenter without controlled DOT. Agitation speed clearly influences biomass production by AQP 4097. The present results are not in accordance with those of L´opez *et al.* (2005) which reported that agitation speed did not have

any effect on biomass production, but significantly influenced pellet morphology, and broth rheology in *A. terreus*.

In terms of lovastatin derivative production, L´opez *et al.* (2005) also found that pellets which had a relatively less dense, open, filamentous morphology were better at producing lovastatin compared to smaller denser pellets. In addition, aeration with oxygen-enriched gas promoted high lovastatin titer by large fluffy pellets, while smaller pellets were obtained at high agitation rates had no effect. This is broadly similar to the study by Lai *et al.* (2002) which added an oxygen carrier (n-dodecane, n-tetradecane,or n-hexadecane) in both shake flask and 5L fermentor cultivations of *A. terreus,* and found lovastatin production was improved. Nevertheless, high DOT levels (> 60%) induced unfavourable morphological changes and the formation of star-like pellets caused an inhibition of lovastatin production. In 2005, Lai *et al*. reported that an increasing agitation speed up to 425 rpm initiated a morphological change in the *A. terreus* mycelium called frayed pellets, and if the agitation was further increased above 425 rpm, the broken hyphae seemed not re-grow, which had an adverse effect on lovastatin productivity. When DOT was reduced to only 3–5%, the culture still produced some lovastatin, but the production diminished to only one-fifth that under conditions where oxygen supply was adequate.

By contrast, Osman *et al.* (2011) showed that lovastatin productivity by *A terreus* was negatively affected by aeration in shake flask experiments, in which non-aerated production medium supported a higher rate of lovastatin synthesis than aerated production medium (160 and 120 μg/ml), respectively.

In other fermentation processes involving culture of filamentous microorganisms, for example, the production of some antibiotics, several

studies have shown that decreased antibiotic production resulted from fragmentation caused by increased agitation speed (Markl and Bronnenmeier, 1985; Smith *et al.*, 1990; Prosser and Tough, 1991; Makagiansar *et al.*, 1993). Xu *et al.* (2006) also found a decrease in exopolysaccharides (EPS) production and morphology changes when agitation speed increased in an enthomopathogenic fungus, *Paecilomyces tenuipes.* The fungal morphology changed from loose clumps with a fluffy perimeter to a smooth perimeter and compact growth with a dense core region, and the maximum yield of EPS (2.33 g/L) was achieved from a culture with a relatively mild agitation rate of 150 rpm at day 10.

3.6.2 Conclusions

3.6.2 Conclusions

Scaling-up the culture process from small to fermenter scale still faces limited-oxygen condition which affects biomass production in AQP 4097. Increased agitation speed was linked to control of DOT and promoted biomass production in AQP 4097 by improving oxygen transfer in the fermenter. Higher agitation speed was also associated with adverse effects both on mycelial morphology and production of the lovastatin derivative by AQP 4097.

3.7 Effect of carbon source on biomass and production of lovastatin derivative

The carbon source normally use for a fungal culture includes simple sugars, (monosaccharide, and disaccharides), common alcohols (methanol, ethanol), polysaccharides, and oils (McNeil and Harvey, 2008). Small molecules such as monosaccharides were taken up by the fungus and converted directly to essential compounds via catabolic pathways in series enzymatic steps (Fekete *et al*., 2004). Catabolite repression is a phenomenon where microorganisms commonly switch off (repress) a large number of genes in the presence of a rapidly metabolisable carbon source such as glucose. This may offer the benefit of saving their energy, as it primarily affects enzymes used to metabolize other carbon sources (Ronne, 1995). In general, carbon sources are used by microorganisms for two major purposes, first, as building blocks for biomolecules, and secondly, as energy sources for the cell's metabolic activities. Cells may produce their energy via the Krebs cycle which in eukaryotes occurs in the mitochondria. Initially, fermentable carbon sources such as glucose are metabolized in the glycolytic pathway to form pyruvate which can be further metabolized via the Krebs cycle. However, when glucose becomes limited or fully exhausted, microorganisms including *Saccharomyces cerevisiae* can also switch pathways to use non-carbohydrate sources such as ethanol to produce energy via the gluconeogenesis process; this phenomenon is called 'diauxic shift' as illustrated in Figure 3.41.

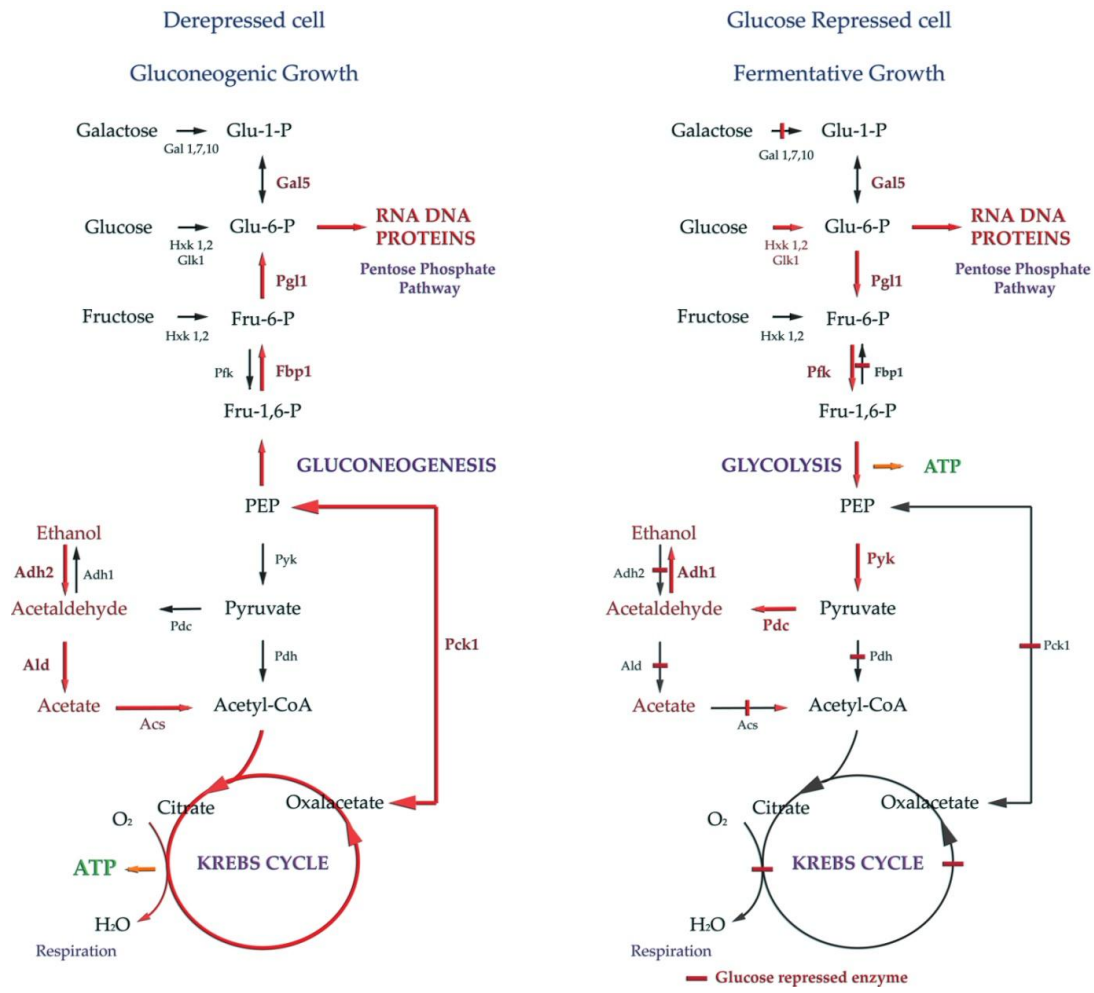

Figure 3.32 Main carbon metabolism pathways in derepressed and in glucose-repressed yeast cells. Specific pathways for utilization of various carbon sources are shown for only two substrates, galactose and ethanol. Adapted from Ronne (1995) Abbreviations: Gal = Galactokinase, Hxk = Hexokinase, Glk = Glucokinase, Pgl = 6-phosphogluconolactonase, Fbp1 = Fructose-1,6-bisphosphatase 1, Pfk = Phosphofructokinase, Pyk = Pyruvate kinase isoenzymes, Pdh = Pyruvate dehydrogenase, Pdc = Pyruvate-decarboxylase, Acs = Acetyl CoA synthetase, Ald = Aldehyde dehydrogenase, Adh = Alcohol dehydrogenase)

Catabolite repression in fungi has been shown to have effects on sporulation (Yi *et al.*, 2008), growth (Flipphi *et al.*, 2003; Nakari-Seta¨la¨ *et al.*, 2009 , Portnoy *et al.*, 2011) , secondary metabolite production (Jia *et al.* 2009, Martín

et al., 1999; Miyake *et al.*,2006); Osman *et al.,* 2011), and virulence of pathogenic fungi (Ospina-Giraldo *et al.*, 2003 ; Walton, 1994; Wu *et al.*,2006; Yi *et al.*,2008;).

The aim of this part of the study was to examine the effect of the nature of the carbon source on lovastatin derivative production and morphology of AQP 4097 by using a readily metabolized carbon source (glucose) and comparing this with two other more slowly utilized carbon sources (lactose and glycerol) as a sole carbon source in the medium.

Inoculums preparation, culture conditions in shake flask experiments, culture conditions in in bioreactor, dry cell weight measurement, statistical analysis of the fungal growth compare in each media, extraction procedure using Bligh and Dyer method, and the metabolomics quantification was performed as described in section 2.12, 2.2.2.2, 2.2.3.4, 2.6.1.1, 2.7, and 2.6.4.1., respectively.

3.7.1 Results and Discussion

3.7.1.1 Effect of carbon source on biomass production of AQP4097

Growth of isolate AQP 4097 was compared in three carbon sources including glucose, lactose, and glycerol in shake flasks initially. As can be seen from Figure 3.42 glucose provided the highest dry cell weight when compared with either lactose or glycerol.

The fungal growth in glucose rapidly increased eight fold between zero and 24 hours, and reached a maximum dry cell weight at 72 hours of 4.95 g/L. Fungal biomass also increased rapidly between zero time and 24 hours, and maximum dry cell weight peaked at 72 hours at 4.72 g/L in a medium with lactose as the C source. The pattern of fungal growth in the medium using

glycerol as C source was distinct from that of both glucose and lactose. The highest dry cell weight in the glycerol medium was only 2.58 g/L at 24 hours after inoculation, around half that of the other two media.

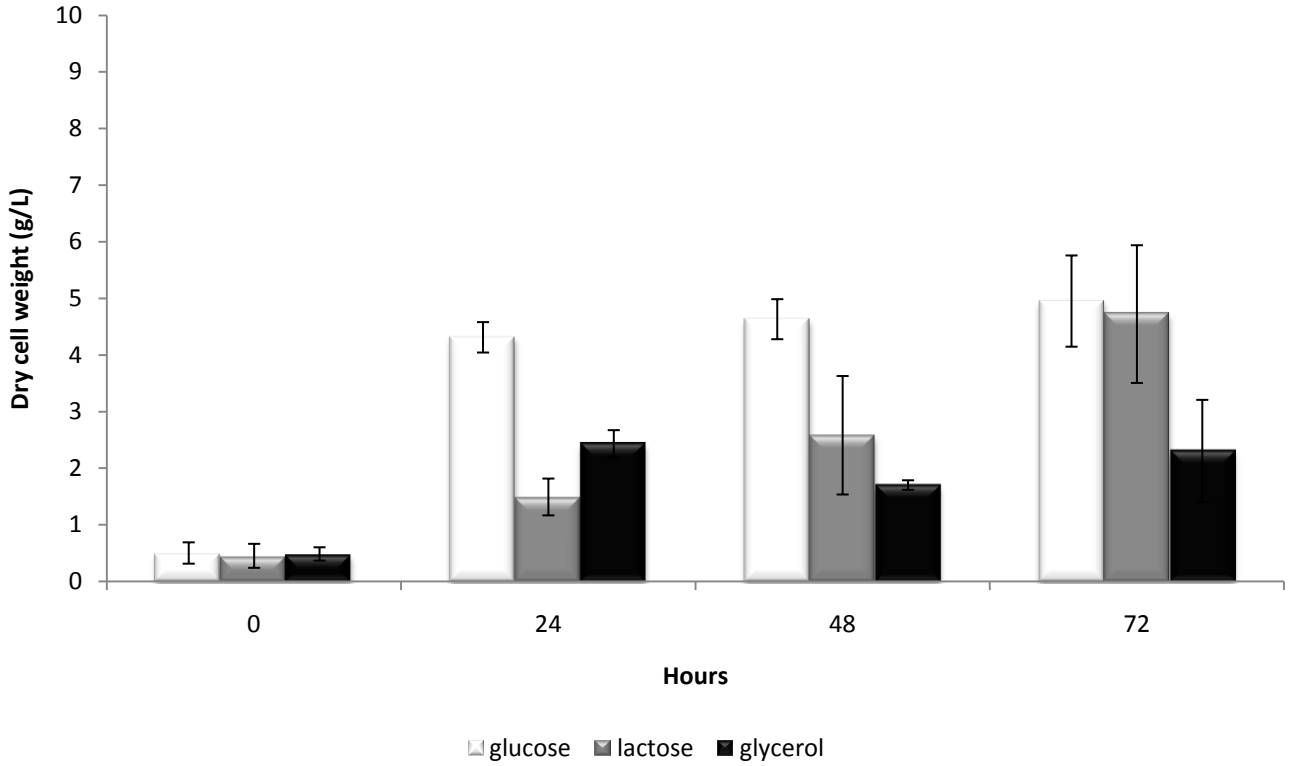

Figure 3.33 The growth of isolate AQP 4097 cultured in three different carbon sources at 0, 24, 48 and 72 hours in a shake flask experiment

3.7.1 2. Statistical analysis of the effects of carbon source upon the biomass production of fungi isolate AQP4097

Statistical analysis of growth based on maximum biomass achieved from AQP 4097 cultured in different types of carbon source (Table 3.5) indicates that glucose was significantly different in terms of fungal growth compared to the other two carbon sources, lactose and glycerol.

Table 3.5 Statistical analysis of influence of growth medium upon fungal growth (AQP 4097) using One-way ANOVA and post-hoc methods (SPSS program, version 16.0)

ANOVA

growthrate

	Sum of Squares	df	Mean Square	F	Sig.
Between Groups	22.719	2	11.359	4.141	.027
Within Groups	74.069	27	2.743		
Total	96.787	29			

Multiple Comparisons

growthrate
Tukey HSD

(I) variable	(J) variable	Mean Difference (I-J)	Std. Error	Sig.	95% Confidence Interval	
					Lower Bound	Upper Bound
Glucose	Lactose	1.83863'	.74071	.050	.0021	3.6752
	Glycerol	1.85333'	.74071	.048	.0168	3.6899
Lactose	Glucose	-1.83863'	.74071	.050	-3.6752	-.0021
	Glycerol	.01470	.74071	1.000	-1.8218	1.8512
Glycerol	Glucose	-1.85333'	.74071	.048	-3.6899	-.0168
	Lactose	-.01470	.74071	1.000	-1.8512	1.8218

*. The mean difference is significant at the 0.05 level.

From these results it is clear that glucose seems to be the best of the three carbon sources in terms of growth of this fungal isolate. Although lactose supported almost as high a maximal cell dry weight, it took much longer

than a glucose based medium to reach this maximum. Conversely, lactose based media are often used to enhance formation of secondary metabolites whose synthesis would have been repressed in the presence of readily utilizable C sources such as glucose. A good example of this is the production of penicillins, where eventually as process control improved a batch lactose based medium was replaced by carefully controlled feeds of glucose such that residual glucose levels were maintained below repressing levels (Chang *et al.*, 1990)

3.7.1.3 Effect of the type of carbon source on lovastatin derivative production by AQP 4097

As can be clearly seen in Figure 3.43, glycerol promoted the highest lovastatin derivative production on AQP 4097, whereas lactose failed to stimulate the productivity by this fungus. The maximum lovastatin derivative production derived from glycerol was 2.56 mg/L at 48 hours, followed by glucose (0.7 mg/L), and lactose (0.6 mg/L) at 24 hours. Glycerol which gave the lowest growth of this fungus (as shown in Figure 3.42) is the best carbon source for lovastatin derivative production.

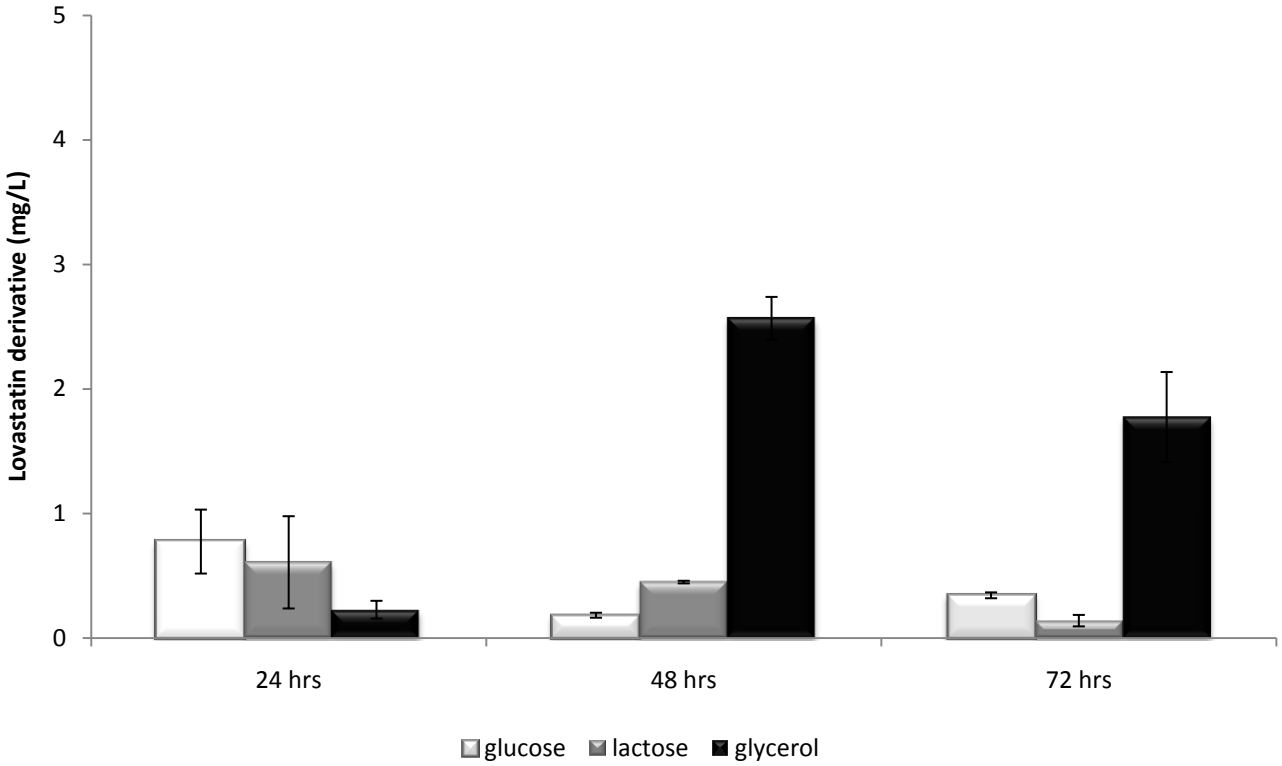

Figure 3.34 Lovastatin derivative concentrations versus time in shake flask cultures of isolate AQP 4097 used different carbon sources, glucose, lactose, and glycerol.

Accordingly, the carbon source concentration selected from experiment 3.6 (30 g/L glucose) was employed in subsequent fermenter experiments to examine scale-up, growth, and lovastatin derivative production in a small STR. Growth of AQP 4097 in this medium is shown in Figure 3.44. It is clear that although some growth occurred in the first 24 hour period, thereafter growth was static. Maximum biomass was achieved at 24 hours (4.6 g/L) and the maximum was much lower than that achieved using glucose at under identical conditions (Figure 3.45).

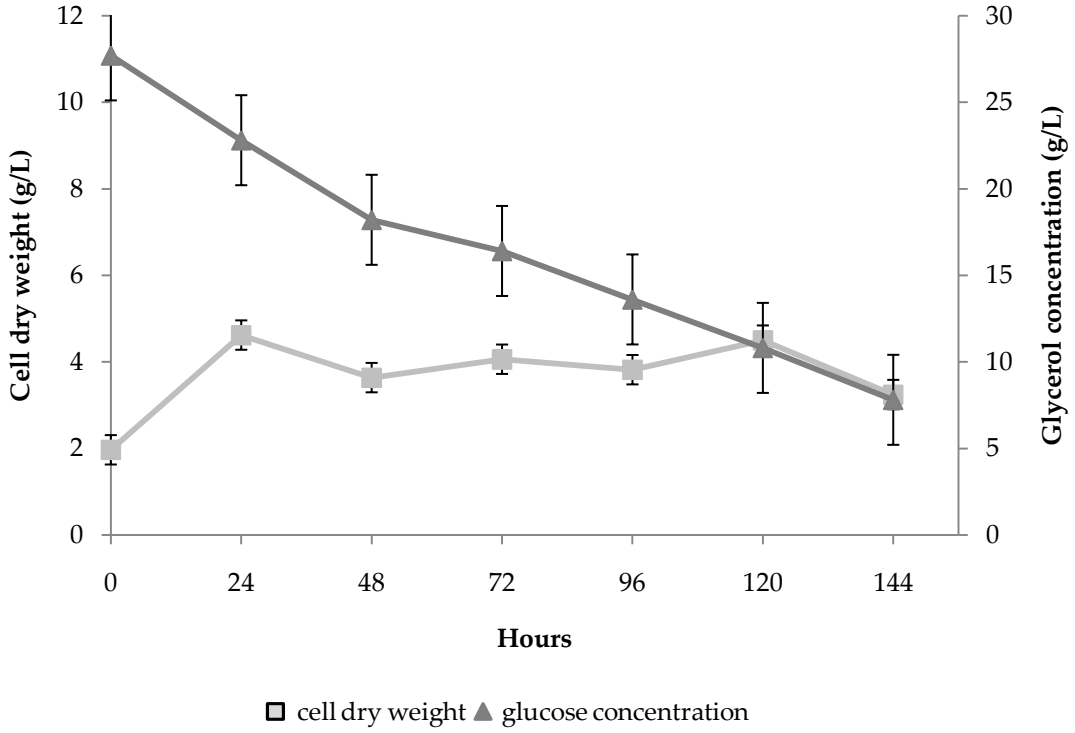

Figure 3.35 Biomass versus time of batch fermenter cultures of AQP 4097 used 30 g/L glycerol as a carbon source.

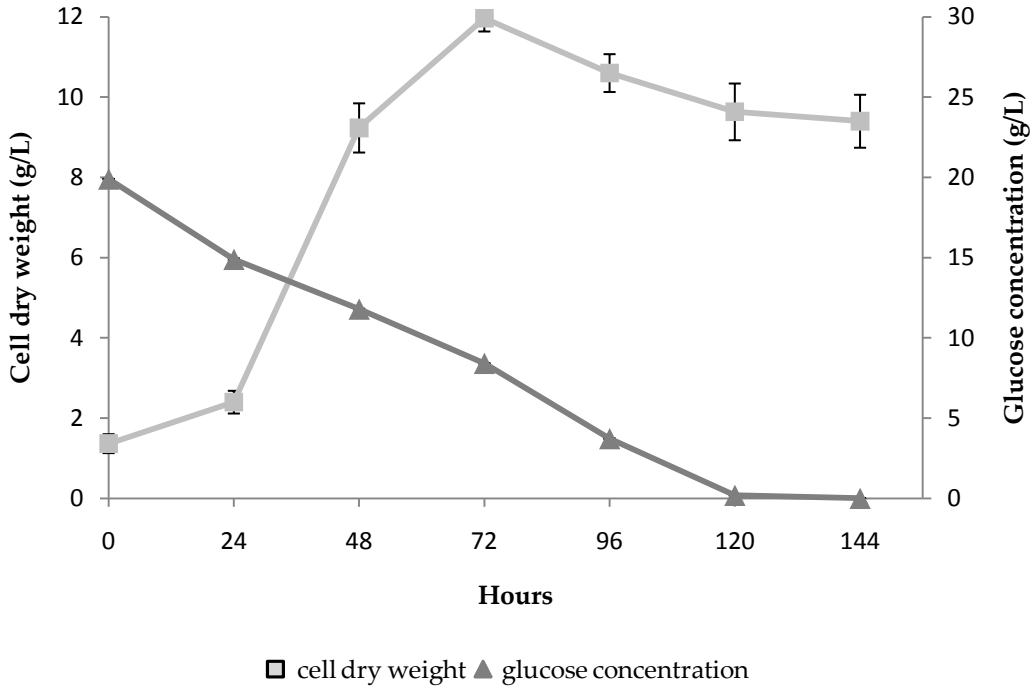

Figure 3.36 Biomass versus time of batch fermenter cultures of AQP 4097 used 30 g/L glucose (from experiment in 3.6) as a carbon source.

The morphology of AQP 4097 in the fermenter culture was also investigated. As can be seen in Figure 3.46A initially the culture was a mix of dispersed hyphal aggregates (Figure 3.46A), and as can be seen in Figure 3.46 B at 48 hours it was mostly in the form of loose fluffy aggregates, which in turn by 72 hours has become denser larger pellets (Figure 3.46 D) showing hyphae with signs of autolysis (red arrow, Fig 3.46E).

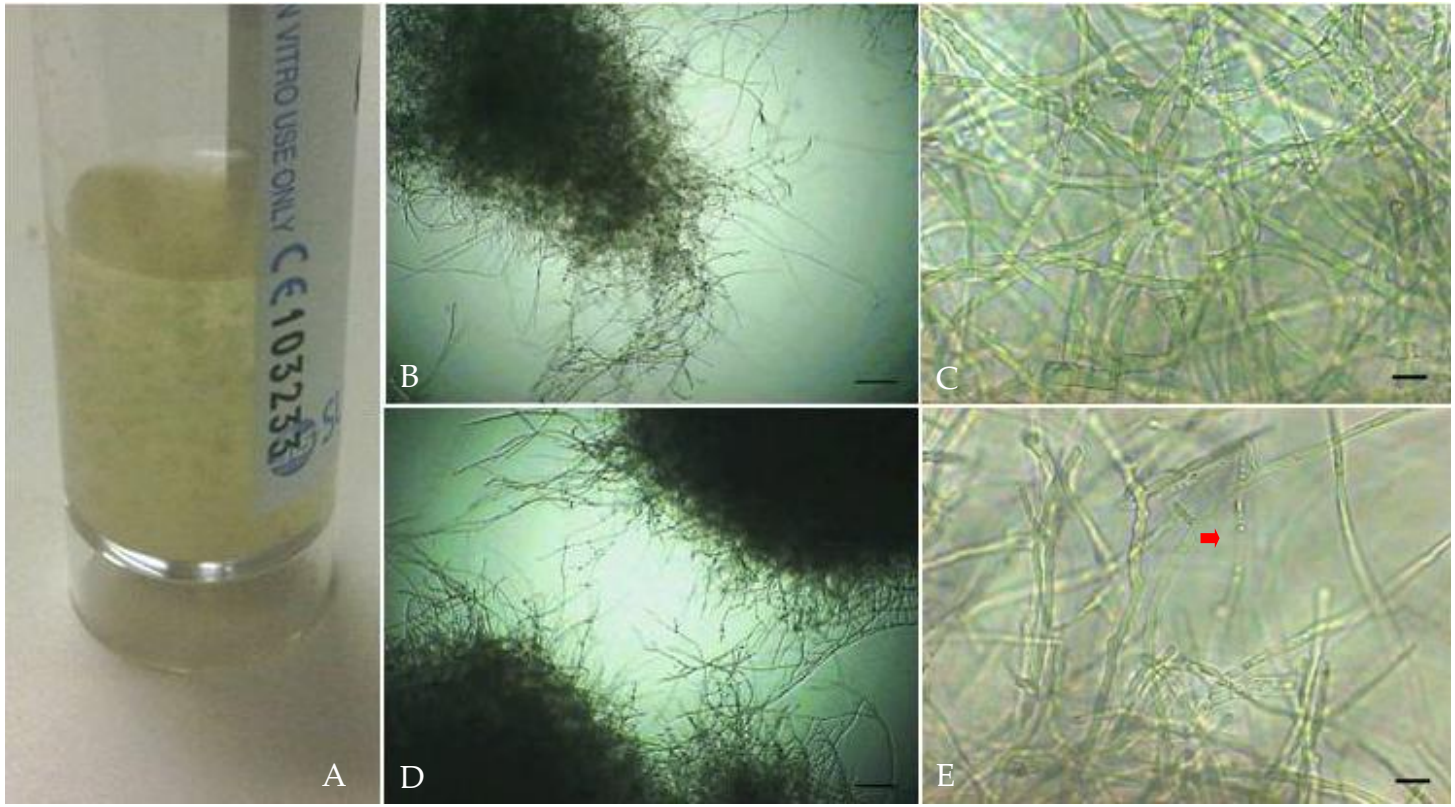

Figure 3.37 Morphological changes in AQP 4097 during batch fermentation: at 48 hours, observed visually (A); under a light microscope at 48 hours (B-C)(with 10x magnification), and 72 hours (D-E))(with 20x magnification) used 30 g/L glycerol as a carbon source. Bar = 10 μm (B-D), and 1 μm (C-E) Legend: red arrow show autolysis mycelium

The diameter of the particles (aggregates, or pellets) was smaller in the later stages of the process (72 hours, Figure 3.46D) than at 48 hours (Figure 3.46B). Glycerol concentration in the medium gradually declined, and there was residual glycerol (around 10 g/L) in the medium until the end of process (Figure 3.44), while the previous experiment (experiment 3.6) using glucose as a sole carbon source (Figure 3.25) glucose has been fully used by 120 hours. Figure 3.48 shows the changes in DOT and stirrer rate in the fermenter culture of AQP 4097 in the glycerol based medium.

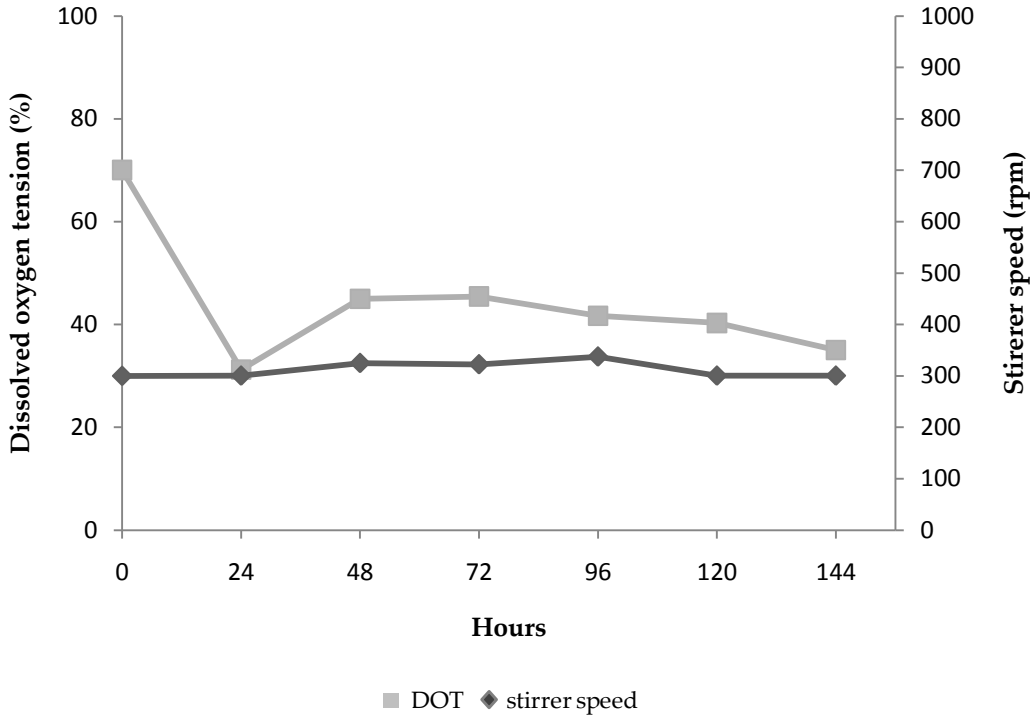

Figure 3.38 A dissolved oxygen tension and stirrer speed versus time of AQP 4097 fermentation cultures in medium used 30 g/L glycerol as a carbon source.

The DOT sharply decreased within 24 hours after inoculation, but afterwards slightly increased and remained constant until the end of experiment. This was broadly similar to the pattern noted with the glucose based medium where DOT also rapidly decreased in the first 24 hours whereas after 24

hours DOT in the glucose based medium gradually decreased down to minus by the process end (Figure 3.48).

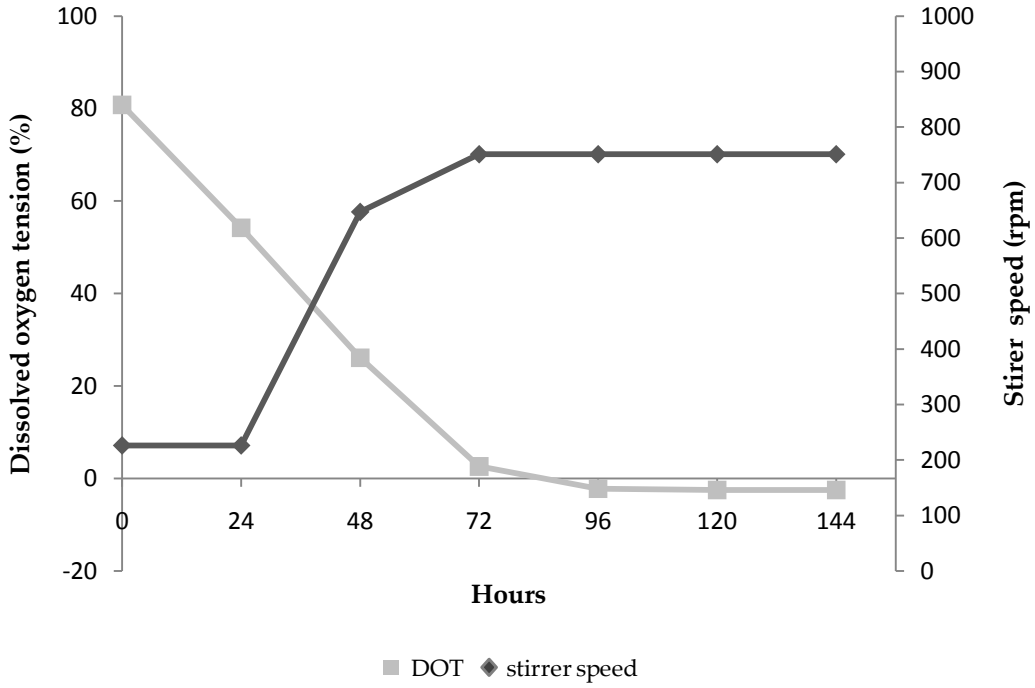

Figure 3.39 A dissolved oxygen tension and stirrer speed versus time of AQP 4097 fermentation cultures in medium used 30 g/L glucose as a carbon source.

The DOT level in the glycerol medium was consistently above 30% so the stirrer speed remained constant throughout the process, by contrast, since the DOT in the glucose medium fell below the set point the stirrer speed automatically increased above 300 rpm in order to attempt to correct this. (Figure 3.47 and 3.48).

As can be seen in Figure 3.49 production of lovastatin derivative by AQP 4097 on two different C sources glycerol and glucose (results from experiment in 3.6), led to markedly differing results. It can be clearly seen that glycerol led to a much higher production of lovastatin derivative

compared to that in the glucose based medium. Lovastatin derivative concentration was gradually increased, and reached a maximum level at 72 hours of 21 mg/L. After which lovastatin derivative fell slowly until the process end. The maximum lovastatin derivative concentration in glycerol was almost 11 times that achieved in glucose although growth was markedly higher in the glucose based medium.

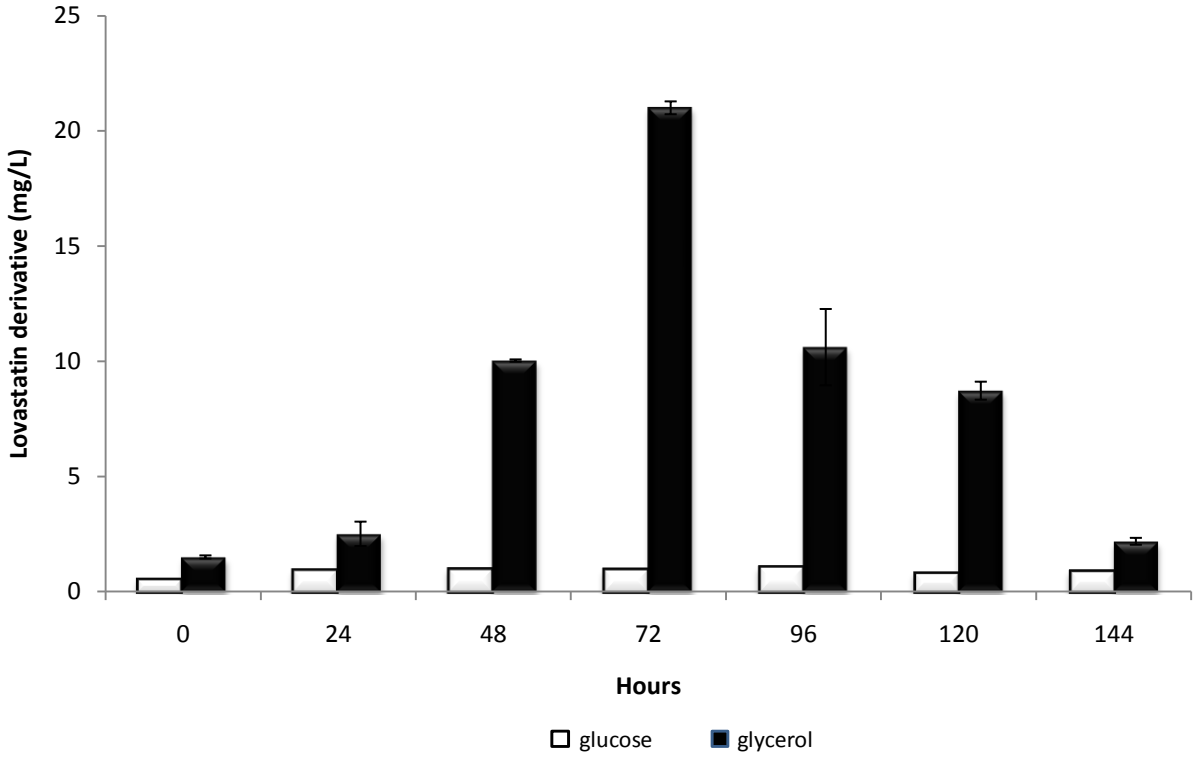

Figure 3.40 Lovastatin derivative concentration versus time produced by AQP 4097 cultured in GY medium using glycerol and glucose (results from experiment in 3.6) as a carbon source 30 g/L in a BiostatQ bioreactor.

In summary, in shake flasks glucose gave best growth of AQP 4097 followed by lactose, and glycerol, whereas the highest lovastatin derivative productivity was achieved in glycerol. In this study, in a lactose medium obviously lovastatin derivative production was poor. By contrast, in the fermenter using a glycerol based medium led to significantly improved lovastatin derivative production. Several studies have demonstrated that lovastatin production depends on the type of carbon source in the fermentation process. The results of Kumar *et al.* (2000) are in agreement with the present findings in that using readily consumable C and N sources like glucose and peptone lead to uncontrolled filamentous type growth of the culture within 24 - 48 hours of fermentation, increase in viscosity, drastic drop of DOT, very poor mass transfer and low lovastatin titres. Jia *et al.* (2009) stated that glycerol led to highest lovastatin production compared to four other carbon sources, glucose, sucrose, lactose, and soluble starch. The authors proposed that this was due to the pathway of glycerol metabolism before being introduced into the glycolytic pathway which led to production of NADPH, which is required for formation of 4a, 5-dihydromonacolin L catalyzed by nonaketide synthase (LNKS), which is an essential intermediate in the lovastatin synthesis pathway. Moreover, it was proposed that a slowly utilized carbon source might also regulate the activity of LovD protein, the last enzyme in the lovastatin biosynthesis pathway. Coincidentally Miyake *et al.* (2006) and Osman *et al.* (2011) both noted that glucose strongly repressed lovastatin synthesis in *M. pilosus* and *A. terreus*, respectively. Moreover, lovastatin synthesis by *A. terreus* in a chemically defined medium was only initiated when glucose concentration levelled off (Hajjaj *et al.*, 2001). López *et al.* (2003) reported that using a slowly metabolized carbon source (lactose) in combination with either soybean meal or yeast extract under N-limited

conditions led to the highest titer and specific productivity (~0.1 mg g−1 h−1) of lovastatin by *A. terreus,* whereas lovastatin production by AQP 4097 in lactose was poor. This may well have been due to the presence of excess N source in the shake flask processes examined here or to related morphological changes dependent on C source or process conditions. In the present study dispersed mycelium of AQP 4097 transformed into relatively dense pellets in the glycerol based medium. Jia *et al.* (2009) reported that cultures of *A. terreus* in a slowly metabolized C source formed small, regular, compact pellets with spongy filaceous outer hairy regions. The size and morphological form of the pellets also affected lovastatin production, López *et al.* (2005) and Porcel *et al.* (2005) both found that less dense, open, pellets of *A. terreus* were better at producing lovastatin compared to small denser pellets, due to the higher oxygen mass transfer. In the present study, when the pellets became denser and larger and showed signs of lysis from 72 hours onwards this was associated with decreases in lovastatin concentration perhaps due to the limited oxygen transfer into the core of the pellets.

3.7.2 Conclusions

Using a slowly utilized carbon source such as glycerol as a sole carbon source promoted lovastatin derivative production, and also affected culture morphology of AQP 4097.

Glucose is suitable for the growth of this fungal isolate, but not for a lovastatin derivative production under the process conditions examined here. Although glycerol that supports lowers growth, it is a good carbon source to produce the lovastatin derivative for this isolate. Interestingly, the results may indicate that lovastatin derivative production may well be related to the morphology of AQP 4097. This is an interesting area for

further quantitative investigation by study the type of morphology characteristic upon the lovastatin derivative production.

Chapter 4 Conclusions and future work

4: Conclusions and future work

The work in this thesis focused on a new marine fungus species, *Trichoderma pseudokoningii* strain AQP 4097, aiming to optimise the cultivation process for biomass and metabolite production from a lab scale - to industrial scale. Morphology changes of the fungus were also observed during the cultivation process. The differential analysis software; Sieve Fiona (v.1.2) and MZMine (v.2.2) were applied to evaluate the mass spectral data from LC-HRFTMS to identify and quantify the metabolites. NMR was also employed to elucidate the structure of some of the compounds with commercial potential that were produced by this strain.

4.1 Conclusions

4.1.1 Effect of salinity and light on sporulation of AQP 4097

AQP 4097 cultured in low concentrations of IO under natural light conditions had a very clear stimulation effect on growth and sporulation. This strain also formed a ring of conidia-bearing mycelium under both dark and natural light incubation conditions. The best conditions for producing spore inocula were growing AQP4097 in PDA with 10 g/L IO and incubation under natural light. It was noticeable that sporulation was poorest in the 33g/L IO medium adopted by Aquapharm Biodiscovery Ltd.

4.1.2 Metabolomics analysis of AQP 4097 cultured on PDA plates with Instant Ocean.

Analysis of LC-HRFTMS results showed that AQP 4097 produced four compounds including virescenoside B, gemfibrozil, γ-linolenic acid, and a

derivative of lovastatin in PDA in varying IO media; however the lovastatin derivative was chosen as the target compound for further study in optimising the fermentation condition for scale up due to its commercial potential.

From LC-MS quantification results, it was revealed that PDA without IO gave the maximum yield of the lovastatin derivative (6.13 μg/plate). NMR also confirmed the presence of a lovastatin congener produced in cultures of AQP 4097 which had a difference in chemical shifts for the olefinic protons which may be due to a change in stereochemistry of one the methyl group and/or migration of the second methyl group on ring B. In addition, the highest concentration of γ-linolenic acid, which is presumed to act as an osmotic pressure maintenance fluid (Raghukumar, 2008) was achieved in PDA with IO 10 g/L (208.46 mg/plate). NMR also confirmed the presence of a structure identical to γ-linolenic acid standard.

4.1.3 Biomass production by AQP 4097 in shake flasks

From statistical analysis of growth of the strain as based on the maximum biomass that could be achieved as shown in Table 3.1., there were no significant differences between PDB plus IO 33 g/L (recommended media from Aquapharm Biodiscovery Ltd.), MYGP and GY media. However, growth was faster and reached the maximum dry cell weight more quickly on simple media which included a rapidly utilised carbon source such as MYGP and GY. Nevertheless, GY was chosen for future cultivation of this fungus for studying the growth and metabolome development in fermenter

cultures due to the fact that it has only one major C energy and one N source, allowing easy optimisation of the ratio of C to N in subsequent research.

4.1.4 The effect of initial glucose concentration on biomass and lovastatin derivative production of AQP 4097

Increasing the concentration of initial glucose in the medium, promoted growth and the production of a lovastatin derivative in AQP 4097 as shown in section 3.5. Initial glucose increased up to 30 g/L and raised the highest biomass to 11 g/L in 72 hours while the production of the lovastatin derivative was at 1.89 mg/L in120 hours. Increased stirring rate affected both biomass and the production of the lovastatin derivative, owing to damage caused on the mycelium.

In spite of the statistical results, there were no significant differences between the growth of AQP 4097 cultured in GY medium containing 20 g/L and 30 g/L glucose; GY medium containing 20 g/L glucose is not entirely suitable for culture of this fungus as a result of the short stationary phase which is an important phase during which it would be expected that secondary metabolite formation would occur. Thus, GY medium with 30 g/L glucose is suitable for this fungus.

4.1.5 Effect of salinity on biomass formation, gamma linolenic acid and lovastatin derivative production in a bioreactor

Statistical analysis of the growth of this strain showed that there are no significant differences between the growth of AQP4097 cultured in GY with varying IO concentrations; although this fungus grew fastest in GY medium with 10 g/L IO and achieved a maximum dry cell weight around 14.8 g/L. Surprisingly, only GY medium with 20 g/L IO showed clear sporulation, in contrast with the results from section 3.2 in which the fungus grows fastest in the media without IO and promoted sporulation when cultured in medium with low concentration IO (10 and 20 g/L IO). Perhaps the controlled conditions in this fermenter batch culture, such as pH and DOT also affected sporulation.

Salinity had a pronounced effect on both the production of γ-linolenic acid and the lovastatin congener. The maximum yield of lovastatin derivative and γ-linolenic acid achieved from GY medium without IO was 1.032 mg/L (at 96 hours) and 125 mg/L (at 96 hours), respectively. Besides, salinity did influence culture morphology; however, this could also be indirectly due to changes in impeller speed.

4.1.6 Process Scale-up: Effect of DOT control on biomass and production of the lovastatin derivative

The DOT had a pronounced effect on the growth of the fungus strain AQP 4097. With a limited DOT, growth of the fungus decreased by 50%; while this had no consequences on the production of the lovastatin derivative.

However, the increased in agitation speed, which can resolve the limited DOT in the fermenter was associated with adverse affects both on mycelial morphology and production of the lovastatin derivative -

4.1.7 Effect of carbon source on biomass and production of the lovastatin derivative

Glycerol which was a slowly utilised carbon source promoted production of a lovastatin congener, besides it also affected the morphology of AQP 4097 which was transformed from loose fluffy aggregates into denser large pellets within 72 hours after inoculation, whereas a fast utilised carbon source such as glucose is more suitable for the growth of this fungal strain.

The maximum concentration of the lovastatin derivative in glycerol was almost 11 fold of what was achieved with glucose although growth was markedly higher in the glucose-based medium.

4.2. Future work

Overall, the work in this thesis has attempted to use new technology such as automated label-free differential expression software (SIEVE and MZMINE) to analyse data from HRFTMS (LTQ-Orbitrap) in the search for bioactive compounds from a new strain of marine fungus provided by Aquapharm Bio-Discovery Ltd. Moreover, it has also developed efficient cultivation and production processes on a small scale, and provided information that has enabled scale up to a fermenter system. This work

identified factors such as salinity, oxygen, and types of carbon sources that effect biomass and bioactive compound production during batch fermentation to generate ideas for further study. Nevertheless, it has been shown in this study that the use of off-line analytical techniques such as infrared spectroscopy can be adapted as real time analytical tools to analyse metabolic flux in microorganism, which will be valuable in bioprocessing. According to the results, the changes in morphology of this strain can be related to the production of the target compound, which will be worth investigating further. Other fermentation techniques such as fed-batch and continuous fermentation should be applied for future studies to improve target yield and solve the limited DOT problem. Searching for suitable extraction methods is another way to achieve a high quality and quantity of product yield, unfortunately this work was time limited; thus it will be more valuable for future work.

Bibliography

Adebayo, A., Harris, R. and Gardner, W. (1971). Turgor pressure of fungal mycelia. *Transactions of the British Mycological Society, 57* (1), 145-151.

Adejoye, O. D. and Fasidi, I. O. (2009). Effect of cultural conditions on biomass and laccase production in submerged medium by *Schizophyllum commune* (fr.), a nigerian edible mushroom. *The Electronic Journal of Environmental, Agricultural and Food Chemistry, 8* (11), 1186-1193.

Alberts, A. C. (1980). Mevinolin, a higher potent competitive inhibitor of hydroxymethylglutaryl-coenzyme A reductase. *Proceedings of the National Academy of Sciences of the United States of America, 77*, 3957–3961.

Atalla, M. M., Hamed, E. R. and El-Shami R. A. (2008). Optimization of a culture medium for increased mevinolin production by *Aspergillus terreus* strain. *Malaysian Journal of Microbiology, 4* (2), 6- 10.

Atkinson, M. J. and Bingman, C. (1997). Elemental composition of commercial seasalts. *Journal of Aquariculture and Aquatic Sciences*, *8* (2), 39-43 .

Avalos, J. and Estrada, A. (2010). Regulation by light in *Fusarium*. *Fungal Genetics and Biology, 47* (11), 930-938.

Balick, M. and Cox, P. (1997). *Plants, People, and Culture : The Science of Ethnobotany.* Nova Iorque: Scientific American Library.

Balunas, M. and Kinghorn, A. D. (2005). Drug discovery from medicinal plants. *Life Sciences, 78* (5), 431 – 441.

Barbesgaard, P., Heldt-Hansen, H. and Diderichsen, B. (1992). On the safety of *Aspergillus oryzae*: A Review. *Applied Microbiology and Biotechnology, 36* (5), 569–572.

Beever, R. E. and Laracy, E. P. (1986). Osmotic adjustment in the filamentous fungus *Aspergillus nidulans*. *Journal of Bacteriology*, *168* (3), 1358-1365.

Beutler, J. A. (2009). Natural products as a foundation for drug discovery. *Current Protocols in Pharmacology* , 46, 9.11.1-9.11.21.

Bhakuni, D. and Rawat, D. (2005). *Bioactive Marine Natural Products.* Co-published by Springer with Anamaya, New Delhi: India.

Bhat, S. V., Nagasampagi, B. A. and Sivakumar, M. (2005). *Chemistry of natural products.* Narosa Publishing House, New Deli, India:

Bligh, E. G. and Dyer, W. J. (1959). A rapid method of total lipid extraction and purification. *Canadian journal of biochemistry and physiology, 37* (8), 911–917.

Blunt, J. W., Copp, B. R., Munro, M. H., Northcotec, P. T. and Prinsep, M. R. (2004). Marine natural products. *Natural Product Reports, 21*, 1-49.

Boothby, D. and Magreola, N. (1984). Production of polysaccharide degrading enzymes by *Cochliobolus Sativus* and *Fusarium Culmorum* grown in liquid culture. *Transactions of the British Mycological Society , 83* (2), 275-280.

Brown, M. S. and Goldstein, J. L. (2004). A tribute to Akira Endo, discoverer of a penicillin for cholesterol. *Atherosclerosis*, 5, 13-16.

Brown, A. D. and Simpson, J. R. (1972). Water relations of sugar-tolerant yeasts: the role of intracellular polyols. *Journal of General Microbiology, 72*, 589-591.

Brown, F. F., Campbell, I. D., Kuchela, P. W. and Rabenstein, D. C. (1977). Human erythrocyte metabolism studies by ^{1}H spin echo NMR. *FEBS Lett. 82* (1), 12-16.

Burke, F. (2008). Scale up and scale down of fermentation processes. In B. McNeil and L. M. Harvey, *Practical fermentation technology* (p. 388). Wiley & Sons. West Sussex: England.

Burke, R. and Jennings, D. (1990). Effect of sodium chloride on growth characteristics of the marine yeast *Debaryomyces hansenii* in batch and continuous culture under carbon and potassium limitation. *Mycological Research , 94* (3), 378-388.

Buss, A. D. and Butler, M. S. (2010). *Natural Product Chemistry for Drug Discovery.* The Royal Society of Chemistry publishing. Piccadilly: England.

Byrne, P. J. and Gareth Jones, E. B. (1975). Effect of salinity on the reproduction of terrestrial and marine fungi. *Transactions of the British Mycological Society, 65* (2), 185-200.

Cagnoli-Bellavita, N., Ceccherelli, P., Ribaldi, M., Polonsky, J. and Baskevitch, Z. (1969). Virescenoside A e virescenoside B: nuovi altrosidi metaboliti dell' *Oospora virescens*. *Wallr. Gazzetta Chimica Italiana, 99*, 1354-1363.

Chang, L., McGrory, E. and R.P., Elander. (1990). Penicillin production by glucose-derepressed mutants of *Penicillium chrysogenum*. *Journal of Industrial Microbiology and Biotechnology, 6* (3), 165-169.

Chen, H. and Chang, C. (1996). Production of γ -linolenic acid by the fungus *Cunninghamella echinulata* CCRC 31840. *Biotechnology Progress, 12*, 338-341.

Chen, H. and Liu, T. (1997). Inoculum effects on the production of γ-linolenic acid by the shake culture of *Cunninghamella echinulata* CCRC 31840. *Enzyme and Microbial Technology, 21*, 137-142.

Claridge, T. D. W. (2006). *High-Resolution NMR Techniques in Organic Chemistry.* v. 19, Elsevier Science. Amsterdam: The Netherlands.

Davis, D. J., Burlak, C. and Money, N. P. (2000). Osmotic pressure of fungal compatible osmolytes. *Mycological Research, 104*, 800-804.

Deacon, J. (2006). *Fungal Biology 4th edition.* Blackwell. Oxford: United Kingdom.

Ebada, S., Edrada, R., Lin, W. and Proksch, P. (2008). Methods for isolation, purification and structural elucidation of bioactive secondary metabolites from marine invertebrates. *Nature Protocols, 3* (12), 1820-1831.

Ebel, R. (2010). Review: Terpenes from Marine-Derived Fungi. *Marine Drugs, 8*, 2340-2368.

Ellis, S., Grindle, M. and Lewis, D. (1991). Effect of osmotic stress on yield and polyol content of dicarboximide-sensitive and -resistant strains of *Neurospora crassa*. *Mycological Research, 95* (4), 457-464.

Endo, A. (1979). Monacolin K, a new hypocholesterolemic agent produced by a *Monascus* species. *The Journal of Antibiotics, 32* (8), 852–854.

Endo, A. (1985). Microbial phosphorylation of compactin (ML-236B) and related compounds. *The Journal of Antibiotics, 38*, 328-332.

Endo, A. (2010). A historical perspective on the discovery of statins. *Proceedings of the Japan Academy, Ser. B*, 484-493.

Endo, A., Hasumi, K. and Negishi, S. (1985). Monacolin J and L, new inhibitors of cholesterol biosynthesis produced by *Monascus tuber*. *The Journal of Antibiotics, 38* (3), 420-422.

Endo, A., Hasumi, K., Nakamura, T., Kunishima, M. and Masuda, M. (1985). Dihydromonacolin L and monacolin X, new metabolites that inhibit cholesterol biosynthesis. *The Journal of Antibiotics, 38* (3), 321-327.

Endo, A., Komagata, D. and Shimada, H. (1986). Monacolin M, a new inhibitor of cholesterol biosynthesis. *The Journal of Antibiotics, 39*, 1670-1673.

Fekete, E., Karaffa, L., Sándor, E., Bányai, I., Seiboth, B., Gyémánt, G. (2004). The alternative D-galactose degrading pathway of Aspergillus nidulans proceeds via L-sorbose. *Archives of Microbiology , 181* (1), 35-44.

Faulkner, D. (2002). Marine natural products. *Natural Product Reports*, 1-48.

Flipphi, M., van de Vondervoort, P., Ruijter, G., Visser, J., Arst Jr., H. and Felenbok, B. (2003). Onset of carbon catabolite repression in *Aspergillus nidulans*. Parallel involvement of hexokinase and glucokinase in sugar signaling. *Journal of Biological Chemistry, 278*, 11849–11857.

Gao, L., Liu, X.-Z. L., Man-Hong, S., Shi-Dong, L. and Jin-Li, W. (2009). Use of a novel two-stage cultivation method to determine the effects of environmental factors on the growth and sporulation of several biocontrol fungi. *Mycoscience, 50* (4), 317-321.

Garraway, M. and Evans, R. (1984). Carbon Nutrition. In Garraway, M. and Evans, R., *Fungal nutrition and physiology.* John Wiley & Sons, Canada.

Gbolagade, J., Sobowale, A. and Adejoye, D. (2006). Optimization of sub-merged culture conditions for biomass production in *Pleurotus florida* (mont.)

Singer, a Nigerian edible fungus. *African Journal of Biotechnology, 5* (16), 1464-1469.

Ghajara, F., Holforda, P., Alhussaena, K., Beattiea, A. and Cotherb, E. (2006). Optimising sporulation and virulence in *Drechslera avenacea*. *Biocontrol Science and Technology, 16* (5), 471-484.

Gindrat, D. (1977). Effects of elevated salt concentrations on growth, sporulation and pigmentation of *Trichoderma spp*. *Canadian Journal of Microbiology 1977, 23* (5), 607-616.

Giorni, P., Battilani, P. and Magan, N. (2008). Effect of solute and matric potential on in vitro growth and sporulation of strains from a new population of *Aspergillus flavus* isolated in Italy. *Fungal Ecology*, *1* (2-3), 102-106.

Griffin, D. H. (1996). Chemical requirements for growth. In Griffin, D. H., *Fungal physiology*. John Wiley & Sons. New Jersey: United States.

Hajjaj, H., Niederberger, P. and Duboc, P. (2001). Lovastatin Biosynthesis by *Aspergillus terreus* in a Chemically Defined Medium. *Applied and Environmental Microbiology, 67* (6), 2596-2602.

Hansson, L., Dostálek, M. and Sörenby, B. (1989). Production of γ-linolenic acid by the fungus *Mucor rouxii* in fed-batch and continuous culture. *Applied Microbiology and Biotechnology, 31* (3), 223-227.

Harold, R., Money, N. and Harold, F. (1996). Growth and morphogenesis in *Saprolegnia ferax*: is turgor required? *Protoplasma, 191*, 105–114.

Hernandez-Saavedra, N., Ochoa, J. and Vazquez-Dulhalt, R. (1995). Osmotic adjustment in marine yeast. *Journal of Plankton Research, 17*, 59-69.

Higashiyama, K., Fujikawa, S., Park, E. Y. and Shimizu, S. (2002). Production of Arachidonic Acid by *Mortierella* fungi. *Biotechnology and Bioprocess Engineering, 7*, 252-262.

Holt, G. A. and Chandra, A. (2002). Herbs in the modern healthcare environment—An overview of uses, legalities, and the role of the healthcare professional. *Clinical Research and Regulatory Affairs (USA), 19* (1), 83–107.

Chen, H-C. and Chang, C-C. (1996). Production of γ-Linolenic Acid by the fungus *Cunninghamella echinulata* CCRC 31840. *Biotechnology Progress, 12* (3), 338–341.

Jaivel, N. and Marimuthu, P. (2010). Isolation and screening of lovastatin producing microorganisms. *International Journal of Engineering Science and Technology, 2* (7), 2607-2611.

Jekosch, K. and Kück, U. (2000). Glucose dependent transcriptional expression of the cre1 gene in *Acremonium chrysogenum* strains showing different levels of cephalosporin C production. *Current genetics, 37* (6), 388-395.

Jennings, D. H. (1984). Polyol metabolism in fungi. *Advances in Microbial Physiology, 25*, 149-193.

Jennings, D. H. (1986). Fungal growth in the sea. In *S.T. Moss, The Biology of Marine Fungi* (pp. 1-10). Cambridge University Press, London

Jia, Z., Zhang, X., Zhao, Y. and Cao, X. (2009). Effects of divalent metal cations on lovastatin biosynthesis from *Aspergillus terreus* in chemically defined medium. *World Journal of Microbiology and Biotechnology, 25* (7), 1235–1241.

Juzlová, P., Martinková, L. and Kren, V. (1996). Secondary metabolites of the fungus *Monascus*: a review. *Journal of Industrial Microbiology, 16* (3), 163–170.

Kang, S-I., Kang, S-Y., Kanaly, R. A., Lee, E., Lim, Y. and Hur, H-G. (2009). Rapid oxidation of ring methyl groups is the primary mechanism of biotransformation of gemWbrozil by the fungus *Cunninghamella elegans*. *Archives of Microbiology, 191* (6), 509–517.

Kazakevich, Y. (2007). Hplc Theory. In Y. Kazakevich, and R. Lobrutto, *Hplc for pharmaceutical scientists* (pp. 25-74). A John Wiley & Sons. New Jersey:United State of America.

Kennedy, J., Auclair, K., Kendrew, S., Park, C., Vederas, J. and Hutchinson, C. (1999). Modulation of polyketide synthase activity by accessory proteins during lovastatin biosynthesis. *Science*, *284* (5418), 1368-1372.

Kerzaona, I., Grovela, O., Robiou Du Ponta, T., Papeb, P. L. and Pouchusa, Y.-F. (2008). Effects of seawater on growth and gliotoxin excretion of marine strains of *Aspergillus fumigatus* Fres. *Toxicon, 51* (3), 398-405.

Khachatourians, G. (2001). *Applied mycology and biotechnology for agriculture and foods*. In Khachatourians, G. and Arora, D., Applied Mycology and Biotechnology: Agriculture and food production (Vol. 1)(pp. 1-11). Elsevier Science. Amsterdam: The Natherlands.

Kimura, K., Komagata, D., Murakawa, S. and Endo, A. (1990). Biosynthesis of monacolins: conversion of monacolin J to monacolin K (mevinolin). *The Journal of Antibiotics, 43* (12), 1621-1622.

King, M. W. (2012, June). *Introduction to Cholesterol Metabolism.* Retrieved from the medicalbiochemistry page: http://themedicalbiochemistrypage.org/cholesterol.php

Kogej, T., Gorbushina, A. A. and Gunde-Cimermana, N. (2006). Hypersaline conditions induce changes in cell-wall melanization and colony structure in a halophilic and a xerophilic black yeast species of the genus *Trimmatostroma*. *Mycological Research, 110* (6), 713-724.

Kok Kheng, T. and Epton, H. (1973). Effect of light on the growth and sporulation of *Botrytis cinerea*. *Transactions of the British Mycological Society, 61* (1), 145-157.

Komagata, D., Shimada, H., Murakawa, S. and Endo, A. (1989.). Biosynthesis of monacolins: conversion of monacolin L to monacolin J by a monooxygenase of *Monascus ruber*. *The Journal of Antibiotics, 42*, 407-412.

Kubicek, C. P. and Druzhinina, I. (2007). *Environmental and Microbial Relationships* (second ed.). In Kubicek, C. P. and Druzhinina, I., THE MYCOTA : A comprehensive treatise on fungi as experimental systems for basic and applied research. Sringer-Verlag. Wiesbaden: Germany.

Kumar, M. S., Jana, S. K., Senthil, V., Shashanka, V., Kumar, S. V. and Sadhukhan, A. K. (2000). Repeated fed-batch process for improving lovastatin production. *Process Biochemistry, 36* (4), 363–368.

Lai, L-S. T., Tai-Her, T. and Wang, T. C. (2002). Application of Oxygen Vectors to *Aspergillus terreus* Cultivation. *Journal of Bioscience and Bioengineering, 94* (5), 453-459.

Lai, L-S. T., Tsai, T-H., Wang, T. C. and Cheng, T-Y. (2005). The influence of culturing environments on lovastatin production by *Aspergillus terreus* in submerged cultures. *Enzyme and Microbial Technology, 36* (5-6), 737–748.

Leach, C. (1964). The relationship of visible and ultraviolet light to sporulation of *Alternaria chrysanthemi*. *Transactions of the British Mycological Society, 47* (2), 153-158.

Lewis, D. H. and Smith, D. C. Sugar alcohols (polyols) in fungi and green plants. II. Methods of detection and quantitative estimation in plant extracts. *New Phytologist, 66* (2), 185-204.

Senn, H. and Schlotterbeck, G. (2007). In Lindon, J., Nicholson, J., and Holmes, E., *The Handbook of Metabonomics and Metabolomics.* Elsevier. Amsterdam: The netherlands.

Liu, G.-Q., Lin, Q.-L., Jin, X.-C., Wang, X.-L. and Zhao, Y. (2010). Screening and fermentation optimization of microbial lipid-producing molds from forest soils. *African Journal of Microbiology Research, 4* (14), 1462-1468.

López, J. C., Pérez, J. S. and Sevilla, J. F. (2003). Production of lovastatin by *Aspergillus terreus*: effects of the C:N ratio and the principal nutrients on growth and metabolite production. *Enzyme and Microbial Technology, 33*, 270–277.

López , J. C., Perez, J. S., Sevilla, J. F., Porcel, E. R. and Chisti, Y. (2005). Pellet morphology, culture rheology and lovastatin production in cultures of *Aspergillus terreus. Journal of Biotechnology, 116*, 61–77.

López, J. C., Pérez, J. S., Sevilla, J. F., Fernández, F. A., Grima, E. M. and Chisti, Y. (2003). Production of lovastatin by *Aspergillus terreus*: effects of the

C:N ratio and the principal nutrients on growth and metabolite production. *Enzyme and Microbial Technology, 33*, 270–277.

Luard, E. J. (1982). Growth and accumulation of solutes by *Phytophthora cinnamomi* and other lower fungi in response to changes in external osmotic potential. *Journal of General Microbiology, 128*, 2583-2590.

Makagiansar, H., Shamalou, P., Thomas, C. and Lilly, M. (1993). The influence of mechanical forces on the morphology and penicillin production of *Penicillium chrysogenum. Biotechnology and Bioprocess Engineering, 9*, 83–90.

Mancini, I., Defant, A. and Guella, G. (2007). Recent synthesis of marine natural products with antibacterial activities. *Anti-Infective Agents in Medicinal Chemistry, 6*, 17-48.

Mann, N. (2008). The potential of phages to prevent MRSA infections. *Research in Microbiology, 159*, 400-5.

Manzoni, M. and Rollini, M. (2002). Biosynthesis and biotechnological production of statins by filamentous fungi and application of these cholesterol lowering drugs. *Applied Microbiology and Biotechnology*, 555-564.

Market, B. R. (2011). *Microbial Products: Technologies, Applications and Global Markets.* Healthcare and Medical. Retrieved from BCC Research: http://www.bccresearch.com/report/microbial-products-markets-bio086a.html

Markl, H. and Bronnenmeier, R. (1985). Mechanical stress and microbial production. *Biotechnology, vol. 2. Fundamentals of biochemical engineering. Berlin: VCH*, 369–392.

Martín, J. F., Casqueiro, J., Kosalkoá. K., Marcos, A. T. and Gutiérrez, S. (1999). Penicillin and cephalosporin biosynthesis: Mechanism of carbon catabolite regulation of penicillin production. *Antonie van leeuwenhoek, 75* (1-2), 21-31.

Masuma, R., Yamaguchi, Y., Noumi, M., Omura, S. and Namikoshi, M. (2001). Effect of sea water concentration on hyphal growth and antimicrobial metabolite production in marine fungi. *Mycoscience, 42* (5), 455-459.

Mayer, A. M., Glaser, K. B., Cuevas, C., Jacobs, R., Kem, W., Little, R. (2010). The odyssey of marine pharmaceuticals: a current pipeline perspective. *Trends in Pharmacological Sciences*, (31), 255–265.

Mayer, A., Rodríguez, A., Berlinck, R. and Hamann, M. (2009). Review Marine pharmacology in 2005–6: Marine compounds with anthelmintic, antibacterial, anticoagulant, antifungal, anti-inflammatory, antimalarial,antiprotozoal, antituberculosis, and antiviral activities; affecting the cardiovascular, immune and nervous. *Biochimica et Biophysica Acta, 1790*, 283–308.

Harvey, L. M., and McNeil, B. (2008). The Design and Preparation of Media for Bioprocesses. In McNeil, B. and Harvey, L. M., *Practical Fermentation Technology.* John Wiley & Sons. West Sussex: England.

McWilliams, A. (2011, April). *Microbial Products: Technologies, Applications and Global Markets.* Retrieved from BCC Research: http://www.bccresearch.com/report/microbial-products-markets-bio086a.html?tab=highlight&highlightKeyword=Microbial+Products

Medicine, N. L. (n.d.). Retrieved from http://pubchem.ncbi.nlm.nih.gov/summary/summary.cgi?cid=280575#x299

Miao, L., Kwong, T. F. and Qian, P.-Y. (2006). Effect of culture conditions on mycelial growth, antibacterial activity, and metabolite profiles of the marine-derived fungus *Arthrinium c.f. saccharicola*. *Applied microbial and cell physiology, 72* (5), 1063-1073.

Miller, J. J. and Reid, J. (1961). Stimulation by light of sporulation in *Trichoderma lignorum* (tode) harz. *Canadian Journal of Botany, 39* (2), 259-262.

Miyake, T., Uchitomo, K., Zhang, M., Kono, I., Nozaki, N., Sammoto, H. and Inaqaki, K. (2006). Effects of the principle nutrients on lovastatin production by *Monascus pilosus*. *Bioscience Biotechnology and Biochemistry, 70* (5), 1154–1159.

Mojsov, K. (2010). The effects of different carbon sources on biosynthesis of pectinolytic enzymes by *Aspergillus Niger*. *ATI - Applied Technologies and Innovations, 3* (3), 23-29.

Money, N. (2001). Biomechanics of invasive hyphal growth. In R. Howard and N. Gow, *The Mycota VIII. Biology of the Fungal Cell* (pp. 3–17). Springer-Verlag. Berlin: Germany.

Nakanishi, K. (1999). An historical perspective of natural products chemistry. *In S. Ushio (Ed.), Comprehensive Natural Products Chemistry, 1*, 23–40.

Nakasone, K., Peterson, S. and Jong, S. (2004). Preservation and distribution fungal cultures. In G. Mueller, G. Bills, and M. Foster, *Biodiversity of Fungi* (pp. 37-47). Elsevier. Amsterdam:The Netherlands.

Neil, E. J. (2007). Fundamentals of NMR Spectroscopy in Liquids. In Neil, E. J., *NMR Spectroscopy Explained: Simplified Theory, Applications and Examples for Organic Chemistry and Structural Biology.* Wiley-Interscience. New Jersey: United State of America.

Newman, D. J., Cragg, G. M. and Snader, K. M. (2000). The influence of natural products upon drug discovery. *Natural Product Reports,* (17), 215–234.

Omura, S. (1992). Trends in the search for bioactive microbial metabolites. *Journal of Industrial Microbiology, 10*, 135-156.

Oshoma, C. and Ikenebomeh, M. (2005). Production of *Aspergillus niger* biomass from rice bran. *Pakistan Journal of Nutrition, 4* (1), 32-36.

Osman, M., Khattab, O., Zaghlol, G. and Abd El-Hameed, R. M. (2011). Optimization of some physical and chemical factors for Lovastatin productivity by local strain of *Aspergillus terreus*. *Australian Journal of Basic and Applied Sciences, 5* (6), 718-732.

Ospina-Giraldo, M. D., Mullins, E. and Kang, S. (2003). Loss of function of the *Fusarium oxysporum* SNF1 gene reduces virulence on cabbage and *Arabidopsis*. *Current Genetics, 44*, 49-57.

Pipe, C. J., Majmudar, T. S. and McKinley, G. H. (2008). High shear rate viscometry. *Rheologica Acta, 47*, 621–642.

Porcel, E. R., López , J. C., Pérez, J. S., Sevilla, J. F. and Chisti, Y. (2005). Effects of pellet morphology on broth rheology in fermentations of *Aspergillus terreus*. *Biochemical Engineering Journal, 26*, 139–144.

Portnoy, T., Margeot, A., Linke, R., Atanasova, L., Fekete E., Sandor, E., Hartl, L., Karaffa, L., Druzhinina, I. S., Seiboth, B., Le Crom, S. and Kubicek,

C. P. (2011). The CRE1 carbon catabolite repressor of the fungus *Trichoderma reesei*: a master regulator of carbon assimilation. *BMC Genomics, 12*, 269.

Prosser, J. and Tough, A. (1991). Growth mechanisms and growth kinetics of filamentous microorganisms. *Critical Reviews in Biotechnology, 10*, 253–274.

Raghukumar, C. (2008). Marine fungal biotechnology: an ecological perspective. *Fungal Diversity, 31, 19-35.*

Ramirez, M. and Chulze, S. (2004). Impact of osmotic and matric water stress on germination, growth, mycelia water potentials and endogenous accumulation of sugars and sugar alcohols in *Fusarium graminearum*. *Mycologia, 96* (3), 470-478.

Ramos, A. J., Magan, N. and Sanchis, V. (1999). Osmotic and matric potential effects on growth, sclerotia and partitioning of polyols and sugars in colonies and spores of *Aspergillus ochraceus*. *Mycological Research, 103* (2), 141-147.

Reader, S., Kennedy, M., Hinkley, S. F. and LAM, K. S. (2007). *Fermentation method.* Retrieved from SumoBrain : http://www.sumobrain.com

Ritchie, F., McQuilken, M. P. and Bain, R. A. (2006). Effects of water potential on mycelial growth, sclerotial production, and germination of *Rhizoctonia solani* from potato. *Mycological Research,* (6), 725-733.

Robinson, J., Frame, E. and Frame II, G. (2005). Mass Spectrometry I: Principles and Instrumentation. In Robinson, J., Frame, E. and Frame II, G., *Undergraduate Instrumental Analysis, Sixth Edition.* CRC Press. New York: United State of America.

Rojas, N. L., Cavalitto, S. F., Mignone, C. F. and Hours, R. A. (2008). Role of PPase-SE in *Geotrichum klebahnii*, a yeast-like fungus able to solubilize pectin. *Electronic Journal of Biotechnology, 11* (1), 1-8.

Ronne, H. (1995). Glucose repression in fungi. Trends in genetics , 11, 12-17.

Rossi, M. J. and Oliveira, V. L. (2011). Growth of the ectomycorrhizal fungus *Pisolithus microcarpus* in different nutritional conditions. *Brazilian Journal of Microbiology, 42*, 624-632.

Ruijter, G. J., Visser, J. and Rinzema, A. (2004). Polyol accumulation by *Aspergillus oryzae* at low water activity in solid-state fermentation. *Microbiology, 150*, 1095–1101.

Samapundo, S., Deschuyffeleer, N., Van Laere, D. and Devlieghere, F. (2010). Effect of NaCl reduction and replacement on the growth of fungi important to the spoilage of bread. *Food Microbiology, 27* (6), 749-756.

Samiee, S., Moazami, N., Haghighi, S., Mohseni, F. A., Mirdamadi, S. and M.R. Bakhtiari, M. R. (2003). Screening of lovastatin production by filamentous fungi. *Iranian Biomedical Journal, 7* (1), 29-33.

Sarker, S., Latif, Z. and Gray, A. (2005). Natural Product Isolation. In S. Sarker, Z. Latif and A. Gray, *Natural Products Isolation* (pp. 1-26). Humana Press. New Jersey:United State of America.

Schliemann, W., Cai, Y., Degenkolb, T., Schmidt, J. and Corke, H. (2001). Betalains of Celosia argentea. *Phytochemistry*, *58* (1), 159-165.

Seenivasan, A., Subhagar, A., Aravindan, R. and Viruthagiri, T. (2008). Microbial production and biomedical applications of Lovastatin. *Indian Journal of Pharmaceutical Sciences, 70* (6), 701–709.

Seidel, V. (2005). Initial and Bulk Extraction. In S. Sarker, Z. Latif and A. Gray, *Natural Products Isolation* (pp. 1-26). Humana Press. New Jersey:United State of America.

Shen, B. (2003). Polyketide biosynthesis beyond the type I, II and III polyketide synthase paradigms. *Current Opinion in Chemical Biology, 7*, 285–295.

Smith, J., Lilly, M. and Fox, R. (1990). The effect of agitation on the morphology and penicillin production of *Penicillium chrysogenum*. *Biotechnology and Bioengineering, 35*, 1011–1023.

Spainhour, C. B. (2005). Introduction. In Spainhour, C. B., *Natural products*. John Wiley & Sons. New Jersey: USA.

Staunton, J. and Weissman, K. (2001). Polyketide biosynthesis: a millennium review. *Natural Product Reports, 18*, 380-416.

Stierle, S., Strobel, G. and Stierle, D. (1993). Taxol and taxane production by *Taxomyces andreanae*, an endophytic fungus of Pacific yew. *Science, 260*, 214-216.

Suleman, P., Al-Musallam, A. and Menezes, C. A. (2001). The effect of solute potential and water stress on black scorch caused by *Chalara paradoxa* and *Chalara radicicola* on Date Palms. *Plant Disease, 85*, 80-83.

Tobert, J. (2003). Lovastatin and beyond:The history of the HMG-COA reductase inhibitors. *Nature Reviews, 2*, 517-526.

Top Therapeutic Classes by Spending. (2011). Retrieved from http://www.imshealth.com: http://www.imshealth.com/ims/Global/Content/Corporate/Press%20Room/T

op-Line%20Market%20Data%20&%20Trends/2011%20Top-line%20Market%20Data/Top_Therapy_Classes_by_Sales.pdf

Top 15 U.S Pharmaceutical Products by Sales. (2009). Retrieved from http://www.imshealth.com: http://www.imshealth.com/ims/Global/Content/Corporate/Press%20Room/Top-line%20Market%20Data/2009%20Top-line%20Market%20Data/Top%2015%20Products%20by%20U.S.Sales.pdf

Wang, L., Ridgway, D., Gu, T. and Moo-Young, M. (2003). Effects of process parameters on heterologous protein production in *Aspergillus niger* fermentation. *Journal of Chemical Technology and Biotechnology*, *78*, 1259–1266.

Weete, J., Shewmaker, F. and Gandhi, S. (1998). γ-Linolenic acid in Zygomycetous Fungi: *Syzygites megalocarpus*. *Journal of the American Oil Chemists' Society*, *75* (10), 1367-1372.

Wu, S. C., Halley, J. E., Luttig, C., Fernekes, L. M., Gutierrez-Sanchez, G., Darvill, A. G. and Albersheim, P. (2006). Identification of an endo-b-1,4-D-xylanase from *Magnaporthe grisea* by gene knockout analysis, purification, and heterologous expression. *Applied and Environmental Microbiology*, *72* (2), 986–993.

Wucherpfennig, T., Hestler, T. and Krull, R. (2011). Morphology engineering - osmolality and its effect on *Aspergillus niger* morphology and productivity. *Microbial Cell Factories*, 10:58.

Xiaoyan, Z., Xianghua, W. and Yan, F. (2007). Influence of glucose feeding on the ligninolytic enzyme production of the white rot fungus *Phanerochaete chrysosporium*. *Frontiers of Environmental Science and Engineering in China*, *1*, 89-94.

Xu, C. P., Kim, S. W., Hwang, H. J. and Yun, J. W. (2006). Production of exopolysaccharides by submerged culture of an enthomopathogenic fungus, *Paecilomyces tenuipes* C240 in stirred-tank and airlift reactors. *Bioresource Technology, 97*, 770–777.

Yen, H. and Zhang, Z. (2011). Enhancement of cell growth rate by light irradiation in the cultivation of *Rhodotorula glutinis*. *Bioresource Technology, 102* (19), 9279-9281.

Yi, M., Park, J., Ahn, J. and Lee, Y. (2008). MoSNF1 regulates sporulation and pathogenicity in the rice blast fungus *Magnaporthe oryzae*. *Fungal Genetics and Biology, 45*, 1172–1181.

Young-Won, C., J., B. M. and Chai H.B., a. K. (2006). Drug discovery from natural sources. *The AAPS Journal, 8* (2), 239-253.

Zhang, L., An, R., Wang, J., Sun, N., Zhang, S., Hu, J. and Kuai, J. (2005). Exploring novel bioactive compounds from marine microbes. *Current Opinion in Microbiology, 8* (3), 276–281.

Appendix I

Table I Commercialised pharmaceutical and agricultural product produced from microbes and their sources. Adapted from Buss A.D. (2010) and Young-Won *et al.* (2006)

Approved drug (Generic Name)	**Producing microorganism**	**Type**	**Application**
Amphotericin	*Streptomyces nodosus*	yeast	Antifungal
Amrubicin hydrochloride	*Streptomyces peucetius* var. *caesius*	yeast	Antitumour
Avermectin	*Streptomyces avermitilis*	yeast	Anthelmintic
Biapenem	*Streptomyces cattleya*	yeast	Antibacterial
Bleomycin	*Streptomyces verticillus*	yeast	Antitumour
Calicheamycin	*Micromonospora echinospora*	bacteria	Antitumour
Caspofungin acetate	*Glarea lozoyensis*	fungus	Antifungal
Cefditoren pivoxil	*Cephalosporium sp.*	fungus	Antibacterial
Cephalosporin	*Acremonium spp.*	fungus	Antibacterial
Chloramphenicol	*Streptomyces venezelae*	yeast	Antibacterial
Clavulanic acid	*Streptomyces clavuligerus*	yeast	β-Lactamase inhibitor
Compactin and related statins	*A. terreus, Penicillium spp., Monascus ruber*	fungus, yeast	Cholesterol biosynthesis inhibitor
Cyclosporin	*Tolypocladium spp.*	fungus	Immunosuppressant
Daptomycin	*Streptomyces roseosporus*	yeast	Antibacterial
Doxorubicin	*Streptomyces peucetius*	yeast	Antitumour
Ergotamine	*Claviceps spp.*	fungus	Migraine relief
Ertapenem	*Streptomyces cattleya*	yeast	Antibacterial
Erythromycin	*Saccharopolyspora erythraea*	bacteria	Antibacterial
Everolimus	*Streptomyces hygroscopicus*	yeast	Immunosuppressant

Approved drug (Generic Name)	Producing microorganism	Type	Application
Fusidic acid	*Fusidium coccineum*	fungus	Antibacterial
Gemtuzumab ozogamicin	*Micromonospora echinospora ssp. calichensis*	bacteria	Antitumour
Gentamicin	*Micromonospora purpurea*	bacteria	Antibacterial
Kanamycin	*Streptomyces kanamycetus*	yeast	Antibacterial
Lincomycin	*Streptomyces linconensis*	yeast	Antibacterial
Lipstatin	*Streptomyces toxytricin*	yeast	Lipase inhibition
Micafungin sodium	*Coleophoma empetri*	fungus	Antifungal
Miglustat	*Streptomyces lavendulae*	yeast	Inhibits glucosylceramide synthase
Milbemycin	*Streptomyces hygroscopicus*	yeast	Anthelmintic
Monensin	*Streptomyces cinnamonensis*	yeast	Feed additive
Mycophenolate sodium	*P. brevicompactum*	fungus	Antiproliferative effect
Mycophenolic acid	*Penicillium spp.*	fungus	Immunosuppressant
Neomycin	*Streptomyces fradiae*	yeast	Antibacterial
Nisin	*Lactococcus lactis*	yeast	Antibacterial
Nystatin	*Streptomyces noursei*	yeast	Antibacterial
Penicillin G	*P. notatum*	fungus	Antibacterial
Pimecrolimus	*Streptomyces hygroscopicus* var. *ascomyceticus*	yeast	Immunosuppressant
Pleuromutilin	*Pleurotus mutilus*	fungus	Antibacterial
Pneumocandin	*Glarea lozoyensis*	fungus	Antifungal
Rapamycin	*Streptomyces hygroscopicus*	yeast	Immunosuppressant
Rifamycin	*Amycolatopsis mediterranei*	bacteria	Antibacterial

Approved drug (Generic Name)	Producing microorganism	Type	Application
Rosuvastatin calcium	*P. citrinum,* *P. brevicompactum*	fungus	HMG-CoA reductase inhibitors
Spinosyn	*Saccharopolyspora spinosa*	yeast	Insecticidal
Streptomycin	*Streptomyces griseus*	yeast	Antibacterial
Strobilurins	*Strobilurus tenacellus*	fungus	Agriculture fungicides
Telithromycin	*Saccharopolyspora erythraea*	yeast	Antibacterial
Tetracycline	*Streptomyces spp.*	yeast	Antibacterial
Tigecycline	*Streptomyces aureofaciens*	yeast	Antibacterial
Tylosin	*Streptomyces viridochromogenes*	yeast	Feed additive
Vancomycin	*Amycolatopsis orientalis*	bacteria	Antibacterial

Appendix II

Table I Bioactive compounds from marine fungi. Adapted from Mayer (2009)

Compound name	Molecular weight	Formula	Chemistry class	Organism	Pharmacologic activity	reference
Abyssomicin C	346.3744	$C_{19}H_{22}O_6$	Polyketide	Actinomycete strain	antimicrobial including *Staphylococcus aureus*, Methicillin-resistant *Staphylococcus aureus*, vancomycin resistant strain,*Bacillus subtilis*, *Rhodococcus erythropois*	Mancini and Guella (2007)
Aigialomycins A	378.3732	$C_{19}H_{22}O_8$	NA	mangrove fungus, *Aigialus parvus*	NA	Blunt *et al.* (2004)
Aigialomycins B	380.3891	$C_{19}H_{24}O_8$	NA	mangrove fungus, *Aigialus parvus*	NA	Blunt *et al*. (2004)
Aigialomycins C	364.3897	$C_{19}H_{24}O_7$	NA	mangrove fungus, *Aigialus parvus*	antimalarial activity in vitro against *Plasmodium falciparum* , moderate cytotoxicity against the KB, BC-1 and Vero cell lines	Blunt *et al*. (2004)

Table I (Continued)

Compound name	Molecular weight	Formula	Chemistry class	Organism	Pharmacologic activity	reference
Aigialomycins D	334.3637	$C_{18}H_{22}O_6$	14-membered resorcyclic macrolide	marine mangrove fungus *Aigialus parvus* BCC5311	moderate antimalarial activity (IC50=6.6 Ag/mL) against the multidrug resistant *Plasmodium falciparum* (K1 strain)	Mayer and Hamann (2005)
Aigialomycins E	334.3637	$C_{18}H_{22}O_6$	NA	mangrove fungus *Aigialus parvus*	NA	Blunt *et al*. (2004)
Ascochitine	276.2845	$C_{15}H_{16}O_5$	Polyketides	fungus	*M. tuberculosis* tyrosine phosphatase inhibition	Mayer *et al.* (2009)
Ascosalipyrone	238.2796	$C_{13}H_{18}O_4$	Polyketides	marine fungus *Ascochyia salicornia*	NA	Faulkner (2002)
Ascosalipyrrolidinones A	427.6193	$C_{27}H_{41}NO_3$	Alkaloids	obligate marine fungus *Ascochyta salicornia*e, isolated from *Ulva sp*., a green alga collected from the German coast of the North Sea	antimicrobial	Blunt *et al*. (2004)
Aspergilloxide	388.5833	$C_{25}H_{40}O_3$	Sesterterpene epoxy-diol	*Aspergillus sp.* from the Bahamas	NA	Blunt *et al*. (2004)
Aspergillamide B	474.5946	$C_{28}H_{34}N_4O_3$	NA	*Aspergillus sp.*	NA	Blunt *et al*. (2004)

Table I (Continued)

Compound name	Molecular weight	Formula	Chemistry class	Organism	Pharmacologic activity	reference
Asperic acid	284.3911	$C_{16}H_{28}O_4$	NA	*A. niger* (culture # 94–1212) obtained from the sponge *Hyrtios proteus* from the Dry Tortugas National Park, Florida	NA	Faulkner (2002)
Azetinone kasarin	325.36	$C_{15}H_{23}N_3O_5$	NA	*Hyphomycetes sp.* cultured from a *Zooanthus sp.*	weak antibacterial and cytotoxic activities	Faulkner (2002)
Chalcomycin B	812.9373	$C_{41}H_{64}O_{16}$	Macrolide	culture broth of a marine *Streptomycete* isolate	particularly potent against *S. aureus* (MIC=0.39 Ag/mL).	Mayer and Hamann (2005)
Corollosporine	250.2903	$C_{14}H_{18}O_4$	Pthalide	fungus	*Staphylococcus aureus* (Sa)	Mancini and Guella (2007)
Coruscol A	176.2102	$C_8H_{16}O_4$	1,3-dioxane	*Penicillium sp.* cultured from the bivalve mollusc *Mytilus coruscus* from Okinawa	NA	Faulkner (2002)

Table I (Continued)

Compound name	Molecular weight	Formula	Chemistry class	Organism	Pharmacologic activity	reference
22-Deacetylyanuthone A	360.4871	$C_{22}H_{32}O_4$	meroterpenoids	*A. niger* isolated from a tissue homogenate of an orange *Aplidium sp*. tunicate	NA	Faulkner (2002)
3,7-Dimethyl-1,8-dihydroxy-6-methoxyisochroman	224.253	$C_{12}H_{16}O_4$	NA	*P. steckii* isolated from an unidentified tunicate	NA	Faulkner (2002)
Drechslerines E	266.3758	$C_{16}H_{26}O_3$	NA	*Drechslera dematioidea,*taken from the inner tissues of the Mediterranean red alga *Liagora viscida*	exhibited antiplasmodial activity against two strains of *P.falciparum*	Blunt *et al*. (2004)
Drechslerines G	252.3493	$C_{15}H_{24}O_3$	NA	*Drechslera dematioidea,*taken from the inner tissues of the Mediterranean red alga *Liagora viscida*	exhibited antiplasmodial activity against two strains of *P. falciparum*	Blunt *et al*. (2004)
Eutypoid A	266.2913	$C_{17}H_{14}O_3$	NA	mangrove fungus *Eutypa sp*. isolated from wood in the South China Sea	NA	Blunt *et al*. (2004)

Table I (Continued)

Compound name	Molecular weight	Formula	Chemistry class	Organism	Pharmacologic activity	reference
Fumiquinazolines A, B	445.4705	$C_{24}H_{23}N_5O_4$	NA	*A. fumigatus* from the gastrointestinal tract of the fish *Pseudolabrus japonicus*	NA	Faulkner (2002)
Fumiquinazolines F, G	443.4546	$C_{24}H_{21}N_5O_4$	NA	*A. fumigatus* from the gastrointestinal tract of the fish *Pseudolabrus japonicus*	NA	Faulkner (2002)
Fumiquinazolines H	485.5344	$C_{27}H_{27}N_5O_4$	NA	An *Acremonium sp*. isolated from the surface of the tunicate *Ecteinascidia turbinata* from the Bahamas	anti-inflammatory activity	Faulkner (2002)
Fumiquinazolines I	487.5503	$C_{27}H_{29}N_5O_4$	NA	An *Acremonium sp*. isolated from the surface of the tunicate *Ecteinascidia turbinata* from the Bahamas	anti-inflammatory activity	Faulkner (2002)
Fusaperazines A	312.4077	$C_{13}H_{16}N_2O_3S_2$	NA	*Fusarium chlamydosporum*, isolated from the Japanese marine red alga *Carpopeltis affinis*	NA	Blunt *et al*. (2004)
Halichoblelide	1039.2492	$C_{54}H_{86}O_{19}$	NA	*Streptomyces hygroscopicus* isolated from The Japanese fish *Halichoeres bleekeri*	potent cytotoxicity against the murine P388 cell line and 39 human cancer cell lines	Blunt *et al*. (2004)

Table I (Continued)

Compound name	Molecular weight	Formula	Chemistry class	Organism	Pharmacologic activity	reference
Halorosellinic acid	432.5497	$C_{25}H_{36}O_6$	Ophiobolane sesterterpene	marine fungus *Halorosellinia oceanica* BCC 5149	moderate anti-malarial activity (IC50=13 Ag/mL) against the parasite *P. falciparum* (K1, multidrug resistant strain)	Mayer and Hamann (2005)
Halorosellins A	396.3885	$C_{19}H_{24}O_9$	Ophiobolane sesterterpene	marine fungus *Halorosellinia oceanica* of Thai origin	NA	Blunt *et al*. (2004)
Halorosellins B	382.3619	$C_{18}H_{22}O_9$	Ophiobolane sesterterpene	the marine fungus *Halorosellinia oceanica* of Thai origin	NA	Blunt *et al*. (2004)
Harzialactone A	192.2112	$C_{11}H_{12}O_3$	NA	isolated from OUPS-N115 strain of *T. harzianum*	NA	Faulkner (2002)
Herbarin A	236.2207	$C_{12}H_{12}O_5$	NA	*Cladosporium herbarum* isolated from the sponges *Aplysina aerophoba* and *Callyspongia aerizusa* collected in the French Mediterranean	active in the brine shrimp assay	Blunt *et al*. (2004)

Table I (Continued)

Compound name	Molecular weight	Formula	Chemistry class	Organism	Pharmacologic activity	reference
Humicolone	220.2213	$C_{12}H_{12}O_4$	Phenolic tetralone in acetal form	*Humicola grisea* isolated from drift wood in New Caledonian waters	cytotoxicity towards KB cell lines	Blunt *et al*. (2004)
4'-N-methyl-5'-Hydroxystaurosporine	496.557	$C_{29}H_{28}N_4O_4$	cytotoxic staurosporine derivatives	marine fungal strain (I96S215) I96S215), which was obtained from a tissue sample of an unidentified marine sponge collected in Indonesia	NA	Faulkner (2002)
Hydroxydebromomarinone	424.4862	$C_{25}H_{28}O_6$	NA		NA	Faulkner (2002)
1-Hydroxyyanuthone A	418.5232	$C_{24}H_{34}O_6$	meroterpenoids	*A. niger* isolated from a tissue homogenate of an orange tunicate *(Aplidium sp*.)	NA	Faulkner (2002)
1-Hydroxyyanuthone C	418.5232	$C_{24}H_{34}O_6$	meroterpenoids	*A. niger* isolated from a tissue homogenate of an orange tunicate *(Aplidium sp*.)	NA	Faulkner (2002)

Table I (Continued)

Compound name	Molecular weight	Formula	Chemistry class	Organism	Pharmacologic activity	reference
5-Hydroxyramulosin	198.2158	$C_{10}H_{14}O_4$	NA	*Phoma tropica*, isolated from the brown alga *Fucus spiralis*	NA	Blunt *et al*. (2004)
10-Hydroxy-18-methoxybetaenone	396.5176	$C_{22}H_{36}O_6$	NA	An undescribed *Microsphaeropsis sp*. from the Mediterranean sponge *Aplysina aerophoba*	tyrosine kinase inhibitors	Faulkner (2002)
IB-96212	999.3146	$C_{54}H_{94}O_{16}$	macrolide	NA	a cytotoxic macrolide from a marine species of *Micromonospora sp.*	Faulkner (2002)
Isomarinone	487.3829	$C_{25}H_{27}BrO_5$	NA	NA	NA	Faulkner (2002)
Isosativenetriol	252.3493	$C_{15}H_{24}O_3$	sesquiterpenoids	*Drechslera dematioidea* from the red alga *Liagora viscida*	NA	Blunt *et al*. (2004)

Table I (Continued)

Compound name	Molecular weight	Formula	Chemistry class	Organism	Pharmacologic activity	reference
JM47	438.5179	$C_{21}H_{34}N_4O_6$	cyclic tetrapeptide	marine *Fusarium* species isolated from the green alga *Codium fragile sub sp. atlanticum* collected in Scottish waters	NA	Blunt *et al*. (2004)
Keisslone	198.2158	$C_{10}H_{14}O_4$	NA	marine fungus *Keissleriella sp.* isolated from a Yellow Sea sediment source	antifungal in vitro against *C. albicans*, *T. rubrum* and *A. niger* (MIC=10–80 Ag/ml)	Blunt *et al*. (2004)
Leptosine M	462.4035	$C_{22}H_{22}O_{11}$	epipolysulfanyl dioxopiperazines	*Leptosphaeria sp*. originating from the Japanese brown alga *Sargassum tortile*	NA	Blunt *et al*. (2004)
Leptosine N	772.9343	$C_{33}H_{36}N_6O_8S_4$	epipolysulfanyl dioxopiperazines	*Leptosphaeria sp*. originating from the Japanese brown alga *Sargassum tortile*	NA	Blunt *et al*. (2004)
Leptosine N1	740.8693	$C_{33}H_{36}N_6O_8S_3$	epipolysulfanyl dioxopiperazines	*Leptosphaeria sp*. originating from the Japanese brown alga *Sargassum tortile*	NA	Blunt *et al*. (2004)

Table I (Continued)

Compound name	Molecular weight	Formula	Chemistry class	Organism	Pharmacologic activity	reference
Leptosine M1	708.8043	$C_{33}H_{36}N_6O_8S_2$	epipolysulfanyl dioxopiperazines	*Leptosphaeria sp*. originating from the Japanese brown alga *Sargassum tortile*	NA	Blunt *et al*. (2004)
Lornemides A	273.37	$C_{17}H_{23}NO_2$	NA	marine actinomycete isolated from beach sand in Southern Australia	mildly antimicrobial aromatic amides	Faulkner (2002)
Lornemides B	273.37	$C_{17}H_{23}NO_2$	NA	NA	NA	Faulkner (2002)
Lunatin	286.2363	$C_{15}H_{10}O_6$	NA	*Curvularia lunata*, isolated from the marine sponge *Niphates olemda* from Indonesian waters	active against *S. aureus*, *E. coli* and *B. subtilis* , inactive against *C. albicans*	Blunt *et al*. (2004)
(+)-Macrosphelide E	342.3411	$C_{16}H_{22}O_8$	NA	*Periconia byssoides* isolated from the gastrointestinal tract of the sea hare *Aplysia kurodai*	NA	Faulkner (2002)

Table I (Continued)

Compound name	Molecular weight	Formula	Chemistry class	Organism	Pharmacologic activity	reference
Macrosphelide H	368.3784	$C_{18}H_{24}O_8$	NA	*Periconia byssoides* cultured from the sea hare *Aplysia kurodai*	NA	Blunt *et al*. (2004)
Macrosphelide L	342.3411	$C_{16}H_{22}O_8$	NA	*Periconia byssoides* cultured from the sea hare *Aplysia kurodai*	inhibited the adhesion of human-leukemia HL-60 cells to human-umbilical-vein endothelial cells (HUVEC)	Blunt *et al*. (2004)
Macrosphelides G	326.3417	$C_{16}H_{22}O_7$	NA	*Periconia byssoides*	NA	Blunt *et al*. (2004)
Mangicols A, B	422.598	$C_{25}H_{42}O_5$	sesterterpene polyols	*Fusarium sp*. (strain # CNC-477), tentatively identified as *F. heterosporum*, that was isolated from driftwood collected in the Bahamas	NA	Faulkner (2002)

Table I (Continued)

Compound name	Molecular weight	Formula	Chemistry class	Organism	Pharmacologic activity	reference
Mangicols G	406.5986	$C_{25}H_{42}O_4$	sesterterpene polyols	*Fusarium sp*. (strain # CNC-477), tentatively identified as *F. heterosporum*, that was isolated from driftwood collected in the Bahamas	NA	Faulkner (2002)
Methoxydebromomarinone	438.5128	$C_{26}H_{30}O_6$	NA	NA	NA	Faulkner (2002)
Microsphaerones A	433.4517	$C_{22}H_{27}NO_8$	NA	*Microsphaeropsis sp*. (endophytic fungus) from the marine sponge *Aplysina aerophoba* collected in French waters	NA	Blunt *et al*. (2004)
Nafuredin	360.4871	$C_{22}H_{32}O_4$	epoxy-y-lactone with a methylated olefinic side chain	*A. niger*	exerted anthelmintic activity against the ruminant parasite worm *Haemonchus contortus* and the dwarf tapeworm *Hymenolepsis nana* in mice	Mayer and Hamann (2005)

Table I (Continued)

Compound name	Molecular weight	Formula	Chemistry class	Organism	Pharmacologic activity	reference
Neomarinone	424.5293	$C_{26}H_{32}O_5$	NA	cytotoxins	an unidentified marine actinomycete (strain # CNH-099) from a sediment obtained near San Diego	Faulkner (2002)
Neurosporaxanthin	498.7385	$C_{35}H_{46}O_2$	carotenoid glycosyl ester	*Fusarium sp.* isolated from the seawater surface at Tanegashima, Japan	NA	Faulkner (2002)
Neurosporaxanthin beta-D-glucopyranoside	677.887	$C_{41}H_{57}O_8$	carotenoid glycosyl ester	*Fusarium sp.* isolated from the seawater surface at Tanegashima, Japan	NA	Blunt *et al*. (2004)
N-methylsansalvamide	600.7892	$C_{33}H_{52}N_4O_6$	NA	a *Fusarium sp*. (strain # CNL-619), which was isolated from the green alga *Avrainvillea sp.* from the US Virgin Islands	NA	Faulkner (2002)

Table I (Continued)

Compound name	Molecular weight	Formula	Chemistry class	Organism	Pharmacologic activity	reference
Oxepinamides A	347.3657	$C_{17}H_{21}N_3O_5$	NA	an *Acremonium sp*. isolated from the surface of the tunicate *Ecteinascidia turbinata* from the Bahamas	good anti-inflammatory activity	Faulkner (2002)
Oxepinamides B	NA	NA	NA	an *Acremonium sp*. isolated from the surface of the tunicate *Ecteinascidia turbinata* from the Bahamas	good anti-inflammatory activity	Faulkner (2002)
Oxepinamides C	361.3923	$C_{18}H_{23}N_3O_5$	NA	an *Acremonium sp*. isolated from the surface of the tunicate *Ecteinascidia turbinata* from the Bahamas	good anti-inflammatory activity	Faulkner (2002)
6-oxo-de-Omethyllasiodiplodin	NA	NA	Polyketide	fungus	*B. subtilis, S. aureus and S. enteritidis* inhibition	Mayer *et al.* (2009)
Paecilospirone	508.6888	$C_{32}H_{44}O_5$	NA	*Paecilomyces sp*. obtained from a coral reef at Yap, Micronesia	an inhibitor of microtubule assembly	Faulkner (2002)

Table I (Continued)

Compound name	Molecular weight	Formula	Chemistry class	Organism	Pharmacologic activity	reference
Parasitenone	156.136	$C_7H_8O_4$	new gabosine derivative	*A. parasiticus* from the Korean red alga *Carpopeltis cornea*	NA	Blunt *et al*. (2004)
Penicillazine	432.3808	$C_{20}H_{20}N_2O_9$	a quinoline derivative	*Penicillium sp*. (strain # 386) from the South China Sea	NA	Faulkner (2002)
Peribysins E	282.3752	$C_{16}H_{26}O_4$	Sesquiterpene	fungus	Cell adhesion inhibition	Mayer *et al.* (2009)
Peribysins F, G	270.3645	$C_{15}H_{26}O_4$	Sesquiterpene	fungus	Cell adhesion inhibition	Mayer *et al.* (2009)
Pestalone	439.2859	$C_{21}H_{20}Cl_2O_6$	chlorinated benzophenone	isolated from a member of the marine fungus in genus *Pestalotia*	potent antibiotic activity against methicillin-resistant *S. aureus* and vancomycin-resistant *Enterococus faecium*	Mayer and Hamann (2005)

Table I (Continued)

Compound name	Molecular weight	Formula	Chemistry class	Organism	Pharmacologic activity	reference
Pestalone	439.2859	$C_{21}H_{20}Cl_2O_6$	Benzophenone	Co-cultured fungus and bacterium	MRSA,VRE	Mancini and Guella (2007)
Phomopsidin (50)	330.4611	$C_{21}H_{30}O_3$	NA	*Phomopsis sp*. cultured from a fallen mangrove branch from Pohnpei, Micronesia	NA	Faulkner (2002)
Pycnidione	548.6665	$C_{33}H_{40}O_7$	Polyketide	fungus	*P. falciparum* W2 and D6 strain inhibition	Mayer *et al.* (2009)
Sansalvamide A	586.7626	$C_{32}H_{50}N_4O_6$	NA	*Fusarium sp*. (strain # CNL-292),63	NA	Mayer *et al.* (2009)
Sativene epoxide	252.3493	$C_{15}H_{24}O_3$	NA	NA	NA	Blunt *et al*. (2004)
Sculezonone A	388.368	$C_{20}H_{20}O_8$	NA	A *Penicillium sp*. from the Okinawan bivalve *Mytilus coruscus*	NA	Faulkner (2002)

Table I (Continued)

Compound name	Molecular weight	Formula	Chemistry class	Organism	Pharmacologic activity	reference
Sculezonone B	404.3674	$C_{20}H_{20}O_9$	NA	A *Penicillium sp*. from the Okinawan bivalve *Mytilus coruscus*	NA	Faulkner (2002)
Seco-macrosphelide E	374.3829	$C_{17}H_{26}O_9$	NA	*P. byssoides* separated from the sea hare *Aplysia kurodai*	NA	Blunt *et al*. (2004)
Shimalactone A	452.6255	$C_{29}H_{40}O_4$	Polyketide	fungus	Induction of neuritogenesis	Mayer *et al.* (2009)
Sumiki's acid	142.1094	$C_6H_6O_4$	Macrolide	marine fungus *Cladosporium herbarum*	active against *Bacillus subtilis* and *S. aureus*	Mayer and Hamann (2005)
Trichodenone A	124.1372	$C_7H_8O_2$	NA	cytotoxic metabolites of a strain of *Trichoderma harzianum* OUPS-N115 isolated from the sponge *Halichondria okadai*	NA	Faulkner (2002)
Varioxirane	280.3163	$C_{15}H_{20}O_5$	NA	NA	NA	Blunt *et al*. (2004)

Table I (Continued)

Compound name	Molecular weight	Formula	Chemistry class	Organism	Pharmacologic activity	reference
Varitriol	280.3163	$C_{15}H_{20}O_5$	NA	*Emericella variecolor* isolated from a sponge collected in the Caribbean Sea (*A. variecolor*, the anamorph of *Emericella variecolor*) off Venezuela	increased potency toward some renal, CNS and breast cancer cell lines in the NCI's 60-cell line panel	Blunt *et al*. (2004)
Varixanthone	468.4957	$C_{26}H_{28}O_8$	NA	NA	antimicrobial activity against a range of bacteria	Blunt *et al*. (2004)
Verrol 4-acetate	420.496	$C_{23}H_{32}O_7$	new trichothecene	deuteromycete *Acremonium neocaledoniae*, which was isolated from driftwood in New Caledonia	NA	Faulkner (2002)
Verrucarin A	502.5535	$C_{27}H_{34}O_9$	Polyketide	fungus	Interleukin-8 inhibition	Mayer *et al.* (2009)

Table I (Continued)

Compound name	Molecular weight	Formula	Chemistry class	Organism	Pharmacologic activity	reference
Virescenoside M	496.5904	$C_{26}H_{40}O_9$	diterpene glycosides	*Acremonium striatisporum* associated with the holothurian *Eupentacta fraudatrix*	NA	Faulkner (2002)
Virescenosides N	498.6063	$C_{26}H_{42}O_9$	diterpene glycosides	NA	NA	Faulkner (2002)
Virescenosides O	482.6069	$C_{26}H_{42}O_8$	diterpene glycosides	*Acremonium striatisporum* associated with the holothurian *Eupentacta fraudatrix*	cytotoxic against Ehrlich carcinoma cells in vitro	Blunt *et al*. (2004)
Virescenoside P	480.591	$C_{26}H_{40}O_8$	diterpene glycosides	NA	cytotoxic to developing eggs of the sea urchin *Strongylocentrotus intermedius*	Blunt *et al*. (2004)
Virescenosides Q	466.6075	$C_{26}H_{42}O_7$	diterpene glycosides	NA	NA	Blunt *et al*. (2004)

Table I (Continued)

Compound name	Molecular weight	Formula	Chemistry class	Organism	Pharmacologic activity	reference
Xestodecalactones A	264.2738	$C_{14}H_{16}O_5$	NA	*Penicillium cf. montanense* isolated from marine sponge *Xestospongia exigua* collected from the Bali Sea	NA	Blunt *et al*. (2004)
Xestodecalactone B	280.2732	$C_{14}H_{16}O_6$	NA	culture filtrates of *Penicillium cf. montanense* obtained from the marine sponge *Xestospongia exigua*	active against *C. albicans.*	Mayer and Hamann (2005)
Yanuthone A, C	402.5238	$C_{24}H_{34}O_5$	Epoxy-cyclohexenoid, meroterpenoids	*A. niger* cultured from a tissue homogenate of an orange tunicate *(Aplidium sp*.)	MRSA,VRE	Faulkner (2002), Mancini and Guella (2007)
Yanuthone B	400.5079	$C_{24}H_{32}O_5$	Epoxy-cyclohexenoid, meroterpenoids	*A. niger* cultured from a tissue homogenate of an orange tunicate *(Aplidium sp*.)	MRSA,VRE	Faulkner (2002), Mancini and Guella (2007)

Table I (Continued)

Compound name	Molecular weight	Formula	Chemistry class	Organism	Pharmacologic activity	reference
Yanuthone D	502.5965	$C_{28}H_{38}O_8$	meroterpenoids	*A. niger* cultured from a tissue homogenate of an orange tunicate (*Aplidium sp*.)	NA	Faulkner (2002)
Yanuthone E	504.6124	$C_{28}H_{40}O_8$	meroterpenoids	*A. niger* cultured from a tissue homogenate of an orange tunicate (*Aplidium sp*.)	NA	Faulkner (2002)
Zopfiellamides A	445.5485	$C_{25}H_{35}NO_6$	polyketides	marine ascomycete *Zopfiella latipes*, originally isolated from Indian Ocean soil	moderately active against *Arthrobacter citreus*, *B. brevis*, *B. subtilis*, *B. licheniformis*,*Corynebacterium insidiosum*, *Micrococcus luteus*, *Mycobacterium phlei*, *Streptomyces sp.* and *Acinetobacter calcoaceticus*	Blunt *et al*. (2004), Mayer and Hamann (2005)
Zopfiellamides B	445.5485	$C_{25}H_{35}NO_6$	polyketides	marine ascomycete *Zopfiella latipes*, originally isolated from Indian Ocean soil	moderately active against *Arthrobacter citreus*, *B. brevis*, *B. subtilis*, *B. licheniformis*,*Corynebacterium insidiosum*, *Micrococcus luteus*, *Mycobacterium phlei*, *Streptomyces sp*. and *Acinetobacter calcoaceticus*	Blunt *et al*. (2004)

Table II Bioactive compounds from marine bacteria adapted from Mayer (2009)

Compound name	Molecular weight	Formula	Chemistry class	Organism	Pharmacologic activity	reference
Antanapeptins A	736.9371	$C_{41}H_{60}N_4O_8$	NA	*L. majuscula*	NA	Blunt *et al*. (2004)
Antanapeptins B	738.953	$C_{41}H_{62}N_4O_8$	NA	*L. majuscule*	NA	Blunt *et al*. (2004)
Antanapeptins C	740.9689	$C_{41}H_{64}N_4O_8$	NA	*L. majuscule*	NA	Blunt *et al*. (2004)
Antanapeptins D	722.9105	$C_{40}H_{58}N_4O_8$	NA	*L. majuscula*	NA	Blunt *et al*. (2004)
Apratoxin B	826.0965	$C_{44}H_{67}N_5O_8S$	NA	*Lyngbya sp.*	less active against KB and LoVo cells	Blunt *et al*. (2004)
Apratoxin C	826.0965	$C_{44}H_{67}N_5O_8S$	NA	*Lyngbya sp.*	cytotoxicity against KB and LoVo cells	Blunt *et al*. (2004)
Ara-C (Cytarabine)	243.2166	$C_9H_{13}N_3O_5$	NA	NA	NA	Zhang *et al*. (2005)
Apramides A–G			Lipopeptide,	Two collections of *L. majuscula* from Apra Harbor, Guam		Faulkner (2002)
Basiliskamides A, B	385.4965	$C_{23}H_{31}NO_4$	Polyketide	*Bacillus laterosporus*, isolated from the tissues of an unidentified tube worm from Loloata Island, Papua New Guinea	antifungal polyketide metabolites : potent in vitro activity against *Candida albicans*	Blunt *et al*. (2004)

Table II (Continued)

Compound name	Molecular weight	Formula	Chemistry class	Organism	Pharmacologic activity	reference
Bogorol A	1584.0811	$C_{80}H_{142}N_{16}O_{16}$	Peptide	culture of a marine *Bacillus sp.*	active against methicillin-resistant *S. aureus* (MIC=2 Ag/mL) and vancomycin-resistant enterococcal strains (MIC=10 Ag/mL).	Mayer and Hamann (2005)
Brunsvicamides B	859.065	$C_{46}H_{66}N_8O_8$	Peptides	cyanobacterium *Tychonema sp*	inhibit the *Mycobacterium tuberculosis* protein tyrosine phosphatase B (MptpB),	Mayer *et al*. (2009)
Brunsvicamides C	877.0373	$C_{45}H_{64}N_8O_{10}$	Peptides	cyanobacterium *Tychonema sp*	inhibit the *Mycobacterium tuberculosis* protein tyrosine phosphatase B (MptpB),	Mayer *et al*. (2009)
Bryostatin	905.0326	$C_{47}H_{68}O_{17}$	NA	bacterial symbiont	NA	Zhang *et al*. (2005)
Caylobolide A	763.0939	$C_{42}H_{82}O_{11}$	NA	*L. majuscula* from the Bahamas	cytotoxicity against human colon tumor cells (HCT-116) in vitro	Blunt *et al*. (2004)

Table II (Continued)

Compound name	Molecular weight	Formula	Chemistry class	Organism	Pharmacologic activity	reference
Chalcomycin B	812.9373	$C_{41}H_{64}O_{16}$	NA	isolated from the culture broth of a *Streptomyces sp.* derived from mangrove sediment collected near Pohoiki, Hawaii	activity against a variety of microorganisms and microalgae	Blunt *et al*. (2004)
Cyanopeptolin 954	955.4918	$C_{46}H_{63}ClN_8O_{12}$	Depsipeptide	bacterium	α-chymotrypsin inhibition	Mayer et. al. (2009)
2,4-Dibromo-6-chlorophenol	NA	NA	NA	*Pseudoalteromonas luteoviolacea*	against methicillin-resistant *Staphylococcus aureus* and *Burkholderia cepacia*	Zhong Jiang (2006),
diketopiperazine cyclo(L-phenylalanyl-4R-hydroxy-L-proline)	NA	NA	NA	*Pseudoalteromonas luteoviolacea* isolated from the surface of the Hawaiian alga Padina australis	antibiotic	Faulkner (2002)
Diphosphatidylglycerol	1151.5107	$C_{58}H_{120}O_{17}P_2$	Phospholipids	*Microbacterium sp.* isolated from the Adriatic sponge *Halichondria panicea*	NA	Faulkner (2002)

Table II (Continued)

Compound name	Molecular weight	Formula	Chemistry class	Organism	Pharmacologic activity	reference
Dolastatin 3	660.8079	$C_{29}H_{40}N_8O_6S_2$	NA	*L. majuscula* isolated from the sea hare *Dolabella auricularia*	minor cytotoxic metabolite, an inhibitor of HIV-1 integrase	Faulkner (2002)
Flavochristamides A	617.9639	$C_{34}H_{67}NO_6S$	sulfonolipids	marine *Flavobacterium sp.*	NA	Faulkner (2002)
Flavochristamides B	618.9724	$C_{34}H_{68}NO_6S$	sulfonolipids	marine *Flavobacterium sp.*	NA	Faulkner (2002)
Gephyromycin	NA	NA	Polyketides	bacterium	Increase of neuronal Ca2+ levels	Mayer *et al*. (2009)
Halolitoralin A	552.7066	$C_{27}H_{48}N_6O_6$	Cyclic hexapeptide	*Halobacillus litoralis*, which had originated from a high-salt sediment from the Huanghai Sea, China	moderate antifungal activity against *C. albicans*, *T. rubrum* and four crop threatening fungi, moderate activity against the human gastric tumour BGC cell line	Blunt *et al*. (2004)

Table II (Continued)

Compound name	Molecular weight	Formula	Chemistry class	Organism	Pharmacologic activity	reference
Halolitoralins B, C	438.604	$C_{23}H_{42}N_4O_4$	Tetrapeptides	*Halobacillus litoralis*, which had originated from a high-salt sediment from the Huanghai Sea, China	NA	Blunt *et al*. (2004)
Hassallidin A	1382.5088	$C_{62}H_{99}N_{11}O_{24}$	Lipopeptide	bacterium	*C. albicans* and *A. fumigates* inhibition	Mayer *et al*. (2009)
Hectochlorin	665.6029	$C_{27}H_{34}Cl_2N_2O_9S_2$	NA	*L. majuscula* collected from Hector Bay, Jamaica, and Boca del Drago Beach, Panama	*C. Albicans* inhibition	Blunt *et al*. (2004)
Heptyl prodigiosin	NA	NA	NA	culture of a proteobacteria from a marine tunicate in the Philippines	in vitro activity of heptyl prodigiosin against *P. falciparum* 3D7.	Mayer and Hamann (2005), (Lazaro *et al*., 2002).
Hermitamides A	359.5454	$C_{23}H_{37}NO_2$	NA	A specimen of *L. majuscula* from Papua New Guinea	toxic to brine shrimp and mildly toxic to goldfish	Faulkner (2002)

Table II (Continued)

Compound name	Molecular weight	Formula	Chemistry class	Organism	Pharmacologic activity	reference
Indanone	132.1592	C_9H_8O		a specimen of *L. majuscula* collected in Guam	inhibited hypoxia-induced activation of the VEGF gene promotor in Hep3B human liver tumour cells in vitro	Faulkner (2002)
Lajollamycin	687.82	$C_{36}H_{53}N_3O_{10}$	Polyketided	bacterium	Inhibited *S. aureus* and *S. pneumonia*	Mayer *et al*. (2009)
Largamides D	1233.2044	$C_{56}H_{82}BrN_9O_{17}$	Depsipeptide	bacterium	α-chymotrypsin type II inhibition	Mayer *et al*. (2009)
Largamides E	1188.7534	$C_{56}H_{82}ClN_9O_{17}$	Depsipeptide	bacterium	α-chymotrypsin type II inhibition	Mayer *et al*. (2009)
Largamides F	1283.22	$C_{59}H_{80}BrN_9O_{18}$	Depsipeptide	bacterium	α-chymotrypsin type II inhibition	Mayer *et al*. (2009)
Largamides G	1297.2466	$C_{60}H_{82}BrN_9O_{18}$	Depsipeptide	bacterium	α-chymotrypsin type II inhibition	Mayer *et al*. (2009)

Table II (Continued)

Compound name	Molecular weight	Formula	Chemistry class	Organism	Pharmacologic activity	reference
Lobocyclamide B	1398.6837	$C_{65}H_{115}N_{13}O_{20}$		isolated from a benthic mat of *L. confervoides* from the Bahamas	antifungal activity against fluconazole-resistant *C. albicans*	Blunt *et al*. (2004)
Loloatin A	1273.4339	$C_{65}H_{84}N_{12}O_{15}$	Peptide	lab. cultures of a bacterium	MRSA, VRE, drug-resistant *Streptococcus pneumoniae*	Blunt *et al*. (2004)
Lyngbouilloside	584.7386	$C_{31}H_{52}O_{10}$		*L. bouillonii* collected from Papua New Guinea	Modest cytotoxicity to neuro-2a neuroblastoma cells	Blunt *et al*. (2004)
Lyngbyabellin A	691.6865	$C_{29}H_{40}Cl_2N_4O_7S_2$	cyclic depsipeptides	*L. majuscula* from Guam and the Dry Tortugas National Park, Florida	cytotoxic and antifungal	Blunt *et al*. (2004)
Lyngbyabellin B	679.6758	$C_{28}H_{40}Cl_2N_4O_7S_2$	cyclic depsipeptides	*L. majuscula* from Guam and the Dry Tortugas National Park, Florida	cytotoxic and antifungal	Blunt *et al*. (2004)
Lyngbyabellin C	609.5396	$C_{24}H_{30}Cl_2N_2O_8S_2$		*Lyngbya sp*. from Palau	activity against KB and LoVo cell lines	Blunt *et al*. (2004)

Table II (Continued)

Compound name	Molecular weight	Formula	Chemistry class	Organism	Pharmacologic activity	reference
Lyngbyaloside B	649.6081	$C_{30}H_{49}BrO_{10}$		marine cyanobacterium *Lyngbya sp.*	weak cytotoxicity against KB cells	Blunt *et al*. (2004)
Lyngbyapeptin A				Guam specimen of L. majuscule and a Papua New Guinea specimen of *L. bouillonii*		Faulkner (2002)
Macrolactin F	402.5238	$C_{24}H_{34}O_5$	peptide	*Bacillus sp.* (Sc026) from a marine sediment	antibacterial activity	Faulkner (2002)
Majusculoic acid	315.2459	$C_{15}H_{23}BrO_2$	Polyketide	bacterium	*C. albicans* inhibition, less potent than fluconazole	Mayer *et al*. (2009)

Table II (Continued)

Compound name	Molecular weight	Formula	Chemistry class	Organism	Pharmacologic activity	reference
Malevamide D	732.9899	$C_{40}H_{68}N_4O_8$	NA	isolated from an Hawaiian collection of *S. hydnoides*	toxicity against P388, A-549, HT-29 and MEL-28 cell lines in the sub-nanomolar range	Blunt *et al*. (2004)
Marinomycins A	997.2156	$C_{58}H_{76}O_{14}$	Polyketides	bacterium	S. *aureus* and *E. faceium* inhibition	Mayer *et al*. (2009)
Marinomycins B	997.215	$C_{58}H_{76}O_{14}$	Polyketids	bacterium	S. *aureus* and *E. faceium* inhibition	Mayer *et al*. (2009)
Marinomycins C	997.2156	$C_{58}H_{76}O_{14}$	Polyketids	bacterium	S. *aureus* and *E. faceium* inhibition	Mayer *et al*. (2009)
Marinomycins D	1011.2422	$C_{59}H_{78}O_{14}$	Polyketids	bacterium	S. *aureus* and *E. faceium* inhibition	Mayer *et al*. (2009)
Micropeptin 88 N	1063.2423	$C_{54}H_{78}N_8O_{14}$	Depsipeptide	bacterium	Chemotrypsin inhibition	Mayer *et al*. (2009)
Micropeptin 88 Y	1085.2048	$C_{55}H_{72}N_8O_{15}$	Depsipeptide	bacterium	Chemotrypsin inhibition	Mayer *et al*. (2009)

Table II (Continued)

Compound name	Molecular weight	Formula	Chemistry class	Organism	Pharmacologic activity	reference
Obyanamide	599.7414	$C_{30}H_{41}N_5O_6S$	NA	*L. confervoides* from Saipan in the Commonwealth of the Northern Mariana Islands	cytotoxic to KB cells	Blunt *et al*. (2004)
Palau'imide	428.5643	$C_{25}H_{36}N_2O_4$	NA	NA	cytotoxic to KB and LoVo cells	Blunt *et al*. (2004)
Petrobactin	718.7944	$C_{34}H_{50}N_6O_{11}$	bis-catechol α-hydroxy acid siderophore	*Marinobacter hydrocarbonoclasticus*	NA	Blunt *et al*. (2004)
Phormidolide	1078.2983	$C_{59}H_{97}BrO_{12}$	NA	*Phormidium sp*. from Sulawesi, Indonesia	a potent brine shrimp toxin	Blunt *et al*. (2004)
Resistoflavin methyl ether	392.3582	$C_{22}H_{16}O_7$	Polyketided	bacteria	*B. subtilis* inhibition	Mayer *et al*. (2009)
Salinosporamide A	313.7766	$C_{15}H_{20}ClNO_4$		*Salinispora tropica.*	anticancer agent	Zhang *et al*. (2005).

Table II (Continued)

Compound name	Molecular weight	Formula	Chemistry class	Organism	Pharmacologic activity	reference
Scytonemin	544.555	$C_{36}H_{20}N_2O_4$	NA	cyanobacterium *Stigonema sp*	anti-inflammatory and anti-proliferative activities	Blunt *et al*. (2004)
Somamide A	966.1503	$C_{48}H_{67}N_7O_{12}S$	NA	assemblages of the cyanobacteria *L. majuscula* and *Schizothrix sp*.	NA	*Alteromonas rava sp*.
Somocystinamide A	759.1596	$C_{42}H_{70}N_4O_4S_2$	cytotoxic disulfide dimer	a mixed assemblage of *L. majuscula* and a *Schizothrix sp*. from Fijian waters	NA	Blunt *et al*. (2004)
Streptomyces anthraquinones	NA	NA	Polyketided	*Streptomyces sp.*	Methicillin-resistant *S. aureus* inhibition	Mayer *et al*. (2009)
Streptomycetaceae quinone	NA	NA	Polyketided	*Streptomyces sp.*	Methicillin-resistant *S. aureus* and vancomicinresistant *Enterococcus* inhibition	Mayer *et al*. (2009)
7-O-succinyl macrolactin A	502.5965	$C_{28}H_{38}O_8$	peptide	NA	NA	Faulkner (2002)

Table II (Continued)

Compound name	Molecular weight	Formula	Chemistry class	Organism	Pharmacologic activity	reference
7-O-succinyl macrolactin F	502.5965	$C_{28}H_{38}O_8$	peptide	NA	NA	Faulkner (2002)
Symplostatin 3	746.9734	$C_{40}H_{66}N_4O_9$	NA	*S. hydnoides* isolated from tumour-selective extract of an Hawaiian collection of *Symploca sp*. VP452	strong cytotoxicity towards a range of human tumour cell lines and disrupts microtubules (*in vitro*)	Blunt *et al*. (2004)
(+)-Tanikolide			NA	isolated from a specimen of *L. majuscula* from Madagascar		Faulkner (2002)
Tasiamide	830.0223	$C_{42}H_{67}N_7O_{10}$	NA	A Palauan collection of *Symploca sp.*	cytotoxic against KB and LoVo cells	Blunt *et al*. (2004)
Thiocoraline	1157.408	$C_{48}H_{56}N_{10}O_{12}S_6$	NA	*Micromonospora sp*. L-13-ACM2–092	potent antitumor, antibiotics	Faulkner (2002)
Thiomarinol	640.8084	$C_{30}H_{44}N_2O_9S_2$	Tetrahydro-pyrane	*Alteromonas rava sp.*	against bacteria Gram (+), Gram(-)	Mancini and Guella (2007)

Table II (Continued)

Compound name	Molecular weight	Formula	Chemistry class	Organism	Pharmacologic activity	reference
Thiomarinol B	672.8072	$C_{30}H_{44}N_2O_{11}S_2$	Tetrahydro-pyrane	*Alteromonas rava sp.*	against bacteria Gram (+), Gram(-)	Mancini and Guella (2007)
Thiomarinol C	624.809	$C_{30}H_{44}N_2O_8S_2$	Tetrahydro-pyrane	*Alteromonas rava sp.*	against bacteria Gram (+), Gram(-)	Mancini and Guella (2007)
Thiomarinol D	654.8349	$C_{31}H_{46}N_2O_9S_2$	Tetrahydro-pyrane	*Alteromonas rava sp.*	against bacteria Gram (+), Gram(-)	Mancini and Guella (2007)
Thiomarinol E	668.8615	$C_{32}H_{48}N_2O_9S_2$	Tetrahydro-pyrane	*Alteromonas rava sp.*	against bacteria Gram (+), Gram(-)	Mancini and Guella (2007)

Table II (Continued)

Compound name	Molecular weight	Formula	Chemistry class	Organism	Pharmacologic activity	reference
Thiomarinol F	638.7925	$C_{30}H_{42}N_2O_9S_2$	NA	*Alteromonas rava* sp.	NA	Mancini and Guella (2007)
Tupuseleiamides A, B	408.4886	$C_{21}H_{32}N_2O_6$	Acyldipeptides	*Bacillus laterosporus*, isolated from the tissues of an unidentified tube worm from Loloata Island, Papua New Guinea	NA	Blunt *et al*. (2004)
Ulongamide A	627.7946	$C_{32}H_{45}N_5O_6S$	β-Amino Acid-Containing Cyclodepsipeptides	*Lyngbya sp*. from various Palauan dive sites	weakly cytotoxic against KB and LoVo cells in vitro	Blunt *et al*. (2004)
Ulongamide B	643.794	$C_{32}H_{45}N_5O_7S$	β-Amino Acid-Containing Cyclodepsipeptides	*Lyngbya sp*. from various Palauan dive sites	weakly cytotoxic against KB and LoVo cells in vitro	Blunt *et al*. (2004)
Ulongamides C	691.8368	$C_{36}H_{45}N_5O_7S$	β-Amino Acid-Containing Cyclodepsipeptides	*Lyngbya sp*. from various Palauan dive sites	weakly cytotoxic against KB and LoVo cells in vitro	Blunt *et al*. (2004)
Ulongamides D	671.8472	$C_{34}H_{49}N_5O_7S$	β-Amino Acid-Containing Cyclodepsipeptides	*Lyngbya sp*. from various Palauan dive sites	weakly cytotoxic against KB and LoVo cells in vitro	Blunt *et al*. (2004)
Ulongamides E	685.8737	$C_{35}H_{51}N_5O_7S$	β-Amino Acid-Containing Cyclodepsipeptides	*Lyngbya sp*. from various Palauan dive sites	weakly cytotoxic against KB and LoVo cells in vitro	Blunt *et al*. (2004)

Appendix III

Table I Elemental compostion of Instant Ocean (IO, synthetic sea salts) compared with Sea water (SW). Adapted from Atkinson and Bingman (1997).

Elemental compostion	Sea water (SW)	Instant Ocean (synthetic sea salts)
ppt	35	29.65
Major Cations (mmol kg-1)		
Na^{+}	470	462
K^{+}	10.2	9.4
Mg^{+2}	53	52
Ca^{+2}	10.3	9.4
Sr^{+1}	0.09	0.19
Sum	607	594
Major Anions (mmol kg-1)		
Cl^{-}	550	521
SO^{4-2}	28	23
TCO_2	1.90	1.90
Sum	608	569
Nutrients (μmol kg-1)		
PO_4:P	0.20	0.05
NO_3:N	0.20	1.00

NH_4:N	0.20	10.2
SiO_3:Si	5	4.2
DOP:P	0.2	0.1
DON:N	10	2.9
TOC:C	50	29

Table I (Continued) 1

Elemental compostion	Sea water (SW)	Instant Ocean (synthetic sea salts)
pH	8.25	8.35
TA	2.3	2.3
Trace (μmol kg-1)		
Li	20	54
Si	5	16
Mo	0.1	1.8
Ba	0.04	0.85
V	0.04	2.9
Ni	0.004	1.7
Cr	0.003	7.5
Al	0.002	240
Cu	0.001	1.8
Zn	0.001	0.50
Mn	0.0004	1.2
Fe	0.0001	0.24
Cd	0.0001	0.24
Pb	0.00006	2.1

Co	0.00005	1.3
Ag	0.00001	2.3
Ti	0.00001	0.67

Appendix IV

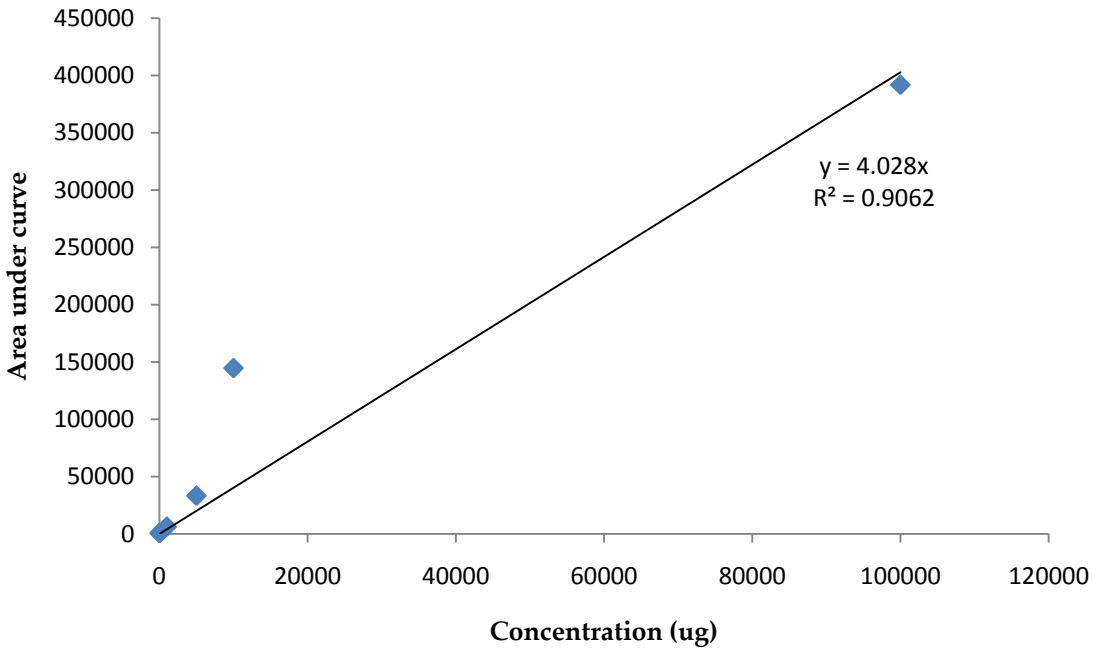

Figure I Calibration curve of gamma-linolenic acid standard.

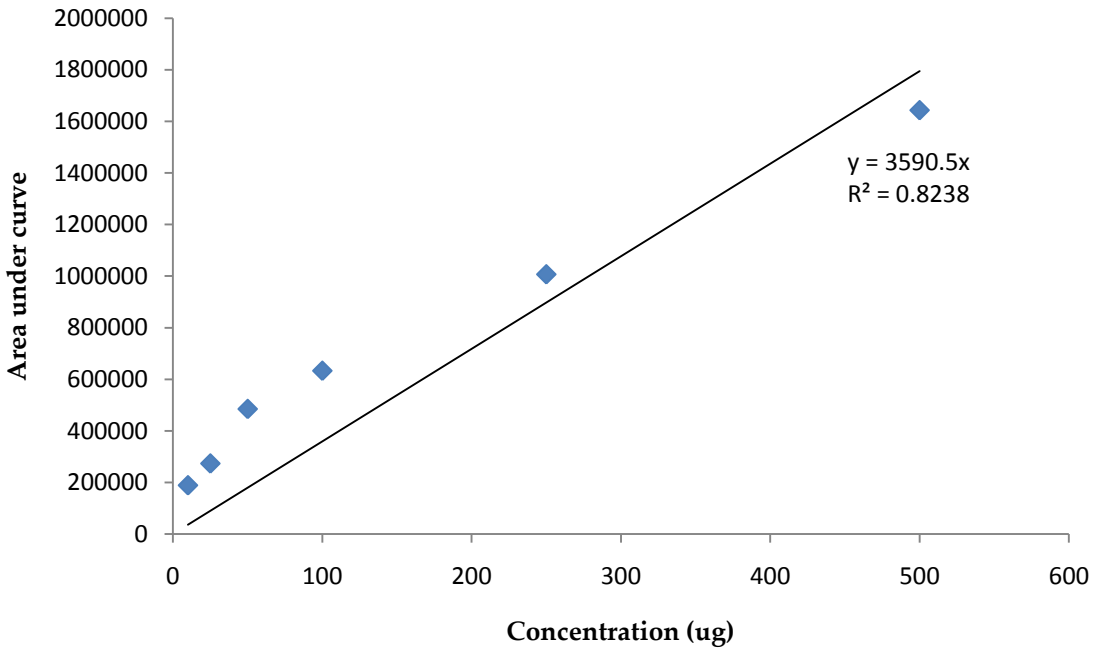

Figure II Calibration curve of lovastatin standard.